APPENDIX F

BIBLIOGRAPHY AND PUBLICATIONS CITED

![Acorn Cardiovascular logo]

CorCap™ Cardiac Support Device
REFERENCES

For detailed information describing use, warnings, precautions and contraindications, refer to the instructions with each device, or contact the manufacturer.

Acorn Cardiovascular, Inc. and CorCap are trademarks of Acorn Cardiovascular, Inc., St. Paul, MN, USA.

CAUTION: In the United States, the CorCap™Cardiac Support Device is limited by USA law to investigational use.

MANUSCRIPTS

Clinical Trial Experience

A. Charité Safety Study

Lembcke A, et al. Early and late effects of passive epicardial constraint on left ventricular geometry: ellipsoidal re-shaping confirmed by electron-beam computed tomography. J of Heart and Lung Transplantation Jan 2006;25(1):90-8. *(ITEM M-A08)*

Lembcke A, Dushe S, Enzweiler CN, Kloeters C, Wiese TH, Hermann KG, Hamm B, Konertz WF. Passive external cardiac constraint improves segmental left ventricular wall motion and reduces akinetic area in patients with non-ischemic dilated cardiomyopathy. Eur J Cardiothorac Surg. 2004 Jan;25(1):84-90. *(ITEM M-A07)*

Lembcke A, Dushe S, Sonntag S, Kloeters C, Enzweiler CN, Wiese TH, Hamm B, Kleber FX, Konertz WF. Changes in right ventricular dimensions and performance after passive cardiac containment. Ann Thorac Surg. 2004 Sep;78(3):900-5. (*ITEM M-A06*)

Lembcke A, Wiese TH, Dushe S, Hotz H, Enzweiler CNH, Hamm B, Konertz WF. Effects of passive cardiac containment on left ventricular structure and function: verification by volume and flow measurements. J of Heart and Lung Transplantation 2004;23:11-19. *(ITEM M-A05)*

Lembcke A, Hotz H, Dushe S, Ensweiler CNH, Wiese TH, Kivelitz DE, Rogalla P, Konertz W, Hamm B. Evaluierung der passiven Kardiomyoplastie mittels links- und rechtsvertrikularer EBCT- und MRT-Volumetrie bei Patienten mit chronischer Herzinsuffizienz. Fortschr Rontgenstr 2003; 175: 1086-1092. *(ITEM M-A04)*

Konertz WF, Dushe S, Hotz H, Spies C, Enzweiler C, Kleber FX. Cardiac Support Device: Novel surgical option for heart failure. Asian Cardiovasc Thorac Ann 2001;9:167-70. *(ITEM M-A03)*

Konertz WF, Shapland JE, Hotz H, Dushe S, Braun JP, Stantke K, Kleber FX. Passive containment and reverse remodeling by a novel textile Cardiac Support Device. Circulation 2001;104(Suppl I):I-270-I-275. *(ITEM M-A02)*

Hotz H, Dushe S, Konertz W. Indikationen, Technik und Erste Ergebnisse der Passiven Kardiomyoplastie. Z Kardiol 2001;90 (Suppl 1):16-21. *(ITEM M-A01)*

B. Melbourne Safety Study

Raman JS, Hata M, Storer M, Power JM, Buxton BG, Alferness C, Hare D. The Mid-term Results of Ventricular Containment (ACORN WRAP) for End-stage Ischemic Cardiomyopathy. Ann Thorac Cardiovasc Surg 2001;7(5):278-81. *(ITEM M-B02)*

Raman JS, Power JM, Buxton BF, Alferness C, Hare D. Ventricular Containment as an Adjunctive Procedure in Ischemic Cardiomyopathy: Early Results. Ann Thorac Surg 2000;70:000-00. *(ITEM M-B01)*

C. CorCap™ Randomized Clinical Trial in Europe and Australia

Franco-Cereceda, A, Lockowandt, U, Liska, J, Alsson, A. Reversal of Ventricular Dilatation in Aortic Regurgitation After Valve Replacement and Cardiac Support Implant Surgery Using the CorCap Cardiac Support Device. Ann Thorac Surg 2005;80:315-316. *(ITEM M-C01)*

D. Acorn Clinical Trial

Acker M, Bolling S, Shemin R, Kirklin J, Oh JK, Mann D, Jessup M, Sabbah H, Starling R, Kubo S. Mitral

valve surgery in heart failure: Insights from the Acorn Clinical Trial. J Thorac Coardiovasc Surg 2006;132:568-77

Hauptman P, Rector T, Wentworth D, Kubo S. Quality of life in advanced heart failure : Role of mitral regurgitation. Am Heart Journal Jan 2006 ;151 :213-8. *(ITEM M-D05)*

Bhat G, Kubo SH. Gender Differences in Heart Failure : Baseline Characteristics from the Acorn Clinical Trial. 2004 HF Society of America poster presentation Sept 14, 2004. *(ITEM M-D04)*

Aranda JM, Beaver TM, Schofield RS, Leach DD, Staples ED, Kubo SH. Predictors of Hospital Length of Stay in a Surgical Approach to the Failing Heart : The ACORN Cardiac Support Device Randomized Trial Experience. 2004 HF Society of America poster presentation Sept 13, 2004. *(ITEM M-D03)*

Mann D et al. Rationale, Design and Methods for a Pivotal Randomized Clinical Trial for the Assessment of the CorCap™ Cardiac Support Device in Patients with NYHA II-IV Heart Failure. J Card Failure. 2004; 10(3):185-192. *(ITEM M-D02)*

Kubo S et al. Development and Validation of a Patient Questionnaire to Determine NYHA Classification. J Card Failure. 2004; 10(3):228-235*(ITEM M-D01)*

E. Implant Technique

Oz MC. Surgical Implantation of the Acorn Cardiac Support Device. Operative Techniques in Thoracic and Cardiovascular Surgery. Vol 7(2) May 2002; 107-110. *(ITEM M-E04)*

Badhwar V, Bolling SF. The Acorn Procedure: Operative Techniques in Thoracic and Cardiovascular Surgery. Vol 7(2) May 2002; 84-89. *(ITEM M-E03)*

Dullum MKC, Carlos BD, Oz MC, Chon CD, Bafi AS, Cooke RH, Harrison J, Bither C, Peel GK. Less Invasive Surgical Management of Heart Failure by Cardiac Support Device Implantation on the Beating Heart. The Heart Surgery Forum 2001-1818. 4(4):361-363, 2001. *(ITEM M-E02)*

Oz MC. Passive ventricular constraint for the treatment of congestive heart failure. Ann Thorac Surg 2001;71:S185-7. *(ITEM M-E01)*

Pre-clinical Experience

F. Global Cardiac Function/Structure

Sabbah H. Commentary: Passive Ventricular Containment in Dilated Ventricular Heart Failure: Experimental insights into clinical benefits. Braunwald's on line 7th edition Jan 2006. *(ITEM M-F14)*

Mann D. Cardiac Remodeling as Therapeutic Target: Treating Heart Failure with Cardiac Support Devices. HF Reviews, 10, 93-94, 2005. (*ITEM M-F13*)

Mann D. Left Ventricular Size and Shape: Determinants of Mechanical Signal Transduction Pathways. HF Reviews, 10, 95-100, 2005. (*ITEM M-F12*)

Walsh R. Design and Features of the Acorn CorCap™ Cardiac Support Device: The Concept of Passive Mechanical Diastolic Support. HF Reviews, 10, 101-107, 2005. *(ITEM M-F11)*

Sabbah HN. Global Left Ventricular Remodeling with the Acorn Cardiac Support Device: Hemodynamic and Angiographic Findings in Dogs with Heart Failure. HF Reviews, 10, 109-115. *(ITEM M-F10)*

Power JM, Raman J, Byrne M, Alferness C. Efficacy of the Acorn Cardiac Support Device in Animals with Heart Failure Secondary to High Rate Pacing. HF Reviews, 10, 117-123, 2005. *(ITEM M-F09)*

Sabbah HN. Effects of Cardiac Support Device on Reverse Remodeling: Molecular, Biochemical, and Structural Mechanisms. J Card Failure 2004; 10 (6):207-214. *(ITEM M-F08)*

Kass DA, Saavedra WF, Sabbah HN. Reverse Remodeling and Enhanced Inotropic Reserve From the Cardiac Support Device in Experimental Cardiac Failure. J Card Failure 2004; 10 (6):215-219. *(ITEM M-F07)*

Sabbah HN. The Acorn Cardiac Support Device and the Myocor Myosplint: treating heart failure by targeting left ventricular size and shape. Ann Thoracic Surg 2003 Jun;75(Suppl 6):S13-9. *(ITEM M-F06)*

Saavedra F, Tunin R, Mishima T Suzuki G, Chaudhry PA, Anagnostopoulos PV, Paolocci N, Sabbah HN, Kass DA. Reverse remodeling and enhanced adrenergic reserve from a passive external ventricular support in experimental dilated heart failure. J Am Coll Cardiol 2002;39:2069-76. *(ITEM M-F05)*

Chaudhry PA, Anagnostopouls PV, Mishima T, Suzuki G, Nair H, Morita H, Sharov VG, Alferness C, Sabbah HN. Acute Ventricular Reduction with the Acorn Cardiac Support Device: Effect on Progressive Left Ventricular Dysfunction and Dilation in Dogs with Chronic Heart Failure. J Card Surg Mar/Apr 2001; 16(2):118-126. *(ITEM M-F04)*

Chaudry PA, Mishima T, Suzuki G, Sharov VG, Anagnostopoulos PV, Undrovinas AI, Nass O, Sabbah HN. Acute ventricular reduction with Acorn's Cardiac Support Device prevents left ventricular dysfunction and remodeling in dogs with advanced heart failure. Surgical Forum 2000;51:146-148. *(ITEM M-F03)*

Chaudhry PA, Mishima T, Sharov VG, Hawkins J, Alferness CA, Paone G, Sabbah HN. Passive epicardial containment prevents ventricular remodeling in heart failure. Ann Thorac Surg 2000;70:1275-80. *(ITEM M-F02)*

Power JM, Raman J, Dornom A, Farish SJ, Burrell LM, Tonkin AM, Buxton B, Alferness CA. Passive ventricular constraint amends the course of heart failure: A study in an ovine model of dilated cardiomyopathy. Cardiovascular Research 1999;44:549-555. *(ITEM M-F01)*

G. Cellular/Molecular

Sharov VG, Todor AV, Sabbah HN. Left Ventricular Histomorphometric Findings in Dogs with Heart Failure Treated with the Acorn Cardiac Support Device. HF Reviews, 10, 141-147, 2005. *(ITEM M-G06)*

Gupta RC, et al. Improvement of Cardiac Sarcoplasmic Reticulum Calcium Cycling in Dogs with Heart Failure Following Long-Term Therapy with the Acorn Cardiac Support Device. HF Reviews, 10, 149-155, 2005. *(ITEM M-G05)*

Rastogi S, et al. Reversal of Maladaptive Gene Program in Left Ventricular Myocardium of Dogs with Heart Failure Following Long-Term Therapy with the Acorn Cardiac Support Device. HF Reviews, 10, 157-163, 2005. *(ITEM M-G04)*

Blom AS, Mukherjee R, Pilla JJ, Lowry AS, Yarbrough WM, Mingoia JT, Hendrick JW, Stroud RE, McLean JE, Affuso J, Gorman RC, Gorman III JH, Acker MA, Spinale FG. Cardiac Support Device Modifies Left Ventricular Geometry and Myocardial Structure After Myocardial Infarction. Circ 2005;112:1274-1283. *(ITEM M-G03)*

Shah PK. Preservation of Cardiac Extracellular Matrix by Passive Myocardial Restraint: An Emerging New Therapeutic Paradigm in the Prevention of Adverse Remodeling and Progressive Heart Failure.   Circ 2005;112:1245-1247. (*ITEM M-G02)*

Sabbah HN, Sharov VG, Gupta RC, Mishra S, Rasogi S, Undrovinas AL, Chaudhry PA, Todor A, Mishima T, Tanhehco EJ, Suzuki G. Reversal of Chronic Molecular and Cellular Abnormalities Due to Heart Failure by Passive Mechanical Ventricular Containment. Circ Res. 2003; 93:1095-1101. *(ITEM M-G01)*

H. Acute Myocardial Infarction

Pilla JJ, et al. Early postinfarction ventricular restraint improves borderzone wall thickening dynamics during remodeling. Ann Thorac Surg 2005;80:2257-62. *(ITEM M-H05)*

Blom AS, et al. Infarct Size Reduction and Attenuation of Global Left Ventricular Remodeling with the CorCap™ Cardiac Support Device Following Acute Myocardial Infarction in Sheep. HF Reviews, 10, 125-139, 2005. *(ITEM M-H04)*

Blom AS, et al. A cardiac support device modifies left ventricular geometry and myocardial structure following myocardial infarction. Circulation 2005;112:1274-1283. *(ITEM M-H03)*

Olsson A, Bredin F, Franco-Cereceda A. Echocardiographic findings using tissue velocity imaging following passive containment surgery with the Acorn CorCap™ cardiac support device. EU Journal of Card-thoracic Surg 28 (2005) 448-453. *(ITEM M-H02)*

Pilla JJ, Blom AS, Brockman DJ, Bowen F, Yuan Q, Giammarco J, Ferrari VA, Gorman JH, Gorman RC, Acker MA. Ventricular Constraint Using the Acorn Cardiac Support Device Reduces Myocardial Akinetic Area in an Ovine Model of Acute Infarction. Circulation. 2002;106[suppl I]:I-207-I-211. *(ITEM M-H01)*

Clinical Reports/Summaries

I. Global Experience/Review

Mann D. Heart Failure; Beyond Practice Guidelines. TX Heart Institue Journal 2006 33;2:201-3

Serri K, Labrousse L, Reant P, Lafitte S, Roudaut R. Significant improvement of myocardial function following cardiac support device implantation: Illustration by two-dimensional strain. Eur J Echo doi:10.1016/j.euje.2005.09.006. *(ITEM M-I13)*

Franco-Cereceda A, Runsio M, Liska J. Passiv volymreducerande kirurgi vid hjärtsvikt och dilaterad Kardiomyopati Resultat från pilotstudie ger anledning till försiktig optimism. Läkartidningen Nr 34 2005 Volym 102. *(ITEM M-I12)*

Thelin S. Polyesternät stramar till sviktande hjärta Kan bli del av framtida behandlingsarsenal vid avancerad hjärtsvikt. Läkartidningen Nr 34 2005 Volym 102 *(ITEM M-I11)*

Oz MC, Konertz WF, Raman J, Kleber FX. Reverse remodeling of the failing ventricle: surgical intervention with the Acorn Cardiac Support Device. Congest Heart Fail. 2004 Mar-Apr;10(2):96-104; discussion 105. (*ITEM M-I10)*

Livi U, et al. One-year clinical experience with the Acorn CorCap™ Cardiac Support Device: results of a limited market release safety study in Italy and Sweden. Ital Heart J. 2005 Jan;6(1):59-65 *(ITEM M-I09)*

Cohn JN. New Therapeutic Strategies for Heart Failure: Left Ventricular Remodeling as a Target. J Card Failure 2004; 10 (6):200-201 *(ITEM M-I08)*

Mann DL. Basic Mechanisms of Left Ventricular Remodeling : The Contribution of Wall Stress. J Card Failure 2004; 10 (6):202-206 *(ITEM M-I07)*

Acker MA. Surgical Therapies for Heart Failure. J Card Failure 2004; 10 (6):220-224 *(ITEM M-I06)*

Starling RC, Jessup M. Worldwide Experience With the CorCap™ Cardiac Support Device. J Card Failure 2004; 10 (6):225-233 *(ITEM M-I05)*

Gummert JF, Rahmel A, Bossert T, Mohr FW. Socks for the dilated heart: Does passive cardiomyoplasty have a role in long-term care for heart failure patients?. Z Kardiol 93:849-854 (2004) *(ITEM M-I04)*

Franco-Cereceda Anders, Lockowandt U, Olsson A, Bredin F, Forssell G, Owall A, Runsio M, Liska J. Early results with cardiac support device implant in patients with ischemic and non-ischemic cardiomyopathy. Scand Cardiovasc J 2004; 38:159-163 *(ITEM M-I03)*

Oz MC, Konertz WF, Kleber FX, Mohr FW, Gummert JF, Ostermeyer J, Lass M, Raman J, Acker MA, Smedira N. Global Surgical Experience with the Acorn Cardiac Support Device. J Thor and CV Surg. 2003; 126:4:983-91 *(ITEM M-I 02)*

Power JM, Byrne M, Raman J, Alferness C. Review: Passive ventricular constraint. Progress in Biophysics & Molecular Biology 82(2003) 197-206. *(ITEM M-I01)*

276

ABSTRACTS

Clinical Trial Experience

A. Charité Safety Study

Dushe, S, Kleber, FX, Konertz, W. The Impact of Passive Diastolic Constraint on Functional Mitral Regurgitation in Patients with Dilative Cardiomyopathy. Society for Heart Valve Disease June 2005 (*ITEM A-A24*)

Konertz WF, Sonntag S, Dushe S, Hotz H. Efficacy trends with the Acorn Cardiac Support Device: 3-Year Follow-Up. American Heart Association Scientific Sessions 2003. Nov 9. *(ITEM A-A23)*

Dushe S, Kleber FX, Sonntag S, Konertz W. Passive Diastolic Containment by a Mesh-Like Device as an Option for Surgical Heart Failure Therapy. EACTS 2003 *(ITEM A-A22)*

Lembcke A, Wiese TH, Dushe S, Hotz H, Enzweiler CNH, Hamm B, Konertz WF. Changes in both left- and right-ventricular volumes and function after passive cardiomyoplasty assessed by electron beam computed tomography. European Heart Journal Vol 4, Abstract Suppl. August 2002:145. *(ITEM A-A21)*

Konertz WF, Dushe S, Enzweiler C, Hamm B. Evidence of decreasing LV size and volume after Cardiac Support Device (CSD) implantation. The Journal of Heart and Lung Transplantation;21:150. *(ITEM A-A20)*

Konertz WF, Kleber FX, Dushe S, Hotz H, Stanke K, Austin L, Walsh R. Efficacy trends with the Acorn Cardiac Support Device: Two year follow-up. Journal of American College of Cardiology;39(Suppl A):142A. *(ITEM A-A19)*

Konertz WF, Kleber FX, Dushe S. Hotz H, Stanke K. Efficacy trends with the Acorn Cardiac Support Device: One year follow-up. Circulation 2001;104(Suppl II):II-357. *(ITEM A-A18)*

Dushe S, Hotz H, Bottner D, Kleber FX, Konertz WF. Passive ventricular constraint for the treatment of heart failure patients - One year follow-up. EACTS/ESTS Joint Meeting Abstract Book September 2001:584. *(ITEM A-A17)*

Konertz WF, Kleber FX, Dushe S, Hotz H, Stantke K. Efficacy trends with the Acorn Cardiac Support Device in patients with advanced heart failure. Journal of Cardiac Failure 2001;7(Suppl 2): 39. *(ITEM A-A16)*

Kleber FX, Sonntag S, Krebs H, Stantke K, Konertz W. Influence of the cardiac support device on left ventricular function. European Journal of Heart Failure 2001;3(Suppl 1): S65. *(ITEM A-A15)*

Konertz W, Kleber FX, Dushe S, Hotz H, Stantke K. Efficacy trends with the acorn cardiac support device in patients with advanced heart failure. European Journal of Heart Failure 2001;3(Suppl 1): S93. *(ITEM A-A14)*

Kleber FX, Sonntag S, Krebs H, Stantke K, Konertz W. Follow-up on passive cardiomyoplasty in congestive heart failure: Influence of the Acorn Cardiac Support Device on left ventricular function. J Am Coll Cardiol 2001;37(Suppl A):143A. *(ITEM A-A13)*

Konertz W, Kleber FX, Dushe S, Hotz H, Stantke K. Initial efficacy trends with the Acorn Cardiac Support Device in patients with advanced heart failure. J Am Coll Cardiol 2001;37(Suppl A):143A. *(ITEM A-A12)*

Sabbah HN, Kleber FX, Konertz W. One year follow-up of the Acorn Cardiac Support Device in patients with heart failure: efficacy trends. European Journal of Heart Failure 2001;3(Suppl 1): S65. *(ITEM A-A11)*

Sabbah HN, Kleber FX, Konertz W. Efficacy trends of the Acorn Cardiac Support Device in patients with heart failure: A one year follow-up. J of Heart and Lung Transplantation 2001;20:217. *(previously ITEM A-A10)*

Konertz W, Hotz H, Dushe S, Braun JP, Stantke K, Kleber FX. Passive containment and reverse remodeling by a novel textile cardiac support device. Circulation 2000;102(Suppl):II-683. *(ITEM A-A09)*

Dushe S, Hotz H, Stantke K, Kleber FX, Konertz W. Mid-term follow up of patients after Cardiac Support Device implantation for dilated cardiomyopathy. J of Cardiac Failure 2000;6(suppl 2):35. *(ITEM A-A08)*

Kleber FX, Sonntag S, Krebs H, Stantke K, Konertz W. Passive cardiomyoplasty in congestive heart failure: influence of the passive Acorn Cardiac Support Device on left ventricular function. European Heart Journal 2000;21(suppl):533. *(ITEM A-A07)*

Konertz W, Kleber FX, Rombeck B, Hotz H, Zytowski M, Sonntag S, Stantke K, Sabbah HN. Safety results and initial efficacy trends with the Acorn Cardiac Support Device in patients with advanced heart failure. European Heart Journal 2000;21(suppl):533. *(ITEM A-A06)*

Dusche S, Rombeck B, Hotz H, Stantke K, Sabbah HN, Kleber FX, Konertz W. Initial safety and efficacy results of Acorn's Cardiac Support Device in patients with advanced heart failure. Cardiovascular Surgery 2000;ESCVS Abstracts:11. *(ITEM A-A05)*

Konertz W, Rombeck B, Zytowski M, Hotz H, Sabbah HN, Alferness CA, Kleber FX. Clinical and hemodynamic short term results with passive cardiomyoplasty. J of Heart and Lung Transplantation 2000;19:68. *(ITEM A-A04)*

Konertz W, Rombeck B, Hotz H, Zytowski M, Sonntag S, Kleber FX, Sabbah HN. Short-term safety of the Acorn Cardiac Support Device in patients with advanced heart failure. J Am Coll Cardiol 2000;35(Suppl A):182A. *(ITEM A-A03)*

Kleber FX, Sonntag S, Krebs H, Stantke K, Rombeck B, Konertz W. Influence of the passive Acorn Cardiac Support Device on systolic and diastolic left ventricular function. J Am Coll Cardiol 2000;35(Suppl A):182A. *(ITEM A-A02)*

Rombeck B, Zytowski M, Hotz H, Kleber FX, Konertz W. Cardiomyoplasty with Acorn Cardiac Support Device in patients with Chronic Heart Failure. Poster presentation on October 1-2, 1999 at the Heart Failure Summit V Meeting. *(ITEM A-A01)*

B. Melbourne Safety Study

Raman J, Hata M, Hare DL, Power JM, Jones E, Buxton BF, Alferness CA. Ventricular containment as an adjunct to coronary artery surgery amends the course of heart failure in patients with ischemic cardiomyopathy. Circulation 2000;102(Suppl):II-502. *(ITEM A-B02)*

Raman J, Seevanayagam S, Power JM, Hare D, Buxton BF, Alferness CA. Ventricular containment as an adjunctive procedure in ischemic cardiomyopathy – Results of the Phase I study. The J of Heart Failure 2000;6:121. *(ITEM A-B01)*

C. CorCap™ Randomized Clinical Trial in Europe and Australia

Castel MA, Kotetishvili N, Schomburg R, Lass M. Implantation of a Cardiac Support Device as Adjunct to CABG in Ischemic Cardiomyopathy. ISHLT Annual Meeting; 9-12 April, 2003. *(ITEM A-C01)*

D. Acorn Clinical Trial

Mann DL, et al. Randomized Clinical Assessment of a Cardiac Support Device (CSD) in Advanced Heart Failure Patients Not Requiring Concomitant Valve Surgery. Heart Failure 2005 (Lisbon) June 13, 2005. *(ITEM A-D06)*

Mann D, et al. Results of a Multicenter Randomized Clinical Trial for the Assessment of a Cardiac Support Device in Patients with Heart Failure. J of Heart and Lung Transp. Feb, 2005 :S74 *(ITEM A-D05)*

Acker M, et al. Mitral Valve Surgery in Heart Failure: Results of the Acorn CorCap™ Randomized Trial. AATS Scientific Session April 11, 2005. *(ITEM A-D04)*

Mann D, et al. Results of a Multicenter Randomized Clinical Trial for the Assessment of a Cardiac Support Device in Patients with Heart Failure. ISHLT 2005 Plenary Session April 8, 2005 *(ITEM A-D03)*

Mann D. Clinical Evaluation of the CorCap™ Cardiac Support Device in Patients with Dilated Cardiomyopathy. 2004 AHA Scientific Session Nov. 7, 2004.*(ITEM A-D02)*

Hauptman PJ, Wentworth D, Kubo S. Correlates of Quality of Life in Advanced Heart Failure: Insights from the Acorn Trial. Journal of American College of Cardiology;41(Suppl):212A. *(ITEM A-D01)*

E. Implant Technique

Labrousse L, et al. Implantation of a cardiac support device by the "parachute-like" technique through sternal and trans-abdominal approach. EACTS: Abstract ID: 25254. *(ITEM A-E03)*

Oz MC, Konertz WF, Kleber FX, Mohr FW, Gummert JF, Ostermeyer J, Lass M, Raman J, Acker MA, Smedira N. Global surgical experience with the Acorn Cardiac Support Device. AATS Annual Meeting Program Guide 2002:236. *(ITEM A-E02)*

Dullum MKC, Carlos BD, Oz MC, Chou CD, Bafi AS, Cooke RH, Harrison J, Bither C, Peel GK, Salah Zaki M. Surgical management of heart failure with the Cardiac Support Device: Implantation on the beating heart. Journal of Cardiac Failure 2001;7(Suppl 2): 45. *(ITEM A-E01)*

Pre-clinical Experience

F. Global Cardiac Function/Structure

Walsh RG, Shapland JE, Wojcik LJ. Pre-clinical Histologic Evaluation of a Proprietary Polyester Device for the Treatment of Dilated Cardiomyopathy (Acorn Cardiac Support Device [CSD]): Multiple Species Comparison. Trans Soc Biomaterials 2003;29:701. *(ITEM A-F22)*

Fanous NH, Paone G, Morita H, Suzuki G, Haithcock BE, Sharov VG, Todor A, Brewer R, Sabbah HN. Reverse left ventricular remodeling with the Acorn cardiac support device in dogs with advanced heart failure: A randomized, placebo controlled study. Circulation, Abstract Suppl. 2002:II-550. *(ITEM A-F21)*

Sabbah HN, Suzuki G, Morita H, Chaudhry PA, Mishima T. Chronic therapy with the Acorn Cardiac Support Device in dogs with heart failure affords adequate response to increased demands on the left ventricle. The Journal of Heart and Lung Transplantation;21:153. *(ITEM A-F20)*

Power JM, Raman J, Byrne MJ, Esler M, Kaye D, Alferness C. Passive ventricular constraint significantly lowers left ventricular wall stress in an experimental model of degenerative heart failure and dilated cardiomyopathy. European Heart Journal 2001;22(Suppl): 411. *(ITEM A-F19)*

Sabbah HN, Sharov VG, Chaudhry PA, Suzuki G, Morita H, Todor A. Six months hemodynamic, histologic, and ultrastructural findings in dogs with chronic heart failure treated with the Acorn Cardiac Support Device. European Journal of Heart Failure 2001;3(Suppl 1): S71. *(ITEM A-F18)*

Sabbah HN, Sharov VG, Chaudhry PA, Suzuki G, Todor A, Morita H. Chronic Therapy with the Acorn Cardiac Support Device in dogs with chronic heart failure: Three and six months hemodynamic, histologic and ultrastructural findings. J of Heart and Lung Transplantation 2001;20:189. *(ITEM A-F17)*

Saavedra F, Tunin R, Mishima T, Suzuki G, Chaudhry PA, Anagnostopoulos PV, Paolocci N, Sabbah HN, Kass DA. Reverse remodeling and enhanced adrenergic reserve from a passive external ventricular support in experimental dilated heart failure. Circulation 2000;102(Suppl):II-501. *(ITEM A-F16)*

Power JM, Raman J, Byrne MJ, Alferness CA. Passive ventricular constraint is a trigger for a significant degree of reverse remodeling in an experimental model of degenerative heart failure and dilated cardiomyopathy. Circulation 2000;102(Suppl):II-501. *(ITEM A-F15)*

Sabbah HN, Chaudhry PA, Kleber FX, Konertz W. Passive cardiac support: A surgical approach to the treatment of heart failure. Presented October 13, 2000 at the Mechanical Circulatory Support Meeting. *(ITEM 1-F14)*

Shapland E, Raman J, Byrne M, Power JM, Alferness CA. Passive ventricular constraint is a trigger for a significant degree of reverse remodeling in an experimental model of degenerative heart failure and dilated cardiomyopathy. J of Cardiac Failure 2000;6(suppl 2):32. *(ITEM A-F13)*

Chaudhry PA, Mishima T, Suzuki G, Sharov VG, Anagnostopolos P, Undrovinas AI, Nass O, Alferness CA, Sabbah HN. Acute ventricular reduction with the Acorn Cardiac Support Device prevents progressive left ventricular dysfunction and remodeling in dogs with advanced heart failure. European Heart Journal 2000;21(suppl):534. *(ITEM A-F12)*

Byrne M, Raman J, Power JM, Alferness CA. Passive ventricular constraint; an effective intervention for the treatment of both moderate and severe cardiomyopathy. The J of Heart Failure 2000;6:120. *(ITEM A-F11)*

Power JM, Raman J, Byrne B, Alferness CA. Passive ventricular constraint performed in advanced heart failure prevents mortality in an experimental model of progressive, malignant dilated cardiomyopathy. European J of Heart Failure 2000;2(suppl 2):46. *(ITEM A-F10)*

Power JM, Raman J, Byrne M, Alferness CA. Passive ventricular constraint in advanced heart failure prevents a further decline in cardiovascular function. J Am Coll Cardiol 2000;35(Suppl A):233A. *(ITEM A-F09)*

Byrne M, Raman J, Power JM, Alferness CA. Passive ventricular constraint; an effective intervention for the treatment of both moderate and advanced dilated cardiomyopathy. European Heart Journal 2000;21(suppl):293. *(ITEM A-F08)*

Sabbah HN, Chaudhry PA, Kleber FX, Konertz W. Passive mechanical containment of progressive left ventricular dilation: a surgical approach to the treatment of heart failure. The J of Heart Failure 2000;6:115. *(ITEM A-F07)*

Power JM, Raman J, Burrell LM, Buxton BF, Alferness CA. Passive ventricular constraint in dilated cardiomyopathy does not induce a constrictive cardiovascular pattern. J of Cardiac Failure 1999;5(Suppl 1):32. *(ITEM A-F06)*

Raman J, Power JM, Buxton BF, Alferness CA. Passive ventricular containment in the treatment of experimental dilated cardiomyopathy. Presented May 30, 1999 at the 7th Annual Meeting of the Asian Society for Cardiovascular Surgery. *(ITEM A-F05)*

Chaudhry PA, Paone G, Sharov VG, Mishima T, Hawkins J, Alferness CA, Sabbah HN. Passive ventricular constraint with the Acorn prosthetic jacket prevents progressive left ventricular remodeling and functional mitral regurgitation in dogs with moderate heart failure. AATS 79th Annual Meeting, program page 66, 1999. *(ITEM A-F04)*

Raman J, Power JM, Buxton BF, Alferness CA. Passive ventricular containment in the treatment of experimental dilated cardiomyopathy. J Am Coll Cardiol 1999;33(Suppl A):208A. *(ITEM A-F03)*

Sabbah HN, Chaudhry PA, Paone G, Mishima T, Alferness CA. Passive ventricular constraint with the Acorn prosthetic jacket prevents progressive left ventricular dilation and improves ejection fraction in dogs with moderate heart failure. J Am Coll Cardiol 1999;33(Suppl A):207A. *(ITEM A-F02)*

Power JM, Raman J, Farish SJ, Burrell LM, Tonkin AM, Alferness CA. A novel device for the treatment of rapid pacing induced dilated cardiomyopathy in sheep. J of Cardiac Failure 1998;4(Suppl 1):27. *(ITEM A-F01)*

G. Cellular/Molecular

Rastogi S, Gupta RC, Imai M, Brewer R, Walsh R, Sabbah HN. Chronic Therapy with the *Acorn* Cardiac Support Device normalizes mRNA Gene Expression of Fatty Acid Oxidation Regulatory Enzymes in dogs with heart failure. ISHLT 2006 Annual Meeting, ACC 2006 Annual Meeting. *(ITEM A-G11)*

Rastogi S, Mishra S, Gupta RC, Morita H, Sabbah HN. Chronic Therapy with the Acorn Cardiac Support Device Normalizes Gene Expression of Vascular Endothelial and Basic Fibroblast Growth Factors in Dogs with Heart Failure. ISHLT Annual Meeting; 9-12 April, 2003. *(ITEM A-G10)*

Rastogi S, Gupta RC, Mishra S, Morita H, Sabbah HN. Chronic Therapy with the Acorn Cardiac Support Device Reduces Gene Expression of MMP2 and MMP9 in Dogs with Heart Failure. Journal of American College of Cardiology;41(Suppl):175A. *(ITEM A-G09)*

Rastogi S, Gupta RC, Mishra S, Morita H, Sabbah HN. Long-term therapy with the Acorn cardiac support device normalizes gene expression of -myosin heavy chain in dogs with chronic heart failure. Circulation, Suppl. 2002:II-384. *(ITEM A-G08)*

Rastogi S, Gupta R, Mishra S, Suzuki G, Morita H, Sabbah HN. Therapy with the Acorn Cardiac Support Device reduces mRNA expression of brain and atrial natriuretic peptides in left ventricular myocardium of dogs with heart failure. Journal of American College of Cardiology;39(Suppl A):140A. *(ITEM A-G07)*

Sabbah HN, Gupta RC, Mishra S, Suzuki G, Morita H. Prevention of progressive left ventricular dilation with the Acorn Cardiac Support Device normalizes protein phosphatase activity in dogs with chronic heart failure. Circulation 2001;104 (Suppl II):II-556. *(ITEM A-G06)*

Sabbah HN, Gupta RC, Sharov VG, Todor A, Mishra S, Chaudhry PA, Suzuki G, Morita H. Prevention of progressive LV dilation with the acorn cardiac support device downregulates stretch response proteins and improves sarcoplasmic reticulum calcium cycling in dogs with heart failure. European Heart Journal 2001;22(Suppl): 95. *(ITEM A-G05)*

Gupta RC, Sharov VG, Mishra S, Todor A, Sabbah HN. Chronic therapy with the Acorn Cardiac Support Device (CSD) attenuates cardiomyocyte apoptosis in dogs with heart failure. J Am Coll Cardiol 2001;37(Suppl A):478A. *(ITEM A-G04)*

Sabbah HN, Gupta RC, Sharov VG, Todor A, Mishra S, Chaudhry PA, Suzuki G. Prevention of progressive left ventricular dilation with the Acorn Cardiac Support Device downregulates stretch-response proteins and improves sarcoplasmic reticulum recycling in dogs with chronic heart failure. J Am Coll Cardiol 2001;37(Suppl A):474A. *(ITEM A-G03)*

Sabbah HN, Gupta RC, Sharov VG, Todor A, Mishra S, Chaudhry PA, Nair H. Prevention of progressive left ventricular dilation with the Acorn Cardiac Support Device (CSD) downregulates stretch-mediated p21ras, attenuates myocyte hypertrophy and improves sarcoplasmic reticulum calcium cycling in dogs with heart failure. Circulation 2000;102(Suppl):II-683. *(ITEM A-G02)*

Sabbah HN, Maltsev VA, Chaudhry PA, Mishima T, Undrovinas AI. Contractile function of cardiomyocytes isolated from dogs with heart failure is enhanced after chronic therapy with passive ventricular constraint using the Acorn Cardiac Support Device. Circulation 1999;100(Suppl):439. *(previously ITEM A-G01)*

H. Acute Myocardial Infarction

Pilla JJ, Brockman DJ, Blom AS, Yuan Q, Acker MA. Passive ventricular constraint improves myocardial energetics in a model of heart failure secondary to acute infarction. AATS Annual Meeting Program Guide 2002:76. *(ITEM A-H07)*

Pilla JJ, Brockman DJ, Blom AS, Bowen F, Yuan Q, Gorman JH, Gorman RC, Acker MA. Prevention of dilatation using the Acorn Cardiac Support Device (CSD) results in reversed remodeling and improvement of function. Circulation 2001;104 (Suppl II):II-440. *(ITEM A-H06)*

Pilla JJ, Blom AS, Brockman DJ, Bowen F, Yuan Q, Giammarco J, Gorman JH, Gorman RC, Acker MA. Ventricular constraint using the Acorn Cardiac Support Device (CSD) limits infarct expansion in an ovine model of acute myocardial infarction. Circulation 2001;104(Suppl II):II-480. *(ITEM A-H05)*

Pilla JJ, Brockman DJ, Blom, AS, Bowen F, Gorman, III JH, Gorman RC, Axel L, Acker MA. Placement of the Acorn Cardiac Support Device (CSD) results in left ventricular reversed remodeling and improvement of function in a model of heart failure secondary to acute myocardial infarction. EACTS/ESTS Joint Meeting Abstract Book September 2001:482. *(ITEM A-H04)*

Pilla JJ, Brockman DJ, Blom AS, Yuan Q, Gorman III, JH, Gorman RC, Acker MA. Prevention of dilatation using the Acorn Cardiac Support Device (CSD) results in reversed remodeling and improvement of function in a model of heart failure secondary to myocardial infarction. Journal of Cardiac Failure 2001;7(Suppl 2): 10. *(ITEM A-H03)*

Pilla JJ, Blom AS, Brockman DJ, Bowen FW, Yuan Q, Giammarco J, Gorman III, JH, Gorman RC, Acker MA. Ventricular constraint using the Acorn Cardiac Support Device (CSD) limits infarct expansion in an ovine model of acute myocardial infarction. Journal of Cardiac Failure 2001;7(Suppl 2): 40. *(ITEM A-H02)*

Pilla JJ, Brockman DJ, Blom AS, Yuan Q, Dougherty L, Bowen FW, Giammarco J, Ferrari V, Acker MA. Limiting dilatation results in reversed remodeling and improvement of function in an acute infarct model of heart failure. European Heart Journal 2001;22(Suppl): 679. *(ITEM A-H01)*

Clinical Reports/Summaries

I. Global Experience/Review

Dullum MKC. Update of Restraint Devices for Congestive Heart Failure. TECH-CON 2005 Scientific Session *(ITEM A-I02)*

Sabbah HN, Chaudhry PA, Mishima T, Sharov VG, Maltsev VA, Undrovinas AI, Kleber FX, Konertz W. Passive constraint of the failing ventricle: Impact on ventricular function and remodeling. Proceedings, Cardiomyopathy 2000, page 93. *(ITEM A-I01)*

Meeting:	Scientific Sessions 2003
Session Number:	AOP.81.2a
Session Title:	Device Therapy for End Stage Heart Failure
Presentation Number:	1708
Presentation Title:	Efficacy trends with the Acorn Cardiac Support Device: 3-Year Follow-Up
Author Block:	Wolfgang F Konertz, Steffen Sonntag, Simon Dushe, Holger Hotz, Charite, Berlin, Germany; Franz Kleber; UnfallKrankenhaus, Berlin, Germany
Disclosure Block:	**W**.**F**. **Konertz**, Acorn Cardiovascular, Inc., Clinical Investigator; **S**. **Sonntag**, None; **S**. **Dushe**, None; **H**. **Hotz**, None; **F**. **Kleber**, Acorn Cardiovascular, Inc., Clinical investigator.

Abstract Body:

Background: The Acorn Cardiac Support Device (CSD), a preformed knitted polyester device designed to provide ventricular support, has been shown to reduce wall stress/stretch, limit left ventricular (LV) remodeling, and improve LV function in heart failure (HF) animal models. We previously reported 18-24 month safety and efficacy results for pts in an initial safety study, and now extend these observations to 3 years. **Methods:** Patients (n=29) received the Cardiac Support Device (CSD) with (Group 1; n=17), or without (Group 2; n=12) valve surgery. Most pts. (26/29) had idiopathic cardiomyopathy, and 3 were in NYHA class IV, 15 in class III, and 11 in class II. All pts. were on standard medical treatment, that included beta-blockers and ACE inhibitors for most pts. **Results:** There were no intraoperative complications, and no adverse events or deaths were considered device-related. Sixteen patients were alive at 34-49 months post-implant. Latest follow-up included 8 pts. at 36 months and 4 more pts at 48 months. Although patient numbers were small, improvements in LV end-diastolic dimension (EDD), LV ejection fraction (EF), NYHA class, and quality of life index (Uniscale) were evident at each follow-up. Similar trends were observed for Group 1 and Group 2 pts. Mitral regurgitation (MR) was reduced from 2.5 ± 0.9 to 1.0 ± 1.0 in Group 1 pts. and from 1.4 ± 0.8 to 0.3 ± 0.8 in Group 2 pts. Reductions in MR severity may reflect a change in sphericity index. **Conclusions:** Results indicate that the device is safe, and demonstrated decreases in LVEDD and NYHA class, with increases in LVEF and quality of life index. These beneficial changes were maintained through 36 months follow-up. Randomized clinical trials are in progress to evaluate CSD efficacy in heart failure patients.

	Pre-Implant	6 Months	12 Months	24 Months	36-48 Months
LVEDD(mm)[1]	74.2 ± 6.4 (27)	66.9 ± 10.4 (21)*	66.1 ± 7.2 (18)*	64.4 ± 10.6 (15)*	63.6 ± 11.9 (12)*
LVEF%[1]	21.0 ± 8.8 (29)	29.4 ± 11.9 (22)*	31.4 ± 12.6 (18)*	30.8 ± 13.0 (15)*	31.8 ± 11.3 (12)*
NYHA Class[2]	2.8 ± 0.7 (29)	1.8 ± 0.7 (22)*	1.6 ± 0.7 (18)*	1.6 ± 0.8 (15)*	1.5 ± 0.7 (12)*
Uniscale[2]	4.0 ± 2.4 (27)	6.4 ± 2.4 (19)*	6.7 ± 2.3 (13)*	6.0 ± 2.2 (11)*	6.3 ± 3.5 (8)*
Mean ± (s.d.), *p≤0.05, [1]t-test, [2]Wilcoxon signed-rank test					

Powered by

OASIS

The Online Abstract Submission and Invitation System

Services by

CTT

Coe-Truman Technologies, Inc.

283

Effects of Passive Cardiac Containment on Left Ventricular Structure and Function: Verification by Volume and Flow Measurements

Alexander Lembcke, MD,[a] Till H. Wiese, MD,[a] Simon Dushe, MD,[b]
Holger Hotz, MD,[b] Christian N. H. Enzweiler, MD,[a] Bernd Hamm, MD,[a]
and Wolfgang F. Konertz, MD, PhD[b]

Background: The cardiac support device (CSD, Acorn) is a compliant, textile-mesh graft placed around the ventricles to prevent further dilatation and to improve function in congestive heart failure. The aim of this study was to verify post-operative changes in left ventricular volumes, ejection fraction, blood flow, and myocardial mass.

Methods: Fourteen patients underwent contrast-enhanced, electrocardiography-triggered electron-beam computerized tomography before and 6 to 9 months after CSD implantation. We measured volume and flow using the slice-summation method and the indicator-dilution technique.

Results: We found significant changes for the following parameters: end-diastolic volume decreased from 382.9 ± 140.2 ml to 311.3 ± 138.7 ml, end-systolic volume from 310.4 ± 132.4 ml to 237.4 ± 133.8 ml, end-diastolic diameter from 75.3 ± 7.8 mm to 70.7 ± 11.6 mm, end-systolic diameter from 65.8 ± 7.8 mm to 60.0 ± 14.0 mm, and myocardial mass from 298.6 ± 79.6 g to 263.1 ± 76.8 g. Ejection fraction increased from 20.3% ± 6.4% to 27.8% ± 13.1%. We found no significant differences for stroke volume (from 72.5 ± 24.6 ml to 73.8 ± 23.6 ml), heart rate (from 80.5 ± 11.0 beats per minute to 76.5 ± 6.8 beats per minute), and total cardiac output (from 5.8 ± 1.9 liter/min to 5.6 ± 1.8 liter/min). Mitral regurgitation fraction decreased from 30.5% ± 15.5% to 15.6% ± 12.8%, increasing antegrade cardiac output from 3.8 ± 0.9 liter/min to 4.7±1.5 liter/min. For most parameters, pre- and post-operative values in these patients differed significantly from those in an age- and gender-matched control group. In each patient, we observed a small hyperdense stripe along the pericardium after surgery, but we observed no local complications.

Conclusion: Three-dimensional structural and functional data obtained by computerized tomography volume and flow measurements confirm the safety and efficacy of CSD implantation. J Heart Lung Transplant 2004;23:11–19.

11

Congestive heart failure, based on ischemic or primary dilated cardiomyopathy and characterized by left ventricular dilatation, wall motion abnormality, and decreased ejection fraction, remains one of the most common diseases and has poor long-term clinical outcome. Between 1990 and 1999, patients with heart failure in the Framingham Study cohort had 1-year and 5-year, age-adjusted mortality rates of 24% to 28% and 45% to 59%, respectively.[1] In the Hillingdon Heart Failure Study, individuals with poorer functional status (New York Heart Association [NYHA] Classes III–IV) had a 1-year mortality rate of 38%.[2]

Several clinical trials report the positive effects of drug treatment (primarily angiotensin-converting enzyme inhibitors, possibly combined with beta blockers or spironolactone) on survival in patients in Classes III to IV.[3] Although heart transplantation is the treatment of choice in patients with refractory, advanced cardiac failure, it is limited by the shortage of donor organs, decreased long-term survival because of rejection risks, graft vasculopathy, non-specific graft failure, infection, malignancy, and the high cost of transplantation.[4,5] The surgical treatment options available as alternatives to transplantation (artificial hearts, mechanical cardiac assist devices, dynamic and adynamic cardiomyoplasty, partial left ventriculectomy) continue to be controversial. A new technique, implantation of a cardiac support device (CSD; Acorn Cardiovascular, St. Paul, MN) recently has been added to the range of surgical options. In this new procedure, a compliant polyester-mesh device is implanted around the ventricles to limit cardiac dilatation and thus to improve cardiac function. Currently, the method is undergoing evaluation in a worldwide, randomized, prospective clinical trial.[6] Preliminary results suggest that the technique can be performed safely and has a tendency to improve clinical and hemodynamic parameters.[6–8] Nevertheless, available data remain insufficient for a definitive assessment of this procedure.

The aim of the current study is to supplement initial echocardiographic and angiocardiographic data already published about CSD implantation with precise volumetric measurements obtained using computerized tomography (CT) for comparison. In addition, we present new information pertaining to the behavior of the myocardial mass and individual hemodynamic parameters.

METHODS

The cardiac support device was implanted in 30 patients with advanced congestive heart failure. Among them, a series of 14 consecutive male patients (aged 35–71 years; mean, 56.7 ± 9.9 years; median, 61.0 years) underwent electron-beam CT before and after CSD implantation. These patients form the population for this report. We evaluated patients 1 to 2 weeks before surgery and 6 to 9 months after surgery.

Patients enrolled in the study had NYHA Class III disease or had history of at least 1 Class III episode. All patients were receiving stable drug therapy at the time of surgery (all 14 patients received angiotensin-converting enzyme inhibitors, diuretics, and digoxin; 10 patients received additional beta blockers, and 8 patients also received other cardiac medication) and had no additional systemic disease (no pulmonary, renal, or hepatic dysfunction). Estimated survival of <1 year was an exclusion criterion for surgery.

The surgical procedure was performed as previously described:[6–8] After median sternotomy and opening the pericardium, we measured the diameter and length of the heart to select a CSD of proper size. We placed the appropriate CSD over the ventricles and attached it close to the atrioventricular groove while the heart was beating on cardiopulmonary bypass. With the ventricles fully loaded, the anterior part of the CSD was fitted, trimmed to size, and secured, with the aim of producing a short-term decrease of up to 10% in end-diastolic dimension, based on transesophageal echocardiographic measurements.

In 7 patients, implantation of the CSD was the only surgical procedure, and the other 7 patients underwent concomitant mitral valve repair.

Because CT examination of healthy volunteers is precluded, a control group consisting of 22 retrospectively selected male patients of the same age (aged 46–72 years; mean, 58.8 ± 7.5 years; median, 58.5 years) served for comparison. These control patients had undergone evaluation of left ventricular morphology and function for various established clinical indications but were found retrospectively to have no abnormalities based on echocardiography and electron-beam CT. No patient in the control group had a history of myocardial infarction or of congestive or valvular heart disease. Fourteen of the 22 control patients had mild systemic hypertension controlled with drug treatment.

All patients in the study gave written, informed consent after absolute or relative contraindications to electron-beam CT had been excluded. All patients receiving the CSDs participated in a clinical

feasibility and safety study that the institutional review board had approved previously.

For data acquisition, we followed an established, standardized protocol using an electron-beam CT scanner (Evolution C-150 XP, software version 12.4/GE Imatron, South San Francisco, CA) in the multi-slice mode at 625 mA and 130 kV with an acquisition time of 50 msec, a slice thickness of 8 mm, and a matrix of 256×256.

Patients underwent scanning in the supine position in a section orientation along the approximated short heart axis (table tilt was 17°, table slew was 25°).

For flow measurements, we administered 15 ml contrast medium (iodine content 370 mg/ml; Ultravist, Schering, Berlin, Germany) at a flow of 4 ml/sec, followed by electrocardiography-triggered acquisition of 15 scans in 2 slices each (so-called flow protocol) in the ascending aorta at the level of the pulmonary bifurcation. Using the system's standard software, we calculated time-density curves (Hounsfield units per unit time), the time of maximal contrast medium concentration (transit time), and antegrade cardiac output according to the indicator dilution method.[9,10]

We injected another 90 ml contrast medium at a flow of 3 ml/sec for the subsequent functional study, consisting of acquiring 156 scans at the time of maximum contrast-medium concentration. These electrocardiography-triggered scans were performed in 12 slices each with 13 scans per cardiac cycle (so-called cine protocol) during a single breath-hold period in maximal expiration.

We performed post-processing in the implemented evaluation mode by manually drawing the epicardial and endocardial contours during end-diastole and end-systole on the reconstructed images. The implemented software then calculated ventricular volumes and myocardial mass by multiplying the areas with the slice thickness followed by addition of all slices (slice-summation method) taking into account the 4-mm gaps between adjacent pairs of sections by interpolation (modified Simpson rule). Figures 1 A and B show how the functional electron-beam CT studies were analyzed.

Furthermore, we estimated the mitral regurgitation fraction based on the difference between total and antegrade cardiac output. We also measured the maximal end-diastolic and end-systolic cross-sectional diameters (parallel to the mitral valve) of the left ventricle in a basal section.

Finally, we visually assessed wall motion of all myocardial segments using the workstation in the cine mode, we evaluated for potential areas of decreased opacification or wall thinning, and we inspected for the presence of intracardiac thrombus and pericardial effusion or pericardial adhesion.

Statistical Analysis

We compared the pre- and post-operative values of the patient group using Student's 2-tailed t-test for paired samples. In addition, we compared separately the pre- and post-operative values for the controls using Student's 2-tailed t-test for independent samples. All statistical calculations were performed using a commercially available software package (SPSS version 9.0.1, SPSS; Chicago, IL). The results were given as mean ± standard deviation. Significance was assumed at $p < 0.05$.

RESULTS

None of the 30 patients who received the CSDs had intra-operative complications, and we observed no device-related adverse events after surgery. Three patients died of non-CSD–related causes within 9 months of surgery, and 1 patient required an additional left ventricular assist device. No patient underwent transplantation.

The 14 patients included in the current study recovered smoothly from surgery, were released from the hospital, and showed improved functional status from NYHA Class 2.8 ± 0.6 before surgery to NYHA Class 1.6 ± 0.6 after surgery. Electron-beam CT examinations of all patients yielded adequate data for volumetric and flow measurements. Despite markedly prolonged transit times of the contrast medium, because of severely decreased cardiac function in some cases, we observed good opacification of the left ventricle, whose endocardial and epicardial borders were visible and could be drawn manually in all patients. Despite arrhythmia and occasional ventricular pre-mature beats in several patients without pacemakers, we observed no mistriggering during functional study in any of these patients.

The results presented in Table I show that most left ventricular parameters (both the absolute values and the values indexed for body surface area) differ significantly between the patients and the age- and gender-matched controls. At baseline, patients had considerably greater end-diastolic volume (382.9 ± 140.2 ml vs 132.0 ± 20.2 ml, $p < 0.05$) and end-systolic volume (310.4 ± 132.4 ml vs 50.6 ± 13.2 ml, $p < 0.05$), decreased ejection fraction (20.3% ± 6.4% vs 62.4% ± 6.6%, $p < 0.05$), and decreased antegrade cardiac output (3.8 ± 0.9 liter/min vs 5.1
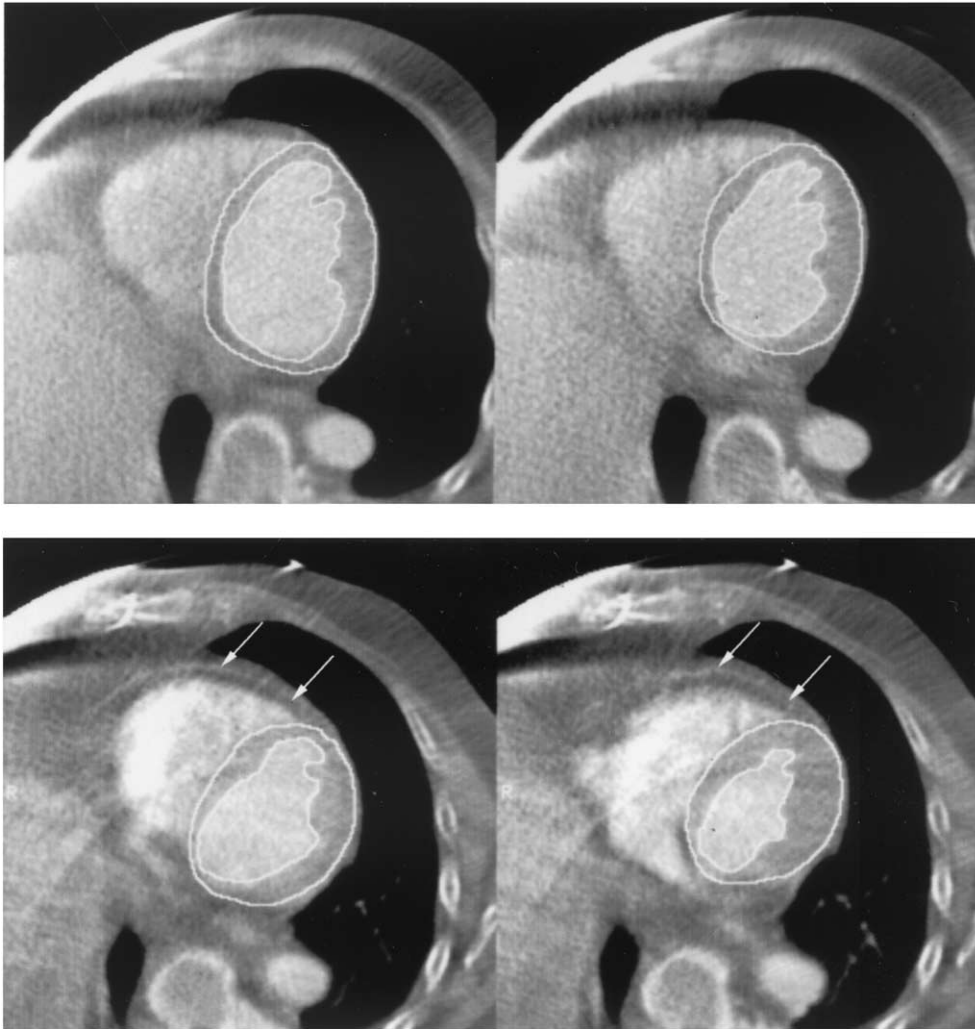
FIGURE 1 A 56-year-old patient with dilated cardiomyopathy. Status before and after implantation of the cardiac support device: section at the same mid-ventricular level along the approximated short heart axis with the manually drawn endocardial and epicardial contours during end-diastole (left) and end-systole (right). Cine protocol: acquisition time, 50 msec; slice thickness, 8 mm; matrix, 256 × 256; FOV 21 cm; contrast agent dose, 90 ml; flow, 3 ml/sec. (A) Two weeks before surgery: EDD = 61 mm, ESD = 50 mm, EDV = 210 ml, SV = 66 ml; EF = 31%, MM = 166 g. (B) Nine months after surgery: EDD = 48 mm, ESD = 30 mm, EDV = 188 ml; ESV = 59 ml, SV = 59 ml, EF = 50%, MM = 148 g. Note the hyperdense stripe along the pericardium after implantation of the cardiac support device (arrows). EDD, end-diastolic diameter; EDV, end-diastolic volume; EF, ejection fraction; ESD, end-systolic diameter; ESV, end-systolic volume; FOV, field of view; MM, myocardial mass; SV, stroke volume.

± 1.5 liter/min, $p < 0.05$) compared with the controls.

The CSD significantly altered morphologic and functional parameters of the left ventricle by decreasing chamber size, improving ejection fraction, and increasing antegrade cardiac output. In detail, the end-diastolic diameter decreased from 75.3 ± 7.8 mm before surgery to 70.7 ± 11.6 mm after surgery, the end-diastolic diameter decreased from 65.8 ± 7.8 mm to 60.0 ± 14.0 mm, the end-diastolic volume decreased from 382.9 ± 140.2 ml to 311.3 ± 138.7 ml, and the end-systolic volume decreased from 310.4 ± 132.4 ml to 237.4 ± 133.8 ml (each with $p < 0.05$). The total stoke volume remained

TABLE I   Left ventricular parameters (mean $\pm$ SD) in 14 male patients before and 6 to 9 months after CSD implantation compared with 22 age- and gender-matched controls

Parameter	Patients pre-operative	Patients post-operative	Control group
EDV (ml)	$382.9 \pm 140.2^{\dagger}$	$311.3 \pm 138.7^{*\dagger}$	132.0 ± 20.2
EDVI (ml/m^2)	$183.1 \pm 65.7^{\dagger}$	$149.3 \pm 66.0^{*\dagger}$	70.6 ± 20.5
ESV (ml)	$310.4 \pm 132.4^{\dagger}$	$237.4 \pm 133.8^{*\dagger}$	50.6 ± 13.2
ESVI (ml/m^2)	$152.1 \pm 60.2^{\dagger}$	$113.9 \pm 63.7^{*\dagger}$	25.8 ± 7.0
SV (ml)	72.5 ± 24.6	73.8 ± 23.6	81.6 ± 16.9
SVI (ml/ml^2)	34.6 ± 11.1	35.2 ± 10.6	35.1 ± 12.7
EF (%)	$20.3 \pm 6.4^{\dagger}$	$27.8 \pm 13.1^{*\dagger}$	62.4 ± 6.6
HR (beats/min)	$80.5 \pm 11.0^{\dagger}$	$76.5 \pm 6.8^{\dagger}$	65.1 ± 13.1
CO (liter/min)	5.8 ± 1.9	5.6 ± 1.8	5.3 ± 1.4
CI (liter/min/m^2)	2.8 ± 0.9	2.7 ± 0.8	2.7 ± 0.7
aCO (liter/min)	$3.8 \pm 0.9^{\dagger}$	$4.7 \pm 1.5^{*}$	5.1 ± 1.5
aCI (liter/min/m^2)	$1.8 \pm 0.4^{\dagger}$	$2.2 \pm 0.6^{*}$	2.6 ± 0.7
CO-aCO (liter/min)	$1.9 \pm 1.4^{\dagger}$	$0.9 \pm 1.0^{*\dagger}$	0.2 ± 0.4
MRF (%)	$30.5 \pm 15.5^{\dagger}$	$15.6 \pm 12.8^{*\dagger}$	2.5 ± 4.6
EDD (mm)	$75.3 \pm 7.8^{\dagger}$	$70.7 \pm 11.6^{*\dagger}$	53.0 ± 3.9
EDDI (mm/m^2)	$36.1 \pm 3.8^{\dagger}$	$33.8 \pm 5.6^{*\dagger}$	27.0 ± 2.7
ESD (mm)	$65.8 \pm 7.8^{\dagger}$	$60.0 \pm 14.0^{*\dagger}$	33.9 ± 3.2
ESDI (mm/m^2)	$31.6 \pm 3.8^{\dagger}$	$29.2 \pm 7.2^{*\dagger}$	17.3 ± 1.8
MM (g)	$298.6 \pm 79.6^{\dagger}$	$263.1 \pm 76.8^{*\dagger}$	166.4 ± 28.5
MMI (g/m^2)	$142.3 \pm 37.2^{\dagger}$	$130.2 \pm 29.6^{*\dagger}$	84.6 ± 14.2

Difference statistically significant ($p < 0.05$) between *post-operative against pre-operative values and †between patients versus controls. aCI, antegrade cardiac index measured in the aorta; aCO, antegrade cardiac output measured in the aorta; CI, (total) cardiac index; CO (total) cardiac output; CO-aCO, difference between total and antegrade cardiac output (yielded the mitral regurgitation volume); EDD, end-diastolic diameter; EDV, end-diastolic volume; EF, ejection fraction; ESD, end-systolic diameter, ESV, end-systolic volume; HR, heart rate; MRF, estimated mitral regurgitation fraction; MM, myocardial mass; SV, (total) stroke volume; I, index related to M^2 body surface area.

nearly constant (72.5 ± 24.6 ml vs 73.8 ± 23.6 ml, $p > 0.05$), and we found a corresponding increase in the left ventricular ejection fraction from $20.3\% \pm 6.4\%$ before surgery to $27.8\% \pm 13.1\%$ after surgery ($p < 0.05$). Although, we saw no significant change in total cardiac output (5.8 ± 1.9 liter/min vs 5.6 ± 1.8 liter/min, $p > 0.05$), we found that antegrade cardiac output increased from 3.8 ± 0.9 liter/min before surgery to 4.7 ± 1.5 liter/min after surgery, resulting in decreased calculated mitral regurgitation volume from 1.9 ± 1.4 liter/min to 0.9 ± 1.0 liter/min as well as decreased estimated mitral regurgitation fraction from $30.5\% \pm 15.5\%$ to $15.6\% \pm 12.8\%$ (each with $p < 0.05$). We saw almost no change in heart rate (from 80.5 ± 11.0/min to 76.5 ± 6.8/min, $p > 0.05$).

Furthermore, the left ventricular myocardial mass decreased slightly but significantly by approximately 10%, from 298.6 ± 79.6 g before surgery to 263.1 ± 76.8 g after surgery ($p < 0.05$).

Although, we noted a tendency toward normalization of morphologic and functional parameters after CSD implantation in the patient group, comparison with the age- and gender-matched control group showed that the significant differences existing between patients and controls in end-diastolic volume index (EDVI), end-systolic volume index (ESVI), end-diastolic diameter index (EDDI), end-systolic diameter index (ESDI), ejection fraction, mitral regurgitation fraction, heart rate, myocardial mass, and myocardial mass index (MMI) persisted after surgery. In contrast, post-operative antegrade cardiac output (4.7 ± 1.5 vs 5.1 ± 1.5 liter/min, $p > 0.05$) and cardiac index (2.2 ± 0.6 vs 2.6 ± 0.7, $p > 0.05$) did not differ significantly between patients and controls.

To eliminate the effects of concomitant mitral valve repair as a potential confounding variable, Table II presents separately the sub-population of patients who underwent CSD implantation as the only surgical procedure (without mitral valve repair). The results from this sub-population confirm that CSD implantation alone significantly altered left ventricular size and myocardial mass as well as left ventricular function in a similar way as described above for the total patient population.

TABLE II   Left ventricular parameters (mean $\pm$ SD) in 7 male patients before and 6 to 9 months after CSD implantation without additional surgical procedure (no concomitant mitral valve repair)

Parameter	Patients pre-operative	Patients post-operative
EDV (ml)	281.8 $\pm$ 89.2	217.1 $\pm$ 112.6*
ESV (ml)	216.7 $\pm$ 83.4	148.3 $\pm$ 103.7*
SV (ml)	63.1 $\pm$ 9.3	68.9 $\pm$ 15.2
EF (%)	23.6 $\pm$ 4.9	35.7 $\pm$ 12.4*
HR (beats/min)	77.9 $\pm$ 11.9	73.4 $\pm$ 5.2
CO (liter/min)	4.9 $\pm$ 1.0	5.1 $\pm$ 1.3
aCO (liter/min)	3.9 $\pm$ 0.9	4.5 $\pm$ 1.3*
CO-aCO (liter/min)	1.0 $\pm$ 0.7	0.6 $\pm$ 0.6*
MRF (%)	19.6 $\pm$ 9.5	11.3 $\pm$ 10.5*
EDD (mm)	70.4 $\pm$ 5.8	63.4 $\pm$ 10.3*
ESD (mm)	60.9 $\pm$ 7.3	52.7 $\pm$ 14.9*
MM (g)	276.4 $\pm$ 56.4	243.7 $\pm$ 51.5*

*Difference statistically significant ($p < 0.05$) between post-operative against pre-operative values. aCO, antegrade cardiac output measured in the aorta; CO (total) cardiac output; CO-aCO, difference between total and antegrade cardiac output (yielded the mitral regurgitation volume); EDD, end-diastolic diameter; EDV, end-diastolic volume; EF, ejection fraction; ESD, end-systolic diameter; ESV, end-systolic volume; HR, heart rate; MRF, estimated mitral regurgitation fraction; MM, myocardial mass; SV, (total) stroke volume.

Nevertheless, in the patients who received only the CSDs, dilatation of the left ventricle and impairment of left ventricular ejection fraction were less pronounced before and after surgery when compared with the patients who underwent CSD implantation with concomitant mitral valve repair. Additionally, patients who received only the CSDs showed a more distinct increase in left ventricular ejection fraction after device implantation (Tables II and III).

After surgery, we observed a small hyperdense stripe along the ventricular pericardium in each patient (Figure 1B). Apart from this pericardial stripe and the pleuromediastinal adhesions typically observed in patients who have undergone median sternotomy, none of the patients showed excessive cardiac scar formation or major, potentially harmful, pericardial adhesions.

Moreover, electron-beam CT demonstrated no local post-operative complications such as pericardial effusion or intracardiac thrombus in any of the patients.

Before surgery, all 14 patients had global hypokinesia of the left ventricular myocardia. Six patients additionally had regional akinesia of the anterior, anteroseptal, or septal ventricular wall. Hypokinetic myocardial segments showed a tendency toward improved contractility after CSD implantation, whereas akinetic segments remained unchanged. We observed no new akinetic or dyskinetic myocardial segments after CSD implantation. Nor did follow-up demonstrate any new areas of decreased opacification, wall thinning, or bulging secondary to disturbed myocardial perfusion.

DISCUSSION

Progressive ventricular dilatation and dysfunction characterize myocardial remodeling in chronic heart failure. All forms of treatment aim at slowing down or preventing this process. The CSD, representing an adaptation of dynamic cardiomyoplasty, has been undergoing clinical testing for approximately 2 years. In this new procedure, a compliant polyester-mesh device is implanted around the heart (Acorn CSD), instead of using an actively stimulated muscle flap. Preliminary early results achieved with the CSD have been published primarily by a small number of study groups investigating this procedure in a Phase I clinical trial.[6–8] These study groups reported that the cardiac support device effectively improves clinical, morphologic, and functional parameters. Initial results show decreased internal left ventricular diameters in association with increased left ventricular ejection fraction.

Imaging Methods and Comparison With Previous Studies

In most studies, echocardiography is the method of first choice for post-implant monitoring because of its wide availability, easy use, and non-invasiveness. However, measurements obtained with this method, in particular with regard to determining ventricular volumes and ejection fraction, may be distorted by the limited accessibility of some patients for ultra-

sound and the fact that the examination crucially relies on the examiner's training and experience. Left ventriculography is occasionally used as an (invasive) alternative, but volumetric measurement by this method is likewise prone to errors because measuring is performed in only 2 planes. This procedure is based on the assumption that the shape of the ventricle corresponds to an ideal ellipsoid, which is rarely the case in patients with abnormal or post-operative changes in heart configuration. The conductance catheter technique is an important clinical tool that allows measurement of pressure-volume loops. However, the accuracy of this method may be limited by electric field homogeneity and parallel conductance, especially at larger volumes. In contrast, sectional imaging modalities, such as electron-beam CT using the so-called slice-summation method, are relatively precise in determining left ventricular volumes and myocardial mass and are characterized by low intra- and inter-observer variation.[11–13] Although currently, magnetic resonance imaging is the accepted gold standard,[14–15] its use in peri-operative monitoring of the patients examined here is limited: In 6 patients from our group, implanted pacemakers were a contraindication for magnetic resonance imaging. In addition, with magnetic resonance imaging, the longer duration in the flat supine position and the repeated breath-hold periods not only are stressful for patients with advanced heart failure and increased dyspnea, but also may cause considerably impaired image quality.

However, because of the close correlation between the results of magnetic resonance imaging and electron-beam CT, despite slight differences in absolute measuring values,[16] the latter is used as an alternative reference procedure to evaluate cardiac function after surgery. Because of their greater precision and detailed anatomic information, the results obtained with electron-beam CT are preferred to echocardiographic measures.[17]

The results obtained by electron-beam CT presented here confirm preliminary positive trends observed after CSD implantation in terms of decreased end-diastolic and end-systolic diameters and increased ejection fraction (Table I). However, the usual measurement of internal diameters alone provides an inadequate description of ventricle size and 3-dimensional ventricular geometry.

This holds true especially in evaluating patients who have undergone cardiac surgery, which may considerably alter ventricular geometry in terms of size and shape. For this reason, changes in volume may not necessarily correlate with proportional changes in diameter and vice versa. Before this report, data reliably reflecting the true extent of such volumetric changes after cardiac support device therapy were lacking.

The presented results confirm earlier animal experiments that demonstrated beneficial effects of the CSD on hemodynamic parameters in experimentally induced dilated cardiomyopathy.[18,19]

Mechanism of Passive Cardiac Containment

The major mechanism on which implantation of a compliant mesh device around the ventricles is based is the so-called girdling effect, which goes back to experience gained with dynamic cardiomyoplasty. Long-term follow-up studies have demonstrated that the patients undergoing dynamic cardiomyoplasty do not seem to benefit from active muscle stimulation, but that passive stabilization alone is responsible for the beneficial therapeutic effect.[20–22] In addition to constraining ventricular dilatation, the girdling effect also is assumed to decrease myocardial wall tension and myocyte overextension, resulting in a decreased myocardial oxygen requirement with a persisting left shift in the pressure-volume relationship. With these effects, ceasing or even reversing cardiac remodeling may be achieved, a therapeutic effect of cardiomyoplasty also known as reverse remodeling.[6]

Alterations in Left Ventricular Muscle Mass

These effects also may underlie the slight but significant decrease in left ventricular muscle mass after implantation of the CSD that we observed in the current study (Tables I, II, and III). Inadequate examination procedures may have prevented making this observation in earlier follow-up studies; we know of no publication that reports such a finding after CSD implantation. The muscle-mass decrease may be a direct result of the decreased ventricular wall tension produced by the CSD implant or may be the result of an indirect effect of the observed decrease in ventricular volume. In our opinion, this observation is consistent with a true reverse-remodeling process, and not just an acute volume decrease that may occur at the time of the CSD implantation. Similar effects have been found in patients receiving effective drug treatment for chronic heart failure[23,24] and in patients after valve replacement and repair for aortic or mitral regurgitation who have not only decreased ventricular blood volume but also regression of ventricular muscle mass as a result of reverse remodeling process.[25,26] Nevertheless, the

TABLE III   Left ventricular parameters (mean $\pm$ SD) in 7 male patients before and 6 to 9 months after CSD implantation and concomitant mitral valve repair

Parameter	Patients pre-operative	Patients post-operative
EDV (ml)	484.0 $\pm$ 104.0	405.4 $\pm$ 91.1*
ESV (ml)	402.1 $\pm$ 106.8	326.6 $\pm$ 97.5*
SV (ml)	81.9 $\pm$ 31.9	78.9 $\pm$ 30.3
EF (%)	17.0 $\pm$ 6.3	19.9 $\pm$ 8.7
HR (beats/min)	77.9 $\pm$ 11.9	73.4 $\pm$ 5.2
CO (liter/min)	6.6 $\pm$ 2.2	6.2 $\pm$ 2.1
aCO (liter/min)	3.8 $\pm$ 1.1	4.9 $\pm$ 1.8*
CO-aCO (liter/min)	2.8 $\pm$ 1.4	1.3 $\pm$ 1.2*
MRF (%)	40.9 $\pm$ 12.8	19.8 $\pm$ 14.2*
EDD (mm)	80.1 $\pm$ 6.7	78.0 $\pm$ 7.9
ESD (mm)	70.9 $\pm$ 4.5	61.4 $\pm$ 19.6
MM (g)	320.7 $\pm$ 97.0	282.6 $\pm$ 96.1[†]

*Difference statistically significant ($p < 0.05$) between post-operative against pre-operative values. aCO, antegrade cardiac output measured in the aorta; CO (total) cardiac output; CO-aCO, difference between total and antegrade cardiac output (yielded the mitral regurgitation volume); EDD, end-diastolic diameter; EDV, end-diastolic volume; EF, ejection fraction; ESD, end-systolic diameter; ESV, end-systolic volume; HR, heart rate; MRF, estimated mitral regurgitation fraction; MM, myocardial mass; SV, (total) stroke volume.

decreased myocardial muscle mass after implantation of the CSD that we observed must be confirmed by additional data.

Severity of Mitral Valve Insufficiency

Furthermore, the fact that total cardiac output differed significantly from antegrade cardiac output remains to be explained; this discrepancy was much more pronounced before than after surgery. In this study, our patients with dilated heart disease typically had accompanying (relative) mitral insufficiency, resulting in decreased antegrade cardiac output compared with total cardiac output. Hence, the extent of the difference between total and antegrade cardiac output is an indirect measure of the degree of mitral insufficiency, unless additional aortic valve insufficiency or intracardiac shunting is present.[9] Thus, the fact that total cardiac output did not change after CSD implantation, whereas antegrade stroke volume tended to increase, is obviously because of decreased mitral regurgitation volume. This supports results reported by other authors[6] who demonstrated post-operative improvement in the degree of mitral insufficiency using color-coded Doppler echocardiography.

Occurrence of Local Complications

Maintaining myocardial perfusion is a potential concern associated with CSD implantation. Although we did not directly measure perfusion in the current study, none of the patients showed any indirect signs of perfusion disturbance or loss. Compared with the pre-operative findings, we saw neither newly occurring areas of decreased opacification nor areas of circumscribed myocardial thinning, nor did we see progression of disturbed myocardial motion at post-operative follow-up. Other complications such as pericardial effusion, major pericardial adhesions, scar formations, and intracardiac thrombus likewise were absent. After surgery, we observed a small hyperdense stripe along the ventricular pericardium in each patient. This was probably the CSD itself or a result of harmless local tissue densification directly around the CSD.

Study Limitations

Although the diagnostic potential of the electron-beam CT has been discussed in detail, some general limitations of the study warrant consideration in drawing conclusions about CSD efficacy. First, this study included a relatively small, select group of patients enrolled as part of an initial non-randomized clinical safety and feasibility study. Second, as part of a pilot study, this investigation lacked a concurrent control group of patients with congestive heart failure who were treated conservatively. Finally, many of the patients received concomitant mitral valve repair, which may have been a confounding variable in interpreting the data of the total patient population. However, the sub-population of patients who received CSDs only (Table II) also showed decreased left ventricular dimensions and even superior improvement in left ventricular function. (Table III)

In summary, electron-beam CT with its well-established measuring precision supplements other diagnostic procedures by providing important additional information about the morphology, 3-dimensional geometry, and function of the left ventricle; about myocardial mass; and about hemodynamic parameters before and after CSD implantation. The results of electron-beam CT presented here corroborate first reports in the literature on the safety as well as the short- and mid-term efficacy of this new surgical procedure. However, long-term results are needed for definitively assessing the benefits of the CSD.

REFERENCES

1. Levy D, Kenchaiah S, Larson MG, et al. Long-term trends in the incidence of and survival in heart failure. N Engl J Med 2002;347:1397–402.
2. Cowie MR, Wood DA, Coats AJS, et al. Survival of patients with new diagnosis of heart failure: a population based study. Heart 2000;83:505–10.
3. Cleland JGF. Improving patient outcomes in heart failure: evidence and barriers. Heart 2000;84(suppl I):I8–10.
4. Hosenpud JD, Bennett LE, Keck BM, Fiol B, Boucek MM, Novick RJ. The Registry of the International Society for Heart and Lung Transplantation: eighteenth official report—2001. J Heart Lung Transplant 2001;20:805–15.
5. Cope JT, Kaza AK, Reade CC, et al. A cost comparison of heart transplantation versus alternative operations for cardiomyopathy. Ann Thorac Surg 2001;72:1298–305.
6. Konertz WF, Shapland JE, Hotz H, et al. Passive containment and reverse Remodeling by a novel textil cardiac support device. Circulation 2001;104(suppl I):I270–5.
7. Raman JS, Power J, Buxton BF, Alferness C, Hare D. Ventricular containment as an adjunctive procedure in ischemic cardiomyopathy: early results. Ann Thorac Surg 2000; 70:1124–6.
8. Oz MC. Passive ventricular constraint for the treatment of congestive heart failure. Ann Thorac Surg 2001;71:S185–7.
9. Kaminaga T, Naito H, Takamiya M, Nishimura T. Quantitative evaluation of mitral regurgitation with ultrafast CT. J Comput Assist Tomogr 1994;18:239–42.
10. Wolfkiel CJ, Ferguson JL, Chomka EV, Law WR, Brundage BH. Determination of cardiac output by ultrafast computed tomography. Am J Physiol Imaging 1986;1:117–123.
11. Pietras RJ, Wolfkiel CJ, Veselik K, Roig E, Chomka EK, Brundage BH. Validation of ultrafast computed tomographic left ventricular volume measurements. Invest Radiol 1991;26: 28–34.
12. Reiter SJ, Rumberger JA, Feiring AJ, Stanford W, Marcus ML. Precision of measurements of right and left ventricular volume by cine computed tomography. Circulation 1986;74: 890–900.
13. Schmermund A, Rensing BJ, Sheedy PF, Rumberger JA. Reproducibility of right and left ventricular measurements by electron-beam CT in patients with congestive heart failure. Int J Card Imaging 1998;14:201–9.
14. Dulce MC, Mostbeck GH, Friese KK, Caputo GR, Higgins CB. Quantification of the left ventricular volumes and function with cine MR imaging: comparison of geometric models with three-dimensional data. Radiology 1993;188:371–6.
15. Sakuma H, Fujita N, Foo TK, et al. Evaluation of left ventricular volume and mass with breath-hold cine MR imaging. Radiology 1993;188:377–80.
16. Kivelitz DE, Enzweiler CNH, Wiese TH, et al. Determination of left ventricular function parameters and myocardial mass: comparison of MRI and EBT. Fortschr Röntgenstr 2000;172:244–50.
17. Konertz W, Hotz H, Khoynezhad A, Zytowski M, Baumann G. Results after partial left ventriculectomy in a European heart failure population. J Card Surg 1999;14:129–35.
18. Chaudhry PA, Mishima T, Sharov VG, et al. Passive epicardial containment prevents ventricular remodeling in heart failure. Ann Thorac Surg 2000;70:1275–80.
19. Chaudhry PA, Anagnostopouls PV, Mishima T, et al. Acute ventricular reduction with the Acorn cardiac support device: effects on left ventricular dysfunction and dilatation in dogs with chronic heart failure. J Card Surg 2001;16:118–26.
20. Mott BD, Oh JH, Misawa Y, et al. Mechanisms of cardiomyoplasty: comparative effects of adynamic versus dynamic cardiomyoplasty. Ann Thorac Surg 1998;65:1039–44.
21. Kass DA, Baughman KL, Pak PH, et al. Reverse remodeling from cardiomyoplasty in human heart failure. Circulation 1995;91:2314–8.
22. Oh JH, Badhwar V, Mott BD, Li CM, Chiu RC. The effects of prosthetic cardiac binding and adynamic cardiomyoplasty in a model of dilated cardiomyopathy. J Thorac Cardiovasc Surg 1998;116:148–53.
23. Groenning BA, Nilsson JC, Sondergaard L, Fritz-Hansen T, Larsson HB, Hildebrandt PR. Antiremodeling effects on the left ventricle during beta-blockade with metoprolol in the treatment of chronic heart failure. J Am Coll Cardiol 2000; 36:2072–80.
24. Khattar RS, Senior R, Soman P, van der Does R, Lahiri A. Regression of left ventricular remodeling in chronic heart failure: comparative and combined effects of captopril and carvedilol. Am Heart J 2001;142:704–13.
25. Legarra JJ, Concha M, Casares J, Merino C, Munoz I, Alados P. Left ventricular remodeling after pulmonary autograft of the aortic valve (Ross operation). J Heart Valve Dis 2001;10:43–8.
26. Badhwar V, Bolling SF. Mitral valve surgery in the patient with left ventricular dysfunction. Semin Thorac Cardiovasc Surg 2002;14:133–6.

Ventricular Constraint Using the Acorn Cardiac Support Device Reduces Myocardial Akinetic Area in an Ovine Model of Acute Infarction

James J. Pilla, PhD; Aaron S. Blom, BA; Daniel J. Brockman, BVSc; Frank Bowen, MD;
Qing Yuan, PhD; Joseph Giammarco, PhD; Victor A. Ferrari, MD; Joseph H. Gorman, III, MD;
Robert C. Gorman, MD; Michael A. Acker, MD

Background—Left ventricular remodeling secondary to acute myocardial infarction (AMI) is characterized by ventricular dilatation and regional akinesis. In this study, we investigated the effect of passive constraint on akinetic area development.

Methods and Results—The effect of passive constraint on akinetic area was investigated in 10 sheep using tissue-tagging magnetic resonance imaging (MRI). A baseline MRI study was followed by the creation of an anterior infarct. After 1 week, the animals received a second MRI study. A cardiac support device (CSD) was then placed over the epicardium in 5 sheep whereas the remaining animals served as controls. A terminal study was performed at the 2-month postinfarct in both groups. The akinetic area at 1-week postinfarct was similar in both groups. At the terminal time-point, the akinetic area in the control group was similar to the 1-week time-point whereas in the CSD group, the area of akinesis decreased ($P=0.001$). A comparison of the 2 groups at the terminal time-point demonstrates a significantly diminished area of akinesis in the CSD group ($P=0.004$). The relative area of akinesis followed a similar pattern. End-systolic and end-diastolic wall thickness was significantly greater in the CSD group at terminal ($P=0.001$). In addition, the minimum wall thickness was greater in the CSD group compared with the controls ($P=0.04$).

Conclusions—Passive constraint reduced akinetic area development secondary to AMI. The attenuation of regional wall stress may prevent the incorporation of the border zone into the infarct, decreasing infarct size and providing a promising new therapy for patients after an AMI. (*Circulation.* 2002;106[suppl I]:I-207-I-211.)

Key Words: ventricles ■ remodeling ■ myocardial infarction ■ magnetic resonance imaging

Acute myocardial infarction can be a stimulus for left ventricular remodeling, which is characterized by dilatation and global and regional functional impairment with an increased risk of heart failure.[1-5] Although the left ventricle undergoes significant architectural and functional changes, such as loss of functional cardiac units, myocyte hypertrophy, and interstitial cellular fibrosis[6] because of myocardial loss by infarction, the mechanisms underlying this remodeling process are not completely understood. Additionally, the degree of left ventricular enlargement has been identified as being associated with an unfavorable clinical outcome.[7]

The increase in ventricular volume after myocardial infarction (MI) is fueled by an increase in wall stress, which increases the workload of the left ventricle. Subsequently, the heart enters into a positive feedback loop of dilatation and further exaggeration of wall stress, which leads, ultimately, to progressive global and regional dysfunction and end-stage heart failure. Studies using pharmacological therapy such as β-blockers and angiotensin-converting enzyme inhibitors to reduce the loading conditions of the heart post-MI have demonstrated a significant improvement in cardiovascular mortality by curbing the detrimental effects of ventricular remodeling.[8-10] Until recently, medical therapy, as described above, was the mainstay of treatments for patients suffering from the debilitating effects of heart failure. However, the latest advancements in the surgical treatment of heart failure have shown promise in improving cardiac function and promoting reverse remodeling in these patients. Additionally, recent studies using a mesh patch placed directly over the infarct itself have been shown to preserve ventricular geometry and function.[11]

The loss of myocytes after an MI leads to the thinning and elongation of the infarct region and has been described as infarct expansion.[12] Expansion of the infarct occurs early after the event, resulting in an increase in wall stress that promotes the global process of ventricular dilatation. Subsequent ventricular remodeling as well as heart failure and death can be correlated to the extent of infarct expansion.[13]

© 2002 American Heart Association, Inc.

Circulation is available at http://www.circulationaha.org   DOI: 10.1161/01.cir.0000032871.25213.0e

In this study, we investigated an alternative method of reducing wall stress by mechanically limiting progressive myocardial dilatation after an infarct using a bidirectional woven polyester jacket (Acorn Cardiac Support Device [CSD], Acorn Cardiovascular, Inc, St. Paul, MN) with the hypothesis that placement of the CSD postinfarction leads to a decrease in border zone involvement and a decreasing akinetic/thinned area surrounding the ischemic area. Magnetic resonance imaging (MRI) with tissue tagging was used to investigate the effects of passive ventricular constraint in an ovine model of acute MI.

Materials and Methods

All animals used in this study received care in compliance with the "Guide for Care and Use of Laboratory Animals" published by the National Institutes of Health (NIH publication 86 to 23, revised 1985), and the investigation was approved by the Institutional Animal Care and Use Committee.

Study Design

The effect of passive constraint on akinetic area was investigated in 10 Dorset sheep by using MRI with SPAtial Modulation of Magnetization (SPAMM)[14] tissue tagging. The experimental protocol for this study consisted of performing a baseline MRI study followed by the creation of a transmural anterior wall MI, which was accomplished via a left thoracotomy and ligating the coronary arteries supplying the anterior wall. After a 1-week recovery period, the animals received a second MRI study and were randomized to 1 of 2 groups, CSD retention or control. The custom polyester CSD was then placed over the ventricular epicardium in 5 sheep via the same thoracotomy used for infarct creation. All animals received no further medical or surgical intervention for the duration of the study. Additional tissue-tagged MRI studies were performed at the 2-month postinfarct time point in both the control and CSD groups.

Anesthesia

One hour before surgery, the animals were premedicated with 1 mg/kg acepromazine and 0.001 mg/kg glycopyrrolate. General anesthesia was induced with ketamine (10 mg/kg) and diazepam (0.5 mg/kg). Endotracheal intubation was performed, and the anesthesia was maintained with a mixture of isoflurane 1% to 2% in oxygen delivered by a time-cycled ventilator with a tidal volume of 20 mL/kg. Anesthesia was continuously adjusted and monitored to maintain a constant physiological state in the animals. General anesthesia was used for all the surgical procedures and for the duration of the MRI studies.

Animal Model

The anterior infarct model used in this study was originally characterized by Dr. L.H. Edmunds and his group at the University of Pennsylvania. This infarct model was chosen because it results in a significant increase in end-diastolic volume with a concomitant deterioration of function at 8 weeks postinfarct without the development on an apical aneurysm as seen with ligation of the left anterior descending.[15] Moreover, mitral valve regurgitation is not created in this model at 8 weeks.[15]

The infarct was created by exposing the heart via a left thoracotomy through the fifth interspace with a partial fifth rib resection. On opening the pericardium, the coronary anatomy was inspected to determine the vessels that were to be ligated. The criterion for ligation was any diagonal and/or obtuse margin vessel that supplied the anterior portion of the myocardium, excluding the left anterior descending. Before ligation, the animals were prophylaxed with a bolus of lidocaine and started on infusions of lidocaine and epinephrine. Systolic blood pressure was maintained at 80 mm Hg throughout the procedure using successive boluses of phenylephrine. The vessels were then ligated with 3-0 prolene. The chest remained open for an additional 45 minutes while the animal's vital signs and ECG
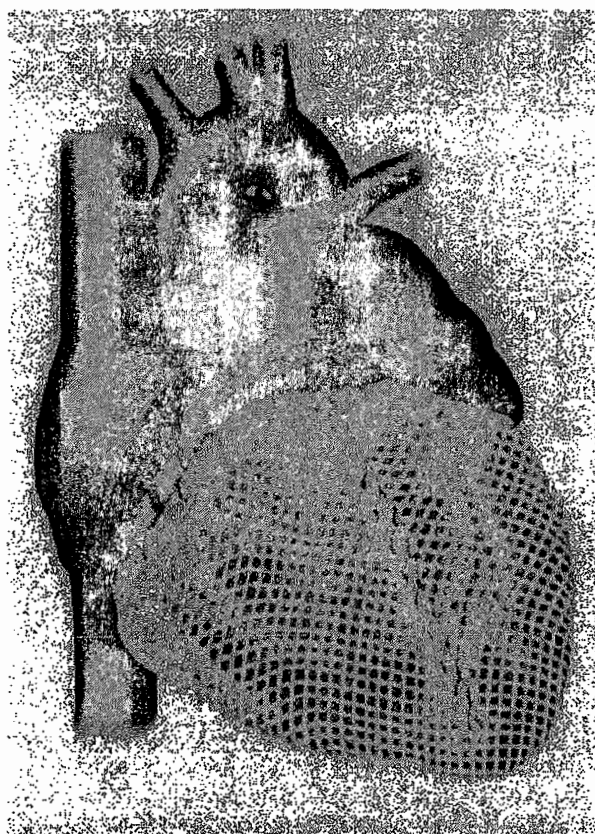

Figure 1. Representative diagram showing placement of the CSD over the ventricular epicardium. The CSD is secured at the base of the heart with interrupted sutures and sized to fit the circumference of the heart with a continuous suture in-line with the long axis of the heart.

were continuously monitored to ensure the animal was stable. After this period, the pericardium in the 5 animals randomized to the CSD group was closed to minimize adhesions to the myocardium whereas the pericardium in the remaining animals was left open. The incision was closed in layers, and a chest tube was placed to drain the chest and evacuate the pneumothorax (the chest tube was removed once the animal became ambulatory). The animal's vital signs and ECG were closely monitored for the initial 24-hour postoperative period before being sent back to the colony.

CSD Placement

One week post-infarct, the CSD was placed on 5 animals. The device is manufactured from a custom-designed bidirectional polyester weave that posses the material properties of being more compliant in the longitudinal direction then in the circumferential thus limiting circumferential dilatation but allowing longitudinal lengthening. The original thoracotomy was reopened and extended dorsally to allow resection of the remainder of the fifth rib. The pericardium was reopened to allow placement of the CSD, which was accomplished by sliding the device over the epicardium, up to the level of the atrioventricular junction. Prolene sutures (4-0) were placed along the base of heart starting on the posterior surface and working around anteriorly, with total of between 8 and 10 sutures depending on the size of the heart. The excess material was gathered up along a line parallel with the long axis of the heart and excised. The ends were resewn to ensure a snug final fit, which entailed having the CSD in contact with the epicardium but exerting little or no tension (Figure 1). The thoracotomy was closed as before, and a chest tube was placed to evacuate the pneomothorax (and again removed when the
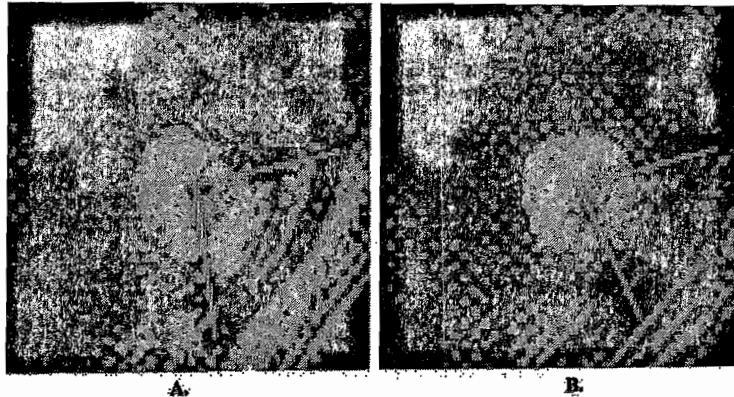
Figure 2. Representative short axis mid-systolic SPAMM tagged images (A, control; B, CSD, right) of the left ventricle at the terminal time point. Notice the increased wall thickness, smaller dysfunctional area, and preservation of normal geometry in the CSD heart as compared with the control.

animal became ambulatory). The animals received the same postoperative recovery measures as they did after the creation of the infarct.

MRI

At baseline, 1 week, and 2 months postinfarct, all animals underwent imaging in a 1.5T whole body high-speed clinical MR system (GE Medical Systems, Milwaukee, WI). Before imaging, the animals were placed under general anesthesia (as described above) and a left ventricular Millar catheter was inserted by means of a carotid artery cut-down. All images were cardiac and respiratory gated to ensure consistent spatial positioning of the heart during each acquisition. Tissue-tagged images in the short axis plane were acquired for this study.

Noninvasive tagging of cardiac tissue in MRI can be achieved by perturbing the local magnetization using SPAMM to create MRI-visible tags within the heart wall. As these tags move with the underlying heart wall, the motion of the tags during the cardiac cycle reveals the internal motion of the otherwise featureless heart wall resulting in a measure of regional strain.

The imaging parameters were as follows: field of view, 22 cm; TR/TE, 8.8/2.2 ms; slice thickness, 6 mm; interslice gap, 0; tag spacing, 5 mm; 2 signal averages; and 6 to 8 k-space lines acquired per cardiac frame (depending on heart rate). Images were acquired in the short axis plane using 2 surface coils (12.7 cm each) placed on the left and right chest. The images were archived and stored for off-line analysis.

Data Analysis

An experienced observer in a blinded fashion performed all MRI image analysis. The short axis-tagged images were analyzed using a custom cardiac MRI analysis program, SPAMMVU.[16] Left ventricular endocardial and epicardial contours were automatically delineated, and tag tracking was performed using an automated algorithm based on recently declassified military software adapted for cardiac MRI analysis.[17] The akinetic area was measured as the portion of myocardium in the infarct zone that exhibited no strain change at end-systole or had thinned sufficiently enough to result in no visible tags. The area of akinesis was then determined by projecting 2 lines from the borders of the infarct to the centroid of the short axis plane. The angle of the intersection of these 2 lines was used to calculate the arc of the akinetic area. Knowing the length of this arc and multiplying by the slice thickness provided a precise measure of the area of akinesis. This procedure was performed for the entire short axis set of images and the measurements from each plane were summed to produce absolute akinetic area. Relative akinetic area was calculated by normalizing the absolute akinetic area by the end-systolic epicardial surface area.

Average end-systolic and end-diastolic wall thickness values were determined from the MRI. In the CSD group, wall-thickness measurements were the sum of myocardial wall thickness and CSD thickness because the MRI pulse sequence used could not differentiate between the two. Wall thickness was determined by fitting the end-diastolic and end-systolic endocardial and epicardial contours to a circle and calculating the difference between the radii of the 2 circles. Minimum wall thickness was ascertained by measuring the length of a line perpendicular to the epicardial and endocardial contours in the infarct zone.

Quantitative results were analyzed using a *t* test to determine significance between time points and groups.

Results

Nineteen sheep initially were in enrolled the study. Eleven of the animals completed the study, of which 6 were controls. Fifty-five percent of the animals that failed to complete the study died within 24 hours postinfarct, and 1 animal died after the baseline study before infarction. After randomization, 1 sheep in each of the 2 groups did not complete the study. The CSD sheep expired during the 2-month pressure-volume analysis (PVA) study because of undetermined causes whereas the control animal died before the 2-month time-point because of a bowel obstruction. A control animal was not included in the final statistical analysis because there was no left ventricular dilatation at 2 months postinfarct.

Representative SPAMM-tagged images of the left ventricle at mid-systole are shown in Figure 2. These images from the 2-month postinfarct study show both control and CSD animals. Note the diminished area of akinesis, as well as the increased wall thickness, in the CSD versus the control animal.

The measured akinetic area (Figure 3) at 1-week postinfarct was similar in both groups (*P*=NS). At the terminal time-point, the akinetic area in the control group was similar to the 1-week time-point (*P*=NS) whereas in the CSD group, the area of akinesis decreased (*P*=0.001). A comparison of the 2 groups at the terminal time point demonstrates a significantly diminished area of akinesis in the CSD group (*P*=0.004).

The relative area of akinesis (Figure 4) followed a similar pattern as that of the absolute area. At 1-week postinfarct, the values for both groups were comparable (*P*=NS). The relative area of the control group at the terminal time-point remained similar to the 1-week point (*P*=NS) whereas in the CSD group, the relative area of akinesis decreased (*P*=0.001). A comparison of the 2 groups at the terminal time point demonstrates a significantly diminished relative akinetic area in the CSD group (*P*=0.013).

Measurements of myocardial wall thickness demonstrate that the CSD group experienced a reduced amount of wall thinning compared with the controls. End-systolic wall thickness measured at the terminal time point was significantly greater in the CSD group compared with the controls (*P*=0.001; Table 1). End-diastolic wall thickness demonstrated similar results with the CSD group having a thicker myocardium (*P*=0.001).
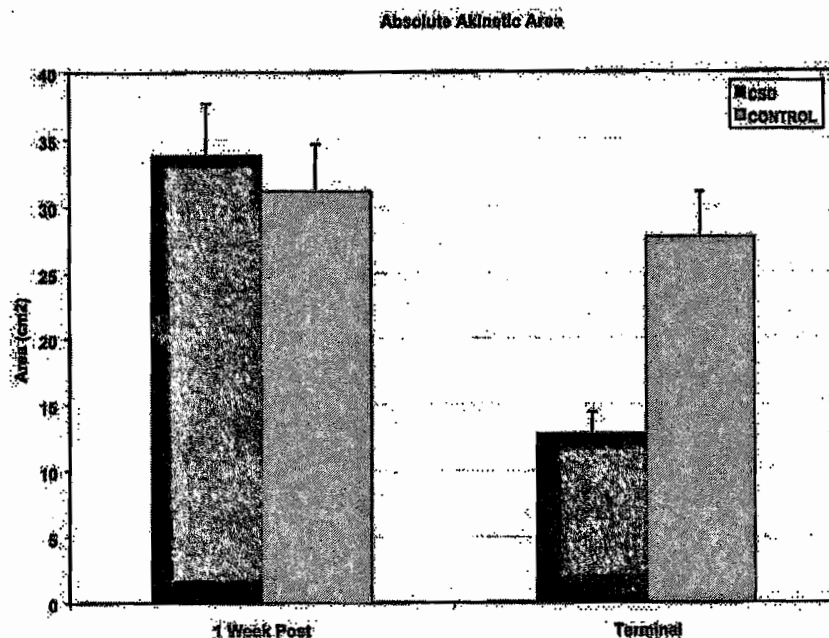
Absolute Akinetic Area

Figure 3. Bar graph indicating the measured area of akinesis at 1 week and 2 months postinfarct for both groups. The measured area of dysfunction at 1 week postinfarct was similar in both groups (*P*=NS). At the terminal time-point, the dysfunctional area in the control group was similar to the 1-week time-point (*P*=NS) whereas in the CSD group, the area of dysfunction decreased (*P*=0.001; *t* test). A comparison of the 2 groups at the terminal time point, however, demonstrates a significantly diminished area of dysfunction in the CSD group (*P*=0.004; *t* test).

1). In addition, the minimum wall thickness was greater in the CSD group compared with the controls (control: 0.277±0.26 versus CSD: 0.50±0.34; *P*=0.04).

Discussion

The results of this study indicate that ventricular constraint using the Acorn CSD attenuates infarct development in an ovine model of acute MI. This is predicated on the assumption that an infarct is defined by thinned and/or akinetic myocardium. In addition, this device diminished end-systolic and end-diastolic myocardial wall thinning, which for the CSD group is the sum of myocardial wall thickness and CSD thickness.

An interesting finding is that the akinetic area and relative akinetic area for the controls did not change from 1 week to terminal whereas in the CSD group, the akinetic area, which was similar to controls at 1-week postinfarct, decreased over the same period. In addition, the results for the control group are consistent with the findings of Gorman et al[15] using the identical ovine model of acute MI. They reported a relative infarct size measured by echocardiogram and postmortem examination at 8 weeks of 23.9%, which is consistent with the measurement we obtained by MRI at the same time point (25%±3%).

The similar akinetic area seen in both groups at 1-week postinfarct could be due to myocardial stunning in the border zone, which is frequently observed early after MI. This stunning in the border myocardium immediately after coronary occlusion has been attributed to differences in local wall stress distribution on the basis of mathematical models of the acutely infarcted left ventricle.[18] In-
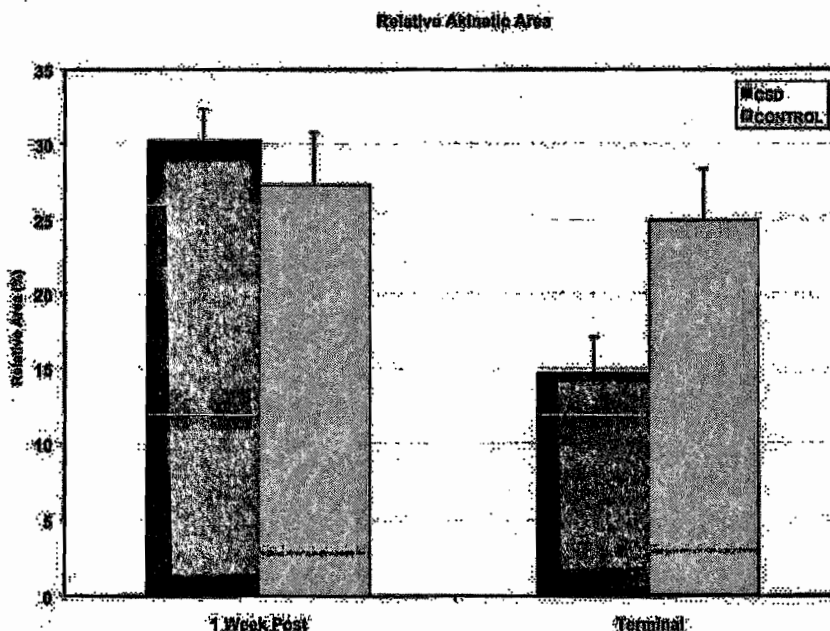
Relative Akinetic Area

Figure 4. Bar graph indicating the relative area of akinesis between the control and CSD groups. At 1 week postinfarct, the values for both groups were comparable (*P*=NS). The relative area of the control group at the terminal time-point remains similar to the 1-week point (*P*=NS), whereas in the CSD group, the relative area of dysfunction decreases (*P*=0.001; *t* test). A comparison of the 2 groups at the terminal time point demonstrates a significantly diminished relative area of dysfunction in the CSD group (*P*=0.013; *t* test).

296

Myocardial Wall Thickness

	Control	CSD	P Value
End-systolic wall thickness	.932±.0029	1.205±.047	0.001
End-diastolic wall thickness	.908±.026	1.140±.039	0.001

creased regional wall stress is due to the reduced end-systolic wall thickness[19] and increased ventricular radius. If left untreated, the increased regional wall stresses favors permanent dysfunction of the border zone and progressive wall thinning.[20] This results in the adjacent akinetic myocardium being pulled into the infarct.

It is hypothesized that placement of the CSD inhibits migration of the akinetic border zone into the infarct by decreasing regional myocardial wall stress. This is accomplished by stabilizing ventricular radius and increasing end-diastolic wall thickness. This results in a reduction of stress in the border zone that leads to improved contractility in this region. It is therefore postulated that the CSD decreases infarct size by halting the migration of the border zone into the infarct. Furthermore, it is postulated that stunned myocardium recovers rather then progressing toward permanent dysfunction.

Passive containment has also been used in an animal model of ischemic-dilated cardiomyopathy.[21] Heart failure was created by microembolization, which results in global dysfunction and an increase in global wall stress, in contrast to the infarct model, which results in acute regional changes. These results demonstrated significantly smaller left ventricular volumes and improvement in cardiac function for CSD-treated animals compared with the controls. In addition, they reported a decrease in stretch proteins and improved Ca^{2+} cycling. The mechanism of action of the CSD is the same as in the acute infarct studies by decreasing wall stress (global or regional); progressive remodeling can be halted and reverse remodeling can occur.

The first Acorn CSD was placed in humans in Germany in 1999. Since that time, nearly 100 patients with dilated cardiomyopathies have had the CSD placed. So far, it has been shown to be safe. In the few patients followed for over 2 years there have been no reports of constriction developing or other major device-related complications. Although many patients have demonstrated significant improvement efficacy has yet to be demonstrated. There is an on-going prospectively randomized multi-institutional study, in both the US and Europe, to study the effectiveness of the CSD inpatients with heart failure and dilated hearts

There are some limitations to this study that deserve consideration. The pericardium on the CSD sheep was closed immediately postinfarct to facilitate CSD placement the following week. This can potentially effect infarct development in the first week between the 2 groups. The results, however, show that at 1-week postinfarct there is no statistical difference in absolute or relative akinetic area between the 2 groups, indicating that closing the pericardium had no observable effect. Another limitation is the lack of a sham operation at 1 week on the control animals. The effect of a sham operation, if anything, would be a negative 1 on the control group.

Additionally, MRI visible markers were not placed on the epicardium at the time of the infarct creation to delineate the baseline infarct zone. As such, we could not serially track infarct zone expansion over the course of the experiment. This would be beneficial in determining the degree of initial infarct zone expansion versus the degree of border zone pulled into the infarct area. Finally, neither pathological studies nor myocardial blood flow (perfusion) studies were performed on the hearts for infarct size determination. Correlation between the pathology, perfusion, and MRI data would be beneficial.

In conclusion, ventricular constraint using the CSD reduced infarct development secondary to acute MI. The reduction in infarct expansion by attenuation in regional wall stress would also predict a modification of the global process of ventricular remodeling. Further studies on the effect of the CSD on the process of ventricular remodeling both on a global and cellular level need to be conducted.

References

1. Eaton LW, Weiss JL, Bulkley Eaton BH, et al. Regional cardiac dilation after acute myocardial infarction. *N Engl J Med.* 1979;300:57–62.
2. Pfeffer MA, Braunwald E. Ventricular remodeling after myocardial infarction: experimental observations and clinical implications. *Circulation.* 1990;81:1161–1172.
3. McKay RG, Pfeffer MA, Pasternak RC, et al. Left ventricular remodeling after myocardial infarction: a corollary to infarct expansion. *Circulation.* 1986;74:693–702.
4. Meizlisch JL, Berger HJ, Plankey M, et al. Functional left ventricular aneurysm formation after acute anterior transmural myocardial infarction: incidence, natural history and prognostic implications. *N Engl J Med.* 1984;311:1001–1006.
5. Kim C, Braunwald E. Potential benefits of late reperfusion of infarcted myocardium: the open artery hypothesis. *Circulation.* 1993;88:2426–2436.
6. Sabbah HN, Goldstein S. Ventricular remodeling: consequences and therapy. *Eur Heart J.* 1993;14:24–29.
7. McKee PA, Castelli WP, McNamara PM, et al. The natural history of congestive heart failure: the Framington study. *N Eng J Med.* 1971;385:1441–1446.
8. Sabbah HN, Shimoyama H, Kono T, et al. Effects of long-term monotherapy with enalapril, metoprolol, and digoxin on the progression of left ventricular dysfunction and dilatation in dogs with reduced ejection fraction. *Circulation.* 1994;84:2852–2859.
9. Pfeffer MA, Launas GA, Vaughan DE, et al. Effect of captopril on progressive ventricular dilatation after anterior myocardial infarction. *N Eng J Med.* 1988;319:80–86.
10. Waagstein F, Caidahl K, Wallentin 1 et al. A. Long-term β-blockade in dilated cardiomyopathy: effect of short- and long-term metoprolol treatment followed by withdrawal and readministration of metoprolol. *Circulation.* 1989;80:551–563.
11. Kelley ST, Malekan RD, Gorman JH III, et al. Restraining infarct expansion preserves left ventricular geometry and function after acute anteroapical infarction. *Circulation.* 1999;1:135–142.
12. Erlebacher JA, Weiss JL, Eaton LW, et al. Late effects of acute infarct dilation on heart size: a two-dimensional echocardiographic study. *Am J Cardiol.* 1982;49:1120–1126.
13. St John Sutton MG. *Left Ventricular Remodeling After Acute Myocardial Infarction.* London: Science Press Limited, 1996.
14. Axel L, Dougherty L. MRI of motion with spatial modulation of magnetization. *Radiology.* 1989;171:841–845.
15. Gorman JH, Gorman RC, Plappert T, et al. Infarct size and location determine development of mitral regurgitation in the sheep model. *J Thorac Cardiovascrg Surg.* 1998;115:615–622.
16. Axel L, Bloomgarden DC, Chang CN, et al. Spammvu: a program for the analysis of dynamic tagged MRI. *Proc Int Soc Magn Reson Med.* 1993;2:724.
17. Dougherty L, Asmuth JC, Blom AS, et al. Validation of an optical flow method for tag displacement estimation. *IEEE Trans Med Imaging.* 1999;18:359–363.
18. Bogen DK, Rabinowitz SA, Needleman A, et al. An analysis of the mechanical disadvantage of myocardial infarction in the canine left ventricle. *Circ Res.* 1980;47:728–741.
19. Heyndrickx GR, Amano J, Patrick TA, et al. Effects of coronary artery reperfusion on regional myocardial blood flow and function in conscious baboons. *Circulation.* 1985;71:1029–1037.
20. Connelly CM, McLaughlin RJ, Vogel WM, et al. Reversible and irreversible elongation of ischemic infarcted and healed myocardium in response to increases in preload and afterload. *Circulation.* 1991;84:387–399.
21. Chaudhry PA, Mishima T, Sharov VG, et al. Passive epicardial containment prevents ventricular remodeling in heart failure. *Ann Thorac Surg.* 2000;70:1275–1280.

297

ELSEVIER

Passive ventricular constraint amends the course of heart failure: a study in an ovine model of dilated cardiomyopathy

J.M. Power[a,*], J. Raman[b], A. Dornom[a], S.J. Farish[c], L.M. Burrell[a], A.M. Tonkin[a], B. Buxton[b], C.A. Alferness[d]

[a]*Department of Medicine, University of Melbourne (Austin and Repatriation Medical Centre Campus), Melbourne, Australia*
[b]*Department of Cardiothoracic Surgery, University of Melbourne (Austin and Repatriation Medical Centre Campus), Melbourne, Australia*
[c]*Department of Public Health and Community Medicine, University of Melbourne (Parkville Campus), Melbourne, Australia*
[d]*Acorn Cardiovascular Inc., St. Paul, MN, USA*

Abstract

Objective: Dilated cardiomyopathy (DCM) is associated with a progressive deterioration in cardiac function. We hypothesised that some of the deleterious effects of DCM could be reduced by mechanically limiting the degree of cardiac dilatation. **Methods:** A Transonic 20A cardiac output (CO) flow-probe was implanted in the pulmonary artery of 12 adult (52 ± 4 kg) sheep. Early heart failure was created by rapid right ventricular (RV) pacing for 21 days at a rate which resulted in an initial 10% decrease in CO (to a maximum of 190 bpm). A custom polyester jacket (Acorn Cardiovascular, St Paul, MN) was then placed, via a partial lower sternotomy, on the ventricular epicardium of all sheep. Animals were randomised either to jacket retention (wrap) or removal (sham). Pacing was recommenced at a higher rate (that initiated a further 10% decrease in CO) for 28 days. Haemodynamic and echocardiographic parameters were determined at baseline, implant and at termination. **Results:** At termination, the left ventricular fractional shortening was significantly higher ($p=0.03$), the degree of mitral valve regurgitation lower (scaled 0–3) ($p=0.03$) and the left ventricular long axis area smaller ($p=0.02$) in the wrap animals compared with sham. **Conclusions:** In this model of heart failure, ventricular constraint with a polyester jacket diminished the deterioration in cardiac function associated with progressive dilated cardiomyopathy. These results suggest that maintainance of a more normal cardiac size and shape may be beneficial in patients with dilated cardiomyopathy. © 1999 Elsevier Science B.V. All rights reserved.

Keywords: Heart failure; Cardiomyopathy; Ventricular function; Remodelling

This article is referred to in the Editorial by S. Goldstein (pages 468–469) in this issue.

1. Introduction

Despite advances in pharmacological therapy, heart failure (HF) remains an unresolved problem in a large patient population. It has been suggested that preventing further ventricular dilatation may impede the progressive deterioration in cardiac function associated with heart failure [1]. Initial interest in this hypothesis emanated from investigations of the mechanisms of the apparent improvement in functional status observed in HF patients who have undergone dynamic cardiomyoplasty [2]. Some results have assigned a dominant role for this outcome to the augmentation of the contractile function of the heart by the paced muscle wrap [3,4], while others have suggested that it is the constraining effect of the wrap on the dilating ventricles that is important [5,6]. The latter hypothesis has been examined in several studies in animal models of heart failure and all have found, in varying degrees and formats, that passive ventricular constraint alone improves outcome in comparison to control [1,7,8]. In one, using a canine

---

*Corresponding author. Tel.: +61-3-9496-4090; fax: +61-3-9496-4099.

E-mail address: jmp@austin.unimelb.edu.au (J.M. Power)

Time for primary review 26 days.

298

model of rapid pacing induced heart failure, a functionally static cardiomyoplasty wrap procedure performed on failed hearts prevented the further remodelling that would normally be expected with continued rapid pacing [1]. This finding complemented other studies in which cardiomyoplasty was performed prospectively in normal hearts, later paced into failure. In the other two studies the heart was wrapped prior to induction of heart failure [7,8].

If indeed passive ventricular constraint can significantly slow or stabilise the usual remodelling process associated with HF, then a synthetic wrap will considerably simplify the procedure in comparison with the major surgical procedure of cardiomyoplasty. Two recent studies have looked at this proposal. In both, the ventricles of normal animal hearts were bound with synthetic membranes and heart failure was induced. In one study, failure was induced by rapid pacing [8] and in the other, by intracoronary artery doxorubicin [7]. In both studies, passive ventricular constraint prevented most of the subsequent ventricular dilatation and preserved much of the left ventricular function compared with nonwrapped animals.

The purpose of this study was to examine the concept of passive ventricular constraint as a treatment for HF in animals that were already in HF at the time of implantation.

We utilised an ovine model of tachycardia-induced progressive heart failure and a purpose designed biocompatible fabric jacket and compared cardiovascular function and structural remodelling in sham operated animals with animals that had undergone a wrap procedure.

2. Methods

The protocol for this study was approved by the Animal Ethics Committee of the Austin Hospital under the guidelines published by the National Health and Medical Research Council of Australia and conforms with the *Guide for the Care and Use of Laboratory Animals* published by the US National Institutes of Health (NIH Publication No. 85-23, revised 1996).

2.1. Initial surgical preparation

Twelve adult merino sheep (mean weight 52 ± 4 kg) were anaesthetised with propofol 2 mg/kg and ventilated with halothane and oxygen. A single 3-cm incision was made in a left intercostal space and a Transonic (Transonic Systems, Ithaca, NY) 20A cardiac output flow-probe was positioned around the pulmonary artery. Permanent indwelling polyethylene catheters were implanted in a carotid artery and a jugular vein. The flow-probe leads and catheters were tunnelled subcutaneously to the dorsum of the animals. A steroid-tipped bipolar ventricular pacing lead (Capsure® SP, Model 4024, Medtronic, MN) was placed transvenously in the apex of the right ventricle. The

proximal lead end was connected to a modified 'data block', which allowed the right ventricle to be paced from wires exiting at the animals dorsum with modified external pacemakers (Medtronic model 5880A).

Antibiotics (1 g ampicillin and 80 mg gentamicin sulphate, both i.v.) were given prophylactically immediately after surgery and for 3 days following. Flunixin meglumine, 50 mg i.m., was given prior to surgery and post-operatively once daily for two days as an analgesic and anti-inflammatory agent.

2.2. Data collection

2.2.1. Echocardiography

Images of the left ventricle (LV) and the left atria (LA) were obtained by right-sided trans-thoracic echocardiography under intravenous anaesthesia (propofol 0.1 mg/kg/min+ketamine 0.2 mg/kg/min) using a 3-MHz probe and a Sonos 1000 unit (Hewlett-Packard). The planimetered LA and LV cross-sectional areas were obtained from a uniform long axis view in diastole and were calculated automatically from a scrolled endocardial outline. Left ventricular fractional shortening was determined in M mode from a short axis view of the LV just below the insertion of the papillary muscles. The degree of mitral valve regurgitation was assessed by colour Doppler and scored, (0–3), in degrees of increasing severity. The images were measured independently by two experienced observers and the mean determined.

2.2.2. Haemodynamic parameters

The animals were anaesthetised (propofol 0.1 mg/kg/min+ketamine 0.2/kg/min) and ventilated with room air supplemented with oxygen. A catheter introducer sheath was placed in a carotid artery and a 5F micro manometer-tipped catheter (Millar Instruments) was introduced into the LV. Haemodynamic signals from these catheters and from the cardiac output (CO) flow-probe together with an ECG recording were processed, digitised and recorded using a MacLab system (MacLab 8, ADI Instruments) and a Macintosh computer. Derived parameters were computed online using this system.

2.2.3. The model of dilated cardiomyopathy and heart failure

The rapid ventricular paced animal model of HF has been widely used and is considered to display many of the features of HF in patients [9]. In our derivative of this model we, as have others [10], utilised the relationship between the rate and duration of pacing initially to create a model of early HF and later to intensify the severity of cardiac dysfunction. In previous pilot studies we found that the response of individual animals to rapid ventricular pacing varies i.e. the relationship between the level of tachycardia induced HF and the pacing rate differs particularly when the desired outcome is not severe endstage

HF. In order to standardise the degree amongst the animals at each stage of the study, we utilised the values from the continuous CO measurement to modify the pacing rates according to the individuals acute response to rapid pacing.

The initial pacing rate was determined as follows. After a post surgical 10–14 day recovery period the CO in normal sinus rhythm (NSR) over a period of 2 min was measured on a minimum of ten different occasions and the mean determined. Pacing was commenced (at twice pacing threshold, range 2–6 ma) and the rate increased, to a maximum value of 190 bpm, until the mean paced CO was 90% of the mean CO in NSR (Rate A). After 21 days of pacing at Rate A there were significant changes in cardiovascular function (see below) indicative of moderate or early heart failure.

In order to intensify the degree of HF a second rate (Rate B) was determined immediately prior to the wrap or sham procedure in the same manner as Rate A was previously determined. Twenty four hours after, the surgery pacing was recommenced at Rate B and continued for 28 days.

2.2.4. Surgical procedure in early heart failure (wrap or sham procedure)

In this procedure a biocompatible polyester mesh fabric jacket (Acorn Cardiovascular, St Paul MN), shaped to cup the ventricular apex and with a longitudinal opening for size adjustment, was placed around both ventricles from the apex to the atrio-ventricular junction. The jacket was retained in six (wrap) animals and removed in the other six (sham) animals.

The animals were induced with intravenous propofol (2 mg/kg), intubated and ventilated with 100% oxygen. General anaesthesia was maintained with intravenous propofol (6 mg/kg/h) plus ketamine (3 mg/kg/h). The animals were placed in dorsal recumbency. A lower partial sternotomy was performed, which extended from the xiphoid process to approximately two-thirds of the way to the thoracic inlet. The pericardium was incised longitudinally and a pericardial cradle was formed (Fig. 1). The myocardial jacket was guided over the heart and fixed posteriorly with large titanium ligature clips (Ligaclips® Ethicon) to the parietal pericardium at the level of the atrioventricular groove. The anterior surface of the jacket was sutured to the pericardium, also above the atrioventricular groove with 5/0 sutures (Prolene® Ethicon). The jacket was then wrapped firmly around the heart and the cut edge sutured (2/0 Prolene® Ethicon) and trimmed of excess material. At this stage, the jacket was removed from the sham animals. The pericardium was closed in all animals with 5/0 sutures (Vicryl® Davis and Geck). The sternotomy was closed in layers: initially with stainless
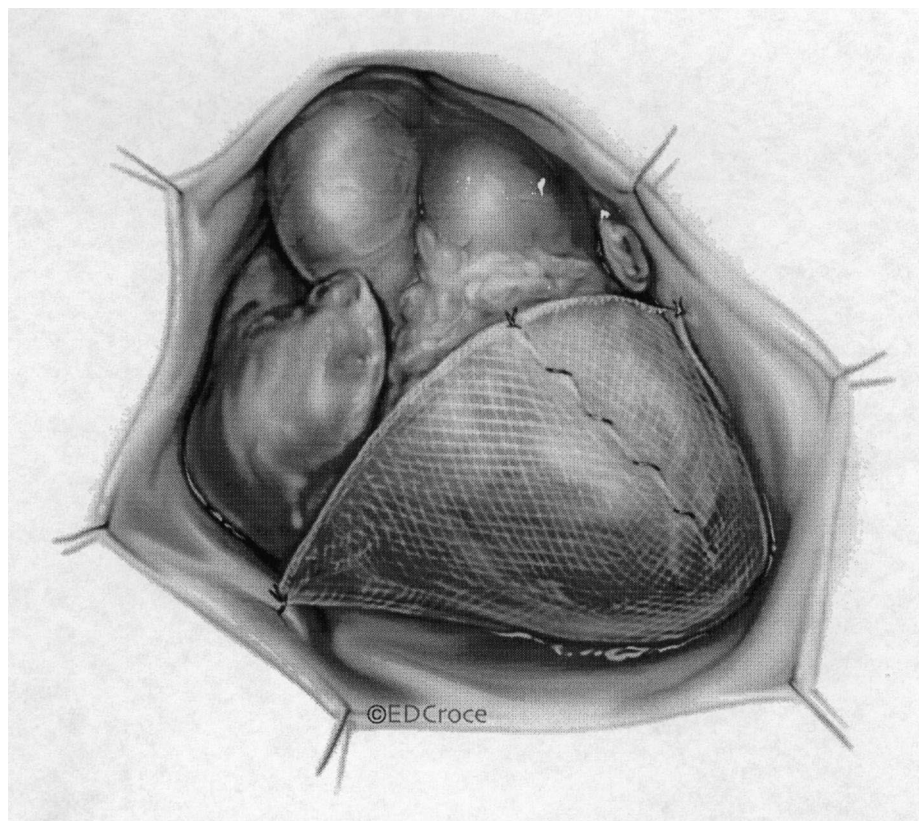

Fig. 1. Position and attachment of the jacket on the epicardial surface of the two ventricles. The Ligaclips® are on the undersurface of the heart and therefore not visible.
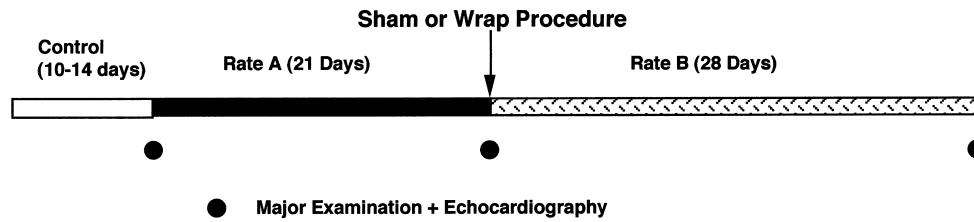
Fig. 2. Schematic representation of the experimental protocol showing periods of pacing at Rate A and Rate B and the data collection points.

steel wire sutures, 2/0 Dexon® (Davis and Geck) in the sternal tissue pad and 1 Ethilon® (Ethicon) skin sutures. Antibiotics (1g ampicillin and 80 mg gentamicin sulphate, both intravenously) were given prophylactically immediately after surgery and for 3 days following. Flunixin meglumine, 50 mg i.m., was given prior to surgery and post-operatively once daily for two days as an analgesic and anti-inflammatory agent.

2.3. Experimental protocol

A schema of the experimental design is shown in Fig. 2. Detailed descriptions of the procedures are given above. After the animals had recovered from an initial surgical preparation they were rapid paced for 21 days to induce early heart failure. A wrap or sham procedure was then performed and pacing continued for an additional 28 days at a higher pacing rate. Animals were then euthanased. A haemodynamic and echocardiographic examination was performed at the end of the baseline period (approximately 14 days after the initial surgical preparation), after 21 days of pacing at rate (A) (immediately prior to the wrap or sham procedure) and after 28 days of pacing at rate (B) (termination).

3. Statistical analysis

Data was analysed using a computerised statistical package (SAS Inst, Gary NC). The two groups (sham and wrap) were compared at baseline, wrap or sham procedure and at termination, using the Wilcoxon rank-sum test. Differences within the wrap and sham treatment groups from control to wrap/sham procedure and from wrap/sham procedure to termination were compared using paired Student's t-test. Results are expressed as mean$\pm$SD and a p value of <0.05 was considered significant.

4. Results

The hearts from the wrap animals were examined at post mortem at the end of the study. In all animals, the position of the jacket remained unchanged from implantation and both ventricles were entirely enclosed. Mean data from animals at baseline and after 21 days of pacing of pacing at Rate (A) and after a further 28 days of pacing at Rate (B) are shown in Table 1. There was no significant differences *between* the wrap and sham groups at baseline. Similarly, after 21 days of pacing at Rate A the parameters from both groups were not significantly different except for $-dP/dt_{max}$. There were, however, significant differences *within* groups with significant changes in cardiac function and structure (Table 2). Left ventricular contractility, expressed as LV fractional shortening (LVFS) decreased by approximately one third in both groups while the LV long axis area more than doubled.

After 28 days of pacing at Rate B there were significant changes *both* between and within the groups (Table 1). Over this pacing period cardiac function deteriorated

Table 1
Between group comparisons of haemodynamic and echo cardiographic parameters

Parameter	Baseline			Paced 21 days at Rate A			Paced 28 days at Rate B		
	Pros. sham	Pros. wrap	p	Pre-sham	Pre-wrap	p	Sham	Wrap	p
RV pacing rate (bpm)	N/A	N/A		188$\pm$4	190$\pm$0	NS	206$\pm$5	213$\pm$4	NS
Normal sinus rhythm (bpm)	75$\pm$18	87$\pm$18	NS	77$\pm$15	93$\pm$20	NS	104$\pm$24	101$\pm$22	NS
Arterial pressure (mm Hg)	94$\pm$8	85$\pm$14	NS	95$\pm$9	87$\pm$20	NS	88$\pm$6	89$\pm$18	NS
Mitral valve regurgitation (0–3)	0	0		0.33$\pm$0.05	0	NS	2.7$\pm$0.52	0.7$\pm$0.82	0.03
$+dP/dt_{max}$ (mm Hg/s)	1060$\pm$265	1102$\pm$487	NS	677$\pm$160	863$\pm$181	0.02	595$\pm$115	676$\pm$276	NS
$-dP/dt_{max}$ (mm Hg/s)	$-$1226$\pm$239	$-$1604$\pm$432	NS	$-$839$\pm$73	$-$1297$\pm$336	NS	$-$997$\pm$296	$-$915$\pm$197	NS
Cardiac output (l/min)	6$\pm$1.3	6$\pm$1.2	NS	4.2$\pm$0.78	4.1$\pm$1.2	NS	3.53$\pm$1.3	3.33$\pm$0.81	NS
Stroke volume (ml)	75$\pm$14	65$\pm$5	NS	55$\pm$16	46$\pm$14	NS	36$\pm$15	34$\pm$10	NS
Minimum LV pressure (mm Hg)	3$\pm$2.48	2$\pm$3.48	NS	9$\pm$2.93	6$\pm$4.62	NS	16$\pm$5.53	9$\pm$3.69	0.027
SVR[a] (dynes/s/cm^{-5})	1437$\pm$346	1256$\pm$285	NS	1827$\pm$364	1853$\pm$881	NS	2167$\pm$810	2232$\pm$657	NS

[a] SVR=Systemic vascular resistance.

Table 2

Within group comparisons of haemodynamic and echo cardiographic parameters[a]

Parameter	A	B	A	B
LVFS (%)	$p=0.03$	$p=0.03$	$p=0.02$	NS
LV Area (cm^2)	$p=0.02$	$p=0.008$	$p=0.02$	NS
RV pacing rate (bpm)	N/A	$p=0.004$	N/A	$p=0.001$
Normal sinus rhythm (bpm)	NS	NS	NS	NS
Arterial pressure (mm Hg)	NS	NS	NS	NS
Mitral valve regurgitation (0–3)	N/A	$p=0.02$	N/A	NS
$+dP/dt_{max}$ (mm Hg/s)	$p=0.01$	NS	NS	NS
$-dP/dt_{max}$ (mm Hg/s)	$p=0.007$	NS	$p=0.04$	NS
Cardiac output (l/min)	NS	NS	NS	NS
Stroke volume (ml)	$p=0.03$	$p=0.002$	$p=0.02$	NS
Minimum LV pressure (mm Hg)	$p=0.03$	$p=0.03$	$p=0.04$	NS
Systemic vas. resist. (dynes/s/cm^{-5})	NS	NS	NS	NS

[a] Columns A are the results of a comparison within the respective groups between values for baseline and after 21 days of pacing at Rate (A). Columns B are the results of a comparison within the respective groups between values after 21 days of pacing at Rate (A) and after 28 days of pacing at Rate (B).

significantly in the sham group compared with the wrap group. At termination LVFS was halved (Fig. 3) and LV long axis area increased by one third in the sham animals (Fig. 4). A significant degree of mitral regurgitation developed in these animals and minimum LV pressure was higher. In contrast, in those animals who underwent the wrap procedure, no significant differences in measured parameters occurred during this second pacing period and very little mitral regurgitation was evident. Overall, there were no significant differences in CO between the two groups.

The two RV pacing rates (Rates A and B) were similar for both groups, however, Rate (B) was significantly higher than Rate (A) in both. Therefore, the effects of a similar mechanism for the intensification of the level of HF produced very different results, which was dependent on the presence of passive ventricular constraint from the fabric wrap.

5. Discussion

Progressive ventricular remodelling, especially dilatation of the left or both ventricles, is a fundamental finding in heart failure and many of the mechanisms of terminal failure are directly related to ventricular enlargement. For the ultimate therapeutic goal of reversing remodelling to occur, cardiac enlargement must first be halted. There are two broad ways this can occur: either indirectly by reversing the remodelling pattern, or directly by surgical reduction. The surgical options currently in use for the treatment of heart failure are based on one or both of these pathways. Direct intervention by surgical reduction of the left ventricle has produced inconclusive results with a decline in cardiac function and resumption of left ventricular dilatation following initial post surgical improvement [11,12]. There are a number of procedures which are based on indirect intervention in the remodelling process. Mitral
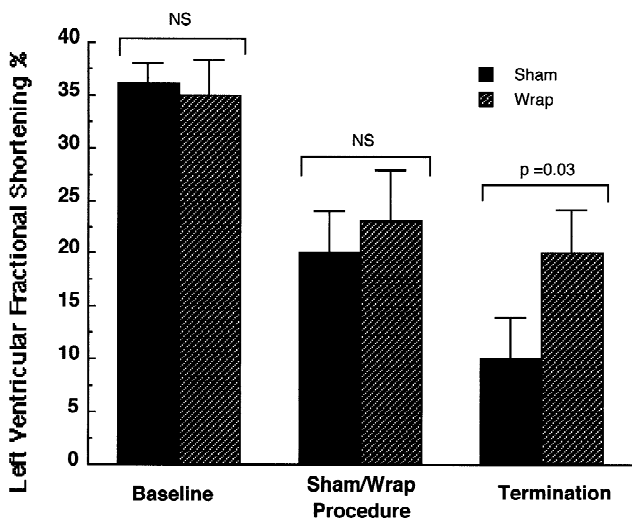

Fig. 3. Mean (±SD) left ventricular fractional shortening at baseline, after 21 days pf pacing at Rate A and following an additional 28 days of pacing at Rate B.
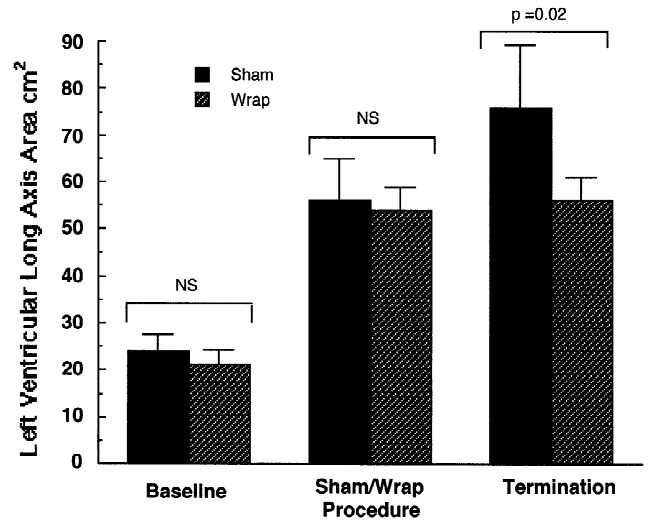

Fig. 4. Mean (±SD) left ventricular long axis area at baseline, after 21 days of pacing at Rate A and following an additional 28 days of pacing at Rate B.

valve regurgitation is a common finding and is associated with a poor prognosis in advanced heart failure. Radical mitral valve annuloplasty has been shown to stabilise cardiac function in some of patients [13]. A broader hypothesis is that if some of the workload of a compromised heart could be relieved, this would allow for reverse remodelling to occur. There is evidence that the chronic implantation of ventricular assist devices may initiate reverse remodelling, although the technology is complex and restricted to relatively few centres [14]. A number of techniques have been devised to co-opt the contractile forces of paced skeletal muscle to enhance circulatory function, however only dynamic cardiomyoplasty has progressed to clinical use. The hypothesis of dynamic cardiomyoplasty was that the failing contractile function of the heart would be augmented by the paced contractions of an electrically transformed latissimus dorsi muscle wrap. Although difficult to quantify, there is evidence that this treatment does improve the condition of many HF patients and that it is associated with demonstrable reverse remodelling [2]. The mechanism behind this improvement, augmented contractility or the constraining effect of the muscle wrap, is subject to debate [15]. A recently published animal study provides evidence that ventricular constraint may play a major role, however in the same report doubt is expressed whether a synthetic wrap would have the structural characteristics necessary to duplicate the protective function of the muscle girdle [1]. Two recent studies [7,8] have looked at this question in two different animal models of heart failure. In both, the normal heart was wrapped prior to the evolution of HF. This has little clinical relevance but they were able to show that this procedure is feasible, stopped much of the increase in LV volume and some of the decrease in function which was exhibited in control animals.

In our study, which utilised an animal model of progressive heart failure, we have shown that passive ventricular constraint with a purposely designed synthetic wrap is feasible and halts the decline in cardiac function and the increase in LV dimensions observed in the parallel sham operated controls.

The work of Sabbah et al. [16–19] provides a partial explanation for the decline in cardiac function that is associated with the assumption of a global profile in dilated cardiomyopathy. They have shown that the severe mitral regurgitation associated with the rounded profile is significantly related to the change in the angle of the mitral valve chordae, resulting in a breakdown of normal mitral valve leaflet coaptation. We believe that this was the mechanism responsible for the dramatic differences in the incidence of mitral valve regurgitation between the two treatment groups.

Further investigation is needed. If the positive outcomes in this study are sustained then passive ventricular constraint with a synthetic wrap may offer a relatively simple and minimally invasive surgical option for the treatment of dilated cardiomyopathy and heart failure. The specific advantages of this technique, no invasion of the circulatory space and minimal surgical trauma, may result in a degree of general acceptance that has alluded other surgical treatments for heart failure.

Acknowledgements

References

[1] Patel HJ, Polidori DJ, Pilla JJ et al. Stabilization of chronic remodeling by asynchronous cardiomyoplasty in dilated cardiomyopathy: effects of a conditioned muscle wrap. Circulation 1997;96:3665–3671.

[2] Kass DA, Baughman KL, Pak PH et al. Reverse remodeling from cardiomyoplasty in human heart failure. External constraint versus active assist. Circulation 1995;91:2314–2318.

[3] Chagas AC, Moreira LF, Da LP et al. Stimulated preconditioned skeletal muscle cardiomyoplasty. An effective means of cardiac assist. Circulation 1989;80:202–208.

[4] Cheng W, Justicz AG, Soberman MS et al. Effects of dynamic cardiomyoplasty on indices of left ventricular systolic and diastolic function in a canine model of chronic heart failure. J Thorac Cardiovasc Surg 1992;103:1207–1213.

[5] Capouya ER, Gerber RS, Drinkwater DJ et al. Girdling effect of nonstimulated cardiomyoplasty on left ventricular function. Ann Thorac Surg 1993;56:867–870.

[6] Mott BD, Oh JH, Misawa Y et al. Mechanisms of cardiomyoplasty: comparative effects of adynamic versus dynamic cardiomyoplasty. Ann Thorac Surg 1998;65:1039–1044.

[7] Vaynblat M, Chiavarelli M, Shah HR et al. Cardiac binding in experimental heart failure. Ann Thorac Surg 1997;64:81–85.

[8] Oh JH, Badhwar V, Mott BD, Li CM, Chiu RC. The effects of prosthetic cardiac binding and adynamic cardiomyoplasty in a model of dilated cardiomyopathy. J Thorac Cardiovas Surg 1998;116:148–153.

[9] Travill CM, Williams TD, Pate P et al. Haemodynamic and neurohumoral response in heart failure produced by rapid ventricular pacing. Cardiovas Res 1992;26:783–790.

[10] Redfield MM, Aarhus LL, Wright RS, Burnett JC. Cardiorenal and neurohumoral function in a canine model of early left ventricular dysfunction. Circulation 1993;87:2016–2022.

[11] Gorcsan JR, Feldman AM, Kormos RL et al. Heterogeneous immediate effects of partial left ventriculectomy on cardiac performance. Circulation 1998;97:839–842.

[12] McCarthy J, McCarthy P, Starling R et al. Partial left ventriculectomy and mitral valve repair for endstage heart failure. Eur J Cardiothorac Surg 1998;13:337–343.

[13] Bolling SF, Pagani FD, Deeb GM, Bach DS. Intermediate-term outcome of mitral reconstruction in cardiomyopathy. J Thorac Cardiovas Surg 1998;115:381–386.

[14] Lee S, Doliba N, Osbakken M, Oz M, Mancini D. Improvement of mitochondrial function after haemodynamic support with left ventricular assist devices in patients with heart failure. J Thorac Cardiovas Surg 1998;116:344–349.

[15] Furnary A, Jessup M, Moreira L. Multicenter trial of dynamic

cardiomyoplasty for chronic heart failure. J Am Coll Cardiol 1996;28:1175–1180.

[16] Kono T, Sabbak H, Rosman H et al. Left ventricular shape is the primary determinant of functional mitral regurgitation in heart failure. J Am Coll Cardiol 1992;20:1594–1598.

[17] Nass O, Rosman H, Al-Kaled N et al. Relation of left ventricular chamber shape in patients with low (<40%) ejection fraction to severity of functional mitral regurgitation. Am J Cardiol 1995;76:402–404.

[18] Sabbah HN, Rosman H, Kono T et al. On the mechanism of functional mitral regurgitation. Am J Cardiol 1993;72:1074–1076.

[19] Sabbah HN, Kono T, Rosman H et al. Left ventricular shape: a factor in the etiology of functional mitral regurgitation in heart failure. Am Heart J 1992;123:961–966.

This information is current as of October 30, 2006

The online version of this article, along with updated information and services, is
located on the World Wide Web at:
http://content.onlinejacc.org/cgi/content/full/39/12/2069

305

EXPERIMENTAL STUDY

Reverse Remodeling and Enhanced Adrenergic Reserve From Passive External Support in Experimental Dilated Heart Failure

W. Federico Saavedra, MD,* Richard S. Tunin, MS,* Nazareno Paolocci, MD, PHD,*
Takayuki Mishima, MD,† George Suzuki, MD,† Charles W. Emala, MD,‡ Pervaiz A. Chaudhry, MD,†
Petros Anagnostopoulos, MD,† Ramesh C. Gupta, PHD,† Hani N. Sabbah, PHD, FACC,†
David A. Kass, MD, FAHA*

Baltimore, Maryland; Detroit, Michigan; and New York, New York

OBJECTIVES	We sought to test the efficacy of a passive elastic containment device to reverse chronic chamber remodeling and adrenergic down-regulation in the failing heart, yet still maintaining preload reserve.
BACKGROUND	Progressive cardiac remodeling due to heart failure is thought to exacerbate underlying myocardial dysfunction. In a pressure–volume analysis, we tested the impact of limiting progressive cardiac dilation by an externally applied passive containment device on both basal and adrenergic-stimulated function in failing canine hearts.
METHODS	Ischemic dilated cardiomyopathy was induced by repeated intracoronary microembolizations in six dogs. The animals were studied before and three to six months after surgical implantation of a thin polyester mesh (cardiac support device [CSD]) that surrounded both cardiac ventricles. Pressure–volume relations were measured by a conductance micromanometer catheter.
RESULTS	Long-term use of the CSD lowered end-diastolic and end-systolic volumes by $-19 \pm 4\%$ and $-22 \pm 8\%$, respectively (both $p < 0.0001$) and shifted the end-systolic pressure–volume relation to the left ($p < 0.01$), compatible with reverse remodeling. End-diastolic pressure and chamber diastolic stiffness did not significantly change. The systolic response to dobutamine markedly improved after CSD implantation ($55 \pm 8\%$ rise in ejection fraction after CSD vs. $-10 \pm 8\%$ before CSD, $p < 0.05$), in conjunction with a heightened adenylyl cyclase response to isoproterenol. There was no change in the density or affinity of beta-adrenergic receptors. Diastolic compliance was not adversely affected, and preload-recruitable function was preserved with the CSD, consistent with a lack of constriction.
CONCLUSIONS	Reverse remodeling with reduced systolic wall stress and improved adrenergic signaling can be achieved by passive external support that does not generate diastolic constriction. This approach may prove useful in the treatment of chronic heart failure. (J Am Coll Cardiol 2002;39:2069–76) © 2002 by the American College of Cardiology Foundation

Chronic cardiac remodeling is a major hallmark of dilated cardiomyopathy and is thought to play a central role in disease progression (1–4). Chamber dilation and wall thinning elevate wall stress, triggering the local release of neurohormones and adversely affecting myocardial molecular biology and physiology (3). Both beta-adrenergic blockade and angiotensin-converting enzyme inhibition enhance heart failure survival and inhibit or reverse remodeling (5–8). Further evidence supporting a pathophysiologic role of remodeling stems from studies of left ventricular assist devices (LVADs). This intervention profoundly unloads the left heart, leading to reverse remodeling (9,10) and improv-

ing myocyte and muscle function (11,12), molecular and calcium signaling (11,13,14) and adrenergic responsiveness (15). However, LVAD studies cannot determine the therapeutic effect of limiting chronic remodeling on the working heart, nor can they easily differentiate unloading influences from changes due to systolic assist and neurohormonal de-activation.

The impact of limiting remodeling on heart failure progression has been directly tested by the application of external containment. An example of this approach is cardiomyoplasty (16,17), in which a flat sheet of skeletal muscle is wrapped around the heart and then stimulated to assist systolic contraction. Intriguingly, both clinical (18) and animal studies (19) have identified a passive girdling effect of the wrap as a dominant mechanism responsible for reverse remodeling and improved function. Such observations have led to the development of a passive polymer jacket that surrounds the heart (cardiac support device [CSD]; Acorn Cardiovascular Inc., St. Paul, Minnesota). In

306

Abbreviations and Acronyms

ATP	=	adenosine triphosphate
cAMP	=	cyclic adenosine monophosphate
CSD	=	cardiac support device
DHA	=	^{3}H-dihydroalprenolol
ESPVR	=	end-systolic pressure–volume relation
LV	=	left ventricle
LVAD	=	left ventricular assist device
PMSF	=	phenylmethylsulfonyl fluoride
RV	=	right ventricle
SDS	=	sodium dodecyl sulfate

recent studies, the CSD has been shown to limit progressive dilation in heart failure (20), enhance fractional shortening and reduce myocyte hypertrophy and interstitial fibrosis (21,22). However, it remains unknown whether this reflects true remodeling or an influence of diastolic constraint, and whether the CSD favorably alters stimulated functional reserve.

Accordingly, the present study tested the following hypotheses: 1) that the CSD induces reverse remodeling, as reflected by a leftward shift in the end-systolic pressure–volume relation (ESPVR); 2) that this is accompanied by enhanced beta-adrenergic signaling; and 3) that both effects are achieved without limiting preload-recruitable reserve or compromising diastolic compliance.

METHODS

Animal model. Heart failure was induced in six adult mongrel dogs (25 to 30 kg) by multiple sequential intracoronary embolizations with polystyrene latex microspheres (70 to 100 μm outer diameter). This model includes many features of human cardiac failure at the chamber, myocardial, cellular and molecular levels (23–25). An average of six microembolizations were performed one to three weeks apart in each animal, until the ejection fraction declined to <35%, a level associated with a 20% to 30% increase in chamber volume. The procedure was performed under sterile conditions and general anesthesia (see next paragraph), and the study approved by the Henry Ford Hospital's Animal Care and Use Committee, in accordance with the guidelines of the National Institutes of Health.

Experimental protocol. After establishing heart failure, the animals underwent cardiac catheterization with a dual-sensor, pressure–volume catheter (SPC 562 Millar Instruments, Houston, Texas) to assess ventricular function. Right and left heart recordings and a contrast ventriculogram were obtained under general anesthesia (0.22 mg/kg oxymorphone; 0.17 mg/kg diazepam; 150 to 250 mg pentobarbital). Left ventricular pressure–volume relations were then measured at rest and during a transient preload reduction induced by inferior vena caval occlusion (NuMed, New York, New York), in accordance with reported protocols (26). Each animal subsequently underwent dobutamine challenge (5 to 10 μg/kg per min), with data recorded at
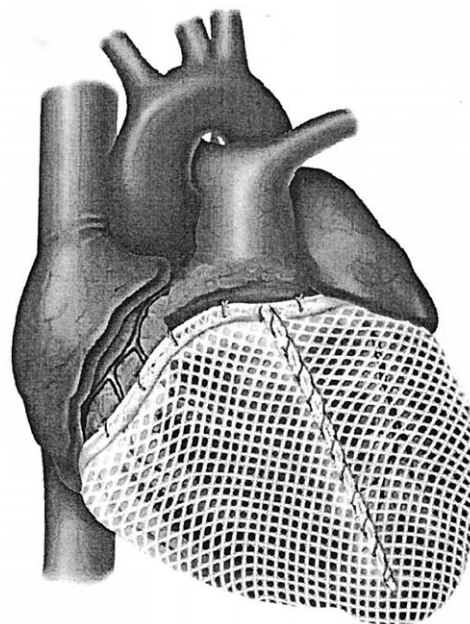

Figure 1. The cardiac support device wrap placed around the heart. The polyester mesh material is sutured along an anterior wall seam to achieve containment around both the right and left ventricles. The material is snug to the surface to remove surface wrinkling, but not to constrict diastolic filling.

steady-state. Dobutamine was then discontinued and baseline was re-established (after 10 to 15 min), and then the dogs were given four sequential bolus injections of 100 ml of dextran to test for preload reserve. All catheters were then removed, and the insertion sites were closed.

The CSD was implanted after completion of the baseline study. Details of the surgical procedure have been reported (20,21,27). After induction with diazepam (0.2 mg/kg intravenously) and oxymorphone (0.1 mg/kg), the animals were intubated, and anesthesia was maintained with 0.5% to 1% isoflurane and supplemental oxygen. The heart was exposed by a median sternotomy, and the parachute technique was used to implant the CSD, by slipping it over the apex of the heart with the full-length seam at the center of the anterior surface. The CSD was placed around both ventricles and anchored with approximately eight sutures at the atrioventricular groove (Fig. 1). The fit was made so that the material was nonwrinkled, thus providing contact with the epicardium throughout the cycle. There was only a small, early volume change with CSD placement (−2.1%), as determined by echocardiography. The chest was closed, and the animals fully recovered from the operation. Once in use, the CSD becomes encased in a thin fibrous sheath without inflammation or progressive fibrosis (21). Follow-up study was performed three to six months after CSD implantation. The dogs were then sacrificed with a barbiturate overdose, and tissues were obtained for biochemical analyses.

Adenylyl cyclase activity. Frozen left ventricular (LV) tissue (300 to 400 mg) was thawed in 5 mmol/l Tris (pH 7.4), 0.25 mol/l sucrose, 1 mmol/l MgCl$_2$, 1 mmol/l EDTA
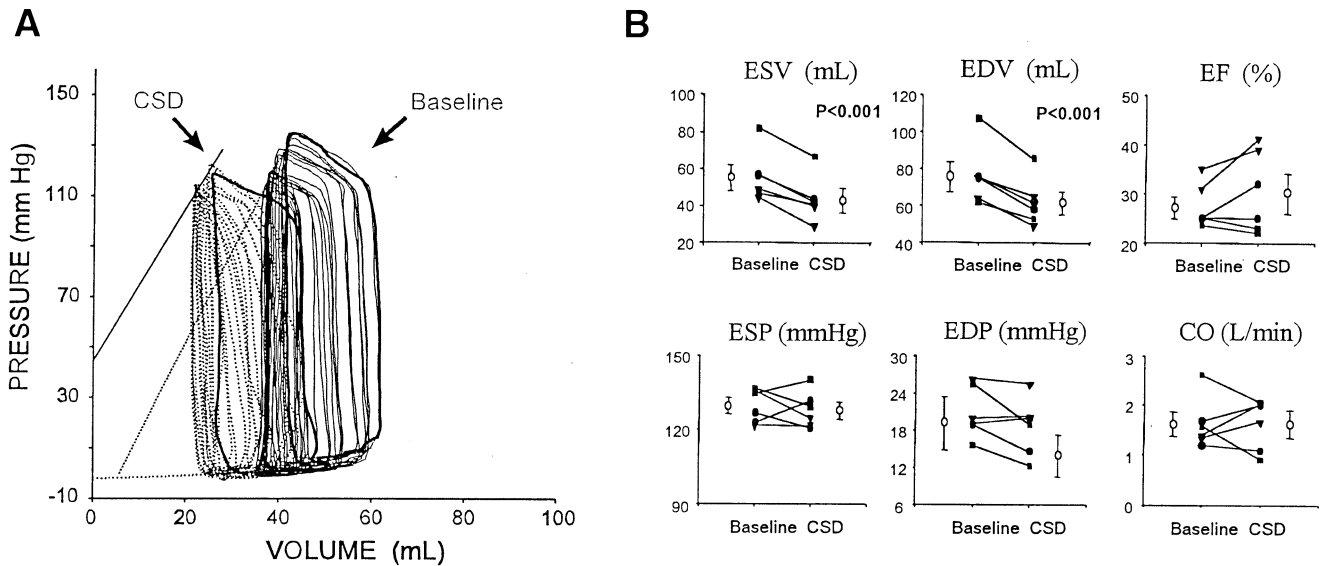
307

Figure 2. Hemodynamic effects of the cardiac support device (CSD). **(A)** Left ventricular pressure–volume relations in one animal before and after long-term CSD use. The **darker loops** for each condition reflect basal conditions, and the **thinner loops** were measured during transient load reduction. There was a reduction in both end-diastolic and end-systolic chamber volumes, with preservation of cardiac stroke volume (loop width), and the end-systolic pressure–volume relation shifted leftward, consistent with reversal of chamber remodeling. The diastolic pressure–volume boundary was not altered. **(B)** Summary of hemodynamic variables before and after long-term CSD use. There was a consistent significant decline in chamber volumes (end-diastolic volume [EDV] and end-systolic volume [ESV]), without a change in cardiac output (CO). End-diastolic pressure (EDP) and end-systolic pressure (ESP) were not significantly changed. EF = ejection fraction.

and 10 μmol/l phenylmethylsulfonyl fluoride (PMSF) and homogenized for 45 s. The homogenates were filtered and centrifuged at 1,000 g (10 min, 4°C); the supernatant was recovered and centrifuged at 45,000 g (25 min, 4°C); and the pellets were resuspended in 25 ml of 50 mmol/l Tris (pH 7.4), 10 mmol/l $MgCl_2$, 1 mmol/l EDTA and 10 μmol/l PMSF and centrifuged at 45,000 g (25 min, 4°C). After rewashing in the same solution, the pellet was resuspended in 0.5 ml of buffer and analyzed immediately. Triplicate samples were incubated for 10 min at 37°C and contained the indicated effector, along with 10 to 20 μg of membrane protein: 25 mmol/l Tris (pH 7.5), 5 mmol/l $MgCl_2$, 0.5 mmol/l EDTA, 1 mmol/l cyclic adenosine monophosphate (cAMP), 1 mmol/l adenosine triphosphate (ATP), [α-^{32}P]ATP (0.5 to 1.5 μCi/tube, 800 Ci/mmol), 5 μmol/l PMSF, 7 mmol/l creatine phosphate, 50 μn/ml creatine kinase and 0.25 mg/ml bovine serum albumin in a final volume of 100 μl. Adenylyl cyclase activity was measured under basal conditions, with 10 μmol/l guanosine triphosphate (GTP) plus 1 nmol/l to 100 μmol/l isoproterenol or 10 μmol/l forskolin. The reactions were terminated by the addition of 100 μl of buffer: 50 mmol/l HEPES (pH 7.5), 2 mmol/l ATP, 0.5 mmol/l cAMP, 2% sodium dodecyl sulfate (SDS) and 1 μCi/ml ^{3}H-cAMP (37 Ci/ mmol). Newly synthesized ^{32}P-cAMP was separated from the precursor [α-^{32}P]ATP by sequential column chromatography with Dowex and aluminum oxide, using recovery of ^{3}H-cAMP to monitor the individual column's efficiency. Eluted radioactivity was quantitated by liquid scintillation.

Beta-adrenergic receptor radioligand binding. Beta-adrenreceptor density was measured using radioligand ^{3}H-dihydroalprenelol (DHA) (New England Nuclear, Boston, Massachusetts), according to published procedures (28). Specific binding to the beta-adrenoceptor population was defined as the difference between the total amount of radioactivity bound in the presence of ^{3}H-DHA alone and the nonspecific binding in the presence of ^{3}H-DHA and 10 μmol/l alprenolol. Receptor density (B_{max}) and the equilibrium dissociation constant (K_d) for ^{3}H-DHA binding to membrane preparations were assessed by Scatchard analysis, using the ReceptorFit Saturation Two-Site Software (Lundon Software, Inc., Cleveland Heights, Ohio).

Data analysis. Pressure–dimension data were recorded at steady-state and during inferior vena caval occlusion; the latter was used to derive pressure–volume relations. Details of the hemodynamic analysis have been reported (29). Systolic function was principally indexed by the ESPVR and preload-recruitable stroke work (30). Preload was expressed as the end-diastolic volume, and arterial load as the effective arterial elastance. The volume signal was calibrated to match the absolute ventricular volumes obtained by contrast ventriculography. All hemodynamic signals were digitally recorded at 200 Hz and analyzed using custom software. Hemodynamic variables before and after CSD implantation were compared by the Student paired t test. The differential effects of dobutamine stimulation before versus after CSD placement were analyzed by three-way analysis of variance (ANOVA), with drug, experimental condi-
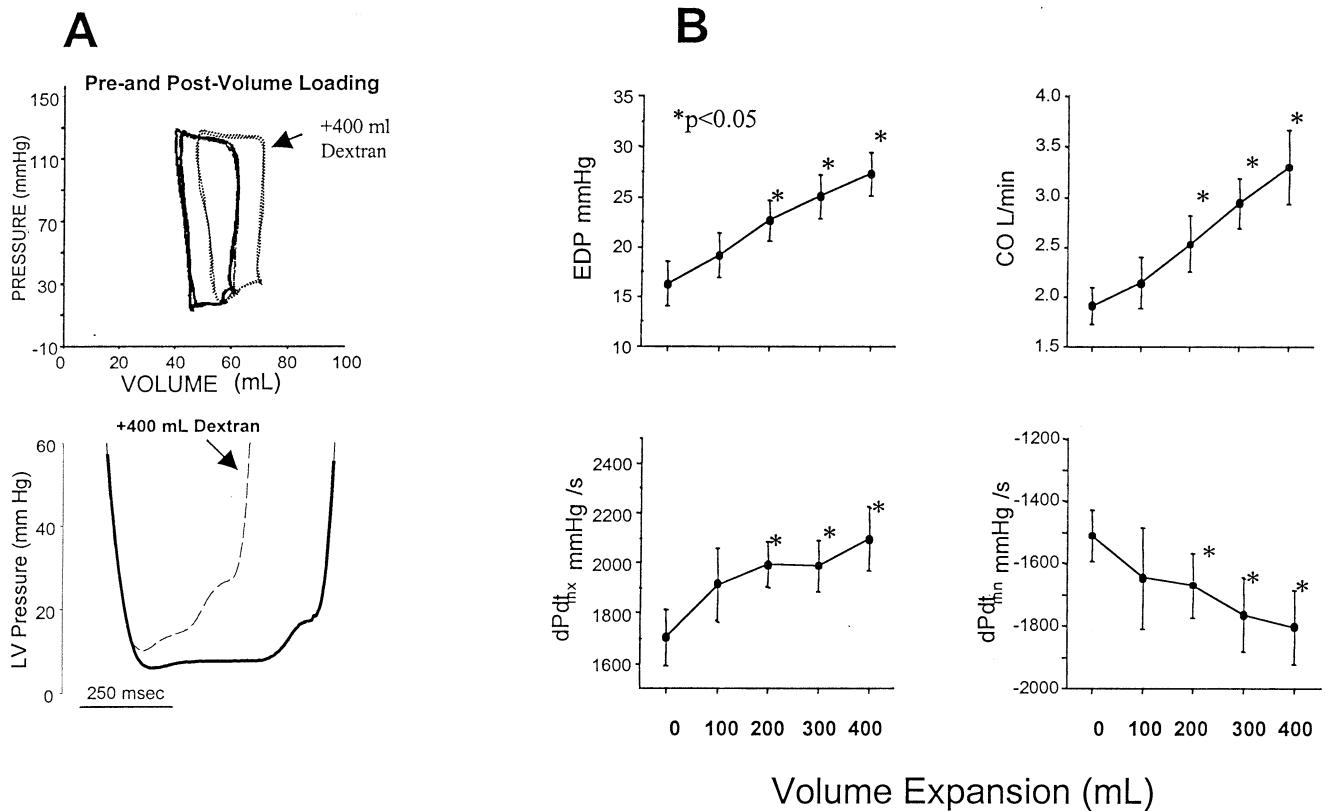
308

Figure 3. Effects of an early preload increase in the failing heart after cardiac support device (CSD) implantation. **(A)** Example of pressure–volume relations before and after infusion of 400 ml of dextran. **(B)** Summary of hemodyanmic variables in relation to incremental volume expansion. For a near 10 mm Hg rise in end-diastolic pressure (EDP), cardiac output (CO) rose by nearly 100%, and there were significant changes in both the maximal and minimal rates of pressure change. Thus, preload-dependent reserve function was not inhibited by CSD placement. dP/dt_{mx} and dP/dt_{mn} = rate of rise in left ventricular pressure, maximal and minimal, respectively. $*p < 0.05$ versus baseline, e.g. 0 volume expansion.

tion and dog as the categorical variables. A different dobutamine response was defined by significance of the cross-term (dobutamine $\times$ condition). Adenylate cyclase data were analyzed by two-way ANOVA. Data are reported as the mean value $\pm$ SEM.

RESULTS

Induction of reverse remodeling in the heart by use of the CSD. Figure 2A displays examples of pressure–volume loops and relations before and after long-term CSD treatment. Placement of the CSD resulted in a leftward shift in the rest pressure–volume loop (thicker lines), as well as in the ESPVR. The latter observation is consistent with reversal of remodeling. In contrast, the diastolic pressure–volume curve was changed only a little. The leftward ESPVR shift was quantified by the end-systolic volume at a matched end-systolic pressure measured in the physiologic range (110 mm Hg, or V_{110}). The V_{110} fell from 44.7 ± 5.2 to 33.9 ± 3.9 ml by long-term CSD treatment ($p < 0.01$). In contrast, the ESPVR slope was not significantly altered (2.5 ± 0.59 before CSD vs. 4.3 ± 2.3 after CSD, $p = NS$).

The diastolic pressure–volume relation was more variably affected, with some animals displaying a leftward shift and others a downward shift, whereas others had no change. Diastolic chamber elastic stiffness (β), as determined from a monoexponential fit ($P = P_{\infty} + \alpha[e^{\beta V} - 1]$) did not significantly change (0.09 ± 0.03 before CSD vs. 0.11 ± 0.02 ml^{-1} after CSD, $p > 0.4$).

Figure 2B provides a summary of the hemodynamic data. Both end-systolic and end-diastolic volumes significantly declined by -22.1 ± 7.6 and $-18.7 \pm 4.2\%$, respectively (both $p < 0.0001$). In contrast, the EF, end-systolic pressure, end-diastolic pressure, cardiac output (Fig. 2B), maximal rate of rise in pressure ($2,025 \pm 130$ vs. $1,765 \pm 67$ mm Hg/s), isovolumic relaxation (49.9 ± 4.5 vs. 51.7 ± 5.4 ms, using a non-zero decay asymptote) and preload-recruitable stroke work (54.1 ± 11.1 vs. 54.4 ± 9.4 mm Hg) were not altered. It should be noted that LV end-diastolic pressure either declined or remained minimally changed. Consistent with previous reports (21), we found no evidence of functional constraint after CSD implantation. Right and left heart diastolic pressures were not equalized (19 ± 3 mm Hg for LV end-diastolic pressure; 8 ± 1 mm Hg for right ventricular [RV] end-diastolic pressure) after long-term CSD use.

Preload-recruitable systolic reserve. Because the CSD imposed an external containment around the heart, one
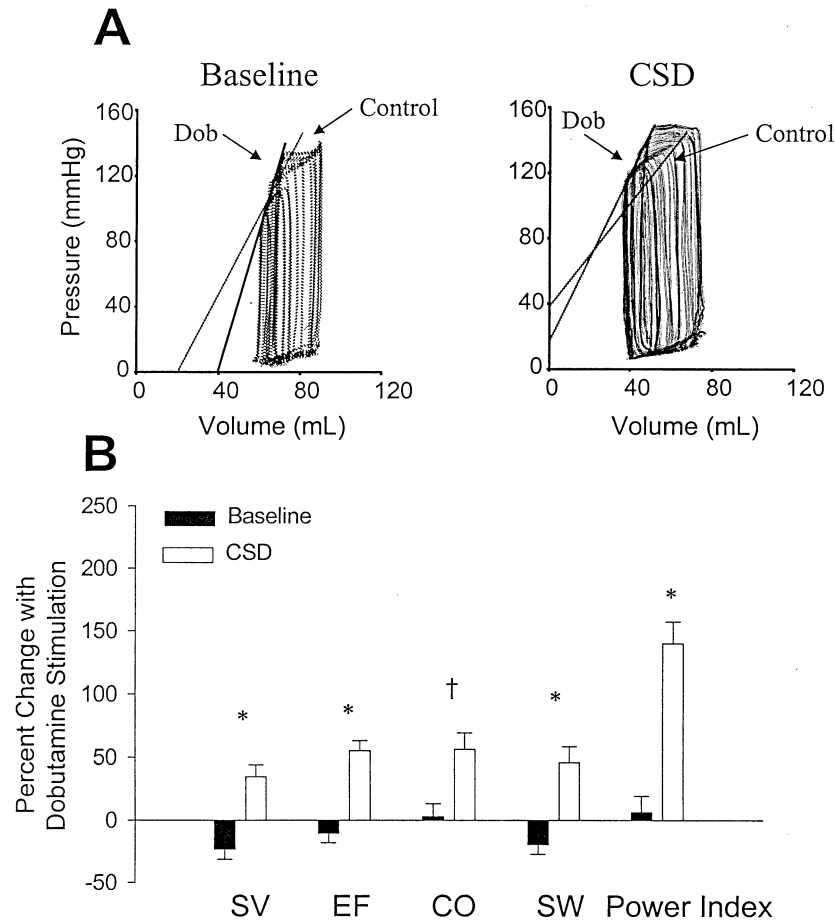
Figure 4. Enhancement of the dobutamine (Dob) response with long-term cardiac support device (CSD) treatment. **(A)** Example of pressure–volume loops and relations during early dobutamine infusion stimulation at baseline and after long-term CSD treatment. The pre-dobutamine end-systolic pressure–volume relation (ESVPR) (control) is shown for baseline and CSD treatment. Before CSD placement, the dobutamine response was very small, with only a slight leftward shift in the ESPVR. However, the magnitude of the response to this same dose was greatly augmented by long-term CSD treatment. **(B)** Percent changes in systolic function in response to dobutamine, comparing baseline with CSD treatment. Substantial increases were observed in response to multiple ejection variables: CO = cardiac output; EF = ejection fraction; SV = stroke volume; SW = stroke work; power index = maximal power/end-diastolic volume (EDV)^2. *p $\leq$ 0.001 and †p $<$ 0.02 compared with baseline response, by three-way analysis of variance of raw data.

concern was that the observed reverse remodeling would be accompanied by inhibition of cardiac preload reserve. Administering dextran infusions in the CSD-treated animals tested this hypothesis. As shown in Figure 3, the preload increased the end-diastolic pressure, as anticipated, but this was accompanied by substantial increases in systolic performance. There was no square-root sign in LV pressure–time tracings (Fig. 3A, bottom graph) before or after volume infusion, supporting the lack of constrictive physiology. Cardiac output rose nearly 100%, and both the maximal rates of rise and decline in pressure were significantly enhanced.

Improved beta-adrenergic reserve and the CSD. Figure 4 shows an example of and summary data on beta-adrenergic reserve before and after CSD placement. In the basal heart failure state, early dobutamine infusion elicited a small systolic response, although this was considerably enhanced after long-term CSD treatment. Stroke volume, stroke work, ejection fraction and cardiac output initially tended to decline with dobutamine, yet each variable rose significantly with the same dobutamine dose after CSD placement (all

p $<$ 0.01 for interaction effect of dobutamine and CSD status by ANOVA).

To further assess the mechanism(s) of the augmented adrenergic response with long-term CSD treatment, LV myocardial isoproterenol-stimulated adenylate cyclase activity was determined. This response was enhanced (Fig. 5A) in CSD-treated animals, as compared with a parallel group of animals (n = 5) with heart failure induced by the same methods and for a similar duration, but without CSD placement. In contrast, adenylate cyclase activity in response to forskolin was similar between the groups (Fig. 5B), supporting signaling changes proximal to the enzyme itself. Neither the beta-adrenergic receptor density (76 $\pm$ 4 vs. 81 $\pm$ 5 fmol/mg with the CSD) nor the binding affinity (1.31 $\pm$ 0.1 vs. 1.3 $\pm$ 0.1 nmol/l) was different between the two groups.

DISCUSSION

This study provides direct evidence that application of a purely passive external containment to a chronically failing
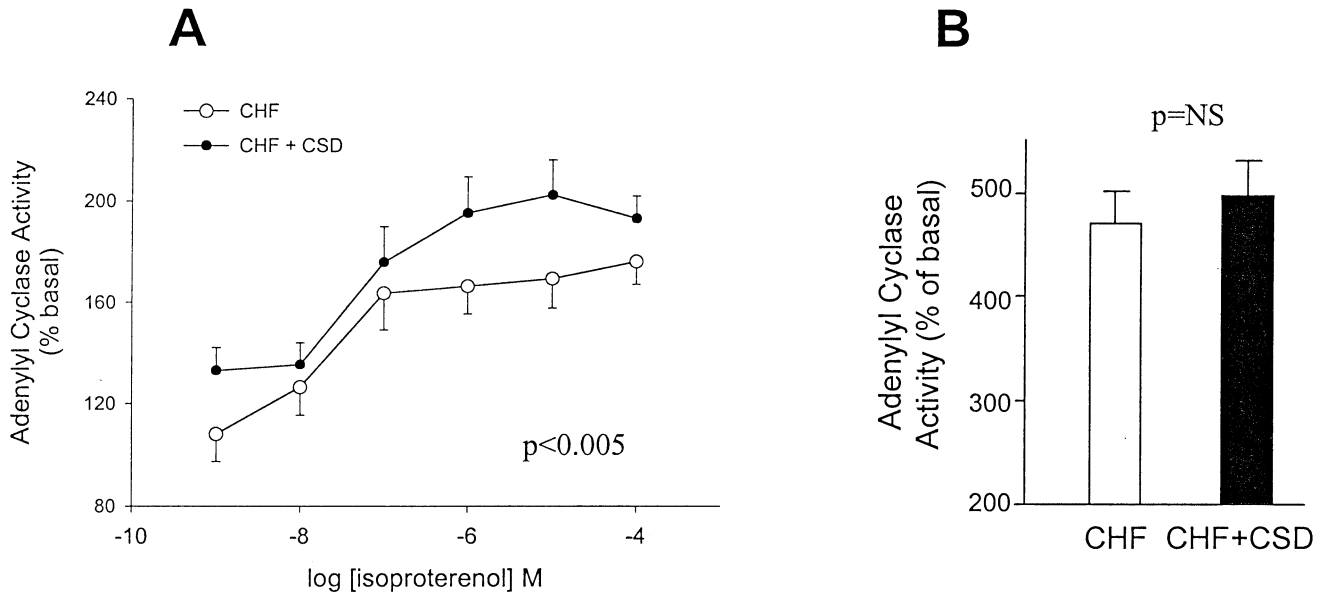
310

Figure 5. **(A)** Isoproterenol-stimulated adenylate cyclase activity in the failing myocardium, with or without cardiac support device (CSD) treatment. The CSD resulted in an enhanced dose response to isoproterenol. The p value is for the CSD effect on the dose response, by two-way analysis of variance. **(B)** Adenylyl cyclase activity with direct activation by forskolin revealed no difference between the groups, suggesting altered up-stream signaling as the major source for the disparity in part **A**. CHF = chronic heart failure.

heart leads to reversal of chamber remodeling, as detected by a leftward ESPVR shift and accompanied by augmented post-receptor sensitivity and responsiveness to beta-adrenergic stimulation. The CSD effect could not be attributed to systolic assistance and, importantly, was achieved in an intact working heart, without causing diastolic constriction that would otherwise inhibit preload reserve.

Reversing remodeling: unloading versus containment. Cessation or reversal of progressive chamber remodeling is an important aim of heart failure therapy (1,3,4,31). Successful pharmacologic approaches have targeted neurohormones, supporting the link between remodeling and angiotensin and catecholamine toxicity. Recent surgical approaches provide a more direct test of the importance of chamber load and structural geometry of the failing heart. The LVAD has been the most widely studied approach, and it can dramatically unload the LV, leading to reverse remodeling (9,32,33). At the cellular level, this results in reversal of many heart failure abnormalities involving gene expression (12,13,34), calcium homeostasis (13,35), hypertrophy (12), energetics (14) and adrenergic signaling (15). This demonstrates remarkable plasticity of the failing heart in response to profound cardiac unloading and systolic assistance. However, such data do not identify an effect of limiting dilation/remodeling, per se, as LVADs also restore cardiac output and markedly reduce neurohormonal activation. Recent comparisons between RV and LV myocardial responses support a load effect from the LVAD (36), but this analysis remains indirect, as RV failure varies among patients, and synergistic influences of neurohormonal deactivation and normalized output on unloading cannot be ruled out.

External containment, such as that provided by the CSD, physically limits cardiac expansion and, in so doing, breaks a positive feedback loop by which progressive dilation and dysfunction are coupled. This strategy of external containment differs from interventions that directly remodel the heart by removing myocardium (37,38) or placing stents to alter its shape and regional load (39). Hints that containment alone might lead to reverse remodeling first came from studies of cardiomyoplasty. Although this method combined an effect of external girdling with systolic assistance from skeletal muscle contraction, clinical data suggest that the former mechanism was particularly potent (18). Passive effects of the wrap were directly tested in an experimental model, where asynchronous, nonburst stimulation was applied to maintain skeletal muscle health, yet not elicit a contraction (19). Intriguingly, reverse remodeling and improved function by this approach were nearly identical to those seen when tetanic systolic cardiomyopathy stimulation was also applied (40), further supporting the notion that containment was a primary mechanism.

The CSD was developed as an artificial material alternative to a passive skeletal muscle wrap. Early reports performed in an ovine model of heart failure induced by rapid pacing found that the CSD limited progressive heart dilation and mitral regurgitation (20). Similar effects were then demonstrated in an ischemic cardiomyopathic model in association with diminished myocyte hypertrophy and fibrosis (21). The present results expand these findings in several major ways. The pressure–volume analysis identified reverse remodeling in the absence of constrictive pathophysiology as hallmarks of the CSD effect. The observed leftward shift in the ESPVR, with little net slope change, is

311

very similar to those experimental and clinical results with cardiomyoplasty (18,41). Also, in concordance with cardiomyoplasty, the CSD did not have a significant net effect on diastolic compliance, although it prevented progressive dilation.

The present data employing the CSD should be compared with time-controlled data from the same model of ischemic dilated cardiomyopathy, but without this device. As previously reported, animals in this latter model display progressive cardiac dilation and a reduced ejection fraction (21)—strikingly different from the results with the CSD. The observation that a purely passive wrap that does not quickly shrink the size of the heart can eventually lead to reverse remodeling is very intriguing. Although the exact mechanism remains unclear, one hypothesis is that the failing heart involves multiple interactive pathways with concomitant changes that can be both adverse and potentially ameliorative. Unchecked, the balance favors adverse factors and results in gradual deterioration. However, simply by limiting one of these important factors—that is, chamber remodeling—the CSD may tip the balance to allow favorable signaling pathways and energy utilization to become effective, and thereby help reverse progressive failure and enhance adrenergic signaling.

Improved adrenergic response. Improved beta-adrenergic signaling observed with the CSD is similar to that reported with LVAD therapy (15). With the CSD, this change occurred despite continued left heart loading and work, and without direct systolic assistance that could reduce the tonic adrenergic tone. Furthermore, the effects were obtained in hearts that were not terminally depressed. Unlike the LVAD, however, there was no change in beta-receptor density (or affinity) with the CSD, despite augmented adenylate cyclase responses to receptor stimulation and functional changes in the whole heart. This may reflect differences between the CSD and LVAD, which is associated with more extreme LV unloading and concomitant systemic changes. The precise mechanism for an enhanced beta-adrenergic response with the CSD remains unknown, but may lie in alterations in beta-adrenergic receptor kinase, G-protein signaling or cyclic guanosine monophosphate metabolism and catabolism.

Containment versus constriction. The major concern regarding external containment devices is whether or not they constrict diastolic filling and, thereby, preload reserve. The pericardium of the failing heart dilates to accommodate myocardial enlargement, but this expansion is generally insufficient to prevent limitations of preload reserve (42). The passive properties of the CSD are less abruptly nonlinear, compared with the pericardium, with a pressure rise of <7 mm Hg for 20% volume expansion, and a rise of 9 mm Hg at 30% expansion. This better enables the material to stretch to accommodate the filling volume. We found that long-term CSD use allowed substantial systolic reserve with early volume expansion. There was no equalization of diastolic pressures between the right and left heart, nor an

LV pressure square-root sign characteristic of restrictive (or constrictive) filling either before or after marked volume loading. Recent clinical studies have found no evidence of interference with coronary flow in either native or bypass vessels in humans (43). The passive properties of the mature CSD, with its fibrous in-growth, remain to be determined, and this is likely to be somewhat stiffer than the CSD alone. Nonetheless, the current data suggest that this combination remains sufficiently pliable to accommodate early volume expansion, yet still limit remodeling/expansion.

Study limitations. We did not perform pressure–volume studies in a parallel sham-operated group, but we did repeat studies in each animal. Previous historic control data in the same experimental model have been reported and support progressive dilation in the absence of the CSD. The duration of CSD treatment was somewhat variable, partially due to practical problems of having to transport co-investigators and equipment from one city to another to perform the studies. Nonetheless, we discerned no significant differences due to this time disparity. Furthermore, the magnitude of the initial volume change with CSD placement was somewhat variable, partly due to the lack of precise on-line measures of CSD snugness and volume change.

Conclusions. We have shown that a purely passive external elastic containment device can reverse remodeling in the failing heart and improve beta-adrenergic signaling, while preserving preload reserve. Preliminary clinical studies with the CSD have been recently reported (27), and the approach appears both safe and generally well tolerated. Ongoing randomized clinical trials in the U.S. and Europe aim to assess the efficacy of the CSD in limiting chronic remodeling in human cardiomyopathy. Such studies should provide the first tests, in humans, of the hypothesis that limiting remodeling alone in the intact working heart can improve long-term function and provide a useful therapy for heart failure.

Reprint requests and correspondence: Dr. David A. Kass, Halsted 500, Johns Hopkins Medical Institutions, 600 N. Wolfe Street, Baltimore, Maryland 21287. E-mail: dkass@bme.jhu.edu.

REFERENCES

1. Cohn JN, Ferrari R, Sharpe N, on behalf of an International Forum on Cardiac Remodeling. Cardiac remodeling—concepts and clinical implications: a consensus paper from an international forum on cardiac remodeling. J Am Coll Cardiol 2000;35:569–82.
2. Anversa P, Olivetti G, Capasso JM. Cellular basis of ventricular remodeling after myocardial infarction. Am J Cardiol 1991;68:7D–16D.
3. Francis GS. Pathophysiology of chronic heart failure. Am J Med 2001;110 Suppl 7A:37S–46S.
4. Goldstein S, Ali AS, Sabbah H. Ventricular remodeling: mechanisms and prevention. Cardiol Clin 1998;16:623–32.
5. Goldstein S, Sabbah H. Ventricular remodeling and angiotensin-converting enzyme inhibitors. J Cardiovasc Pharmacol 1994;24 Suppl 3:S27–31.
6. Jugdutt BI, Schwarz-Michorowski BL, Khan MI. Effect of long-term captopril therapy on left ventricular remodeling and function during

312

healing of canine myocardial infarction. J Am Coll Cardiol 1992;19:713–21.

7. McDonald KM, Rector T, Carlyle PF, et al. Angiotensin-converting enzyme inhibition and beta-adrenoceptor blockade regress established ventricular remodeling in a canine model of discrete myocardial damage. J Am Coll Cardiol 1994;24:1762–8.

8. Pfeffer JM, Pfeffer MA. Angiotensin-converting enzyme inhibition and ventricular remodeling in heart failure. Am J Med 1988;84 Suppl 3A:37–44.

9. Levin HR, Oz MC, Chen JM, et al. Reversal of chronic ventricular dilation in patients with end-stage cardiomyopathy by prolonged mechanical unloading. Circulation 1995;91:2717–20.

10. Barbone A, Oz MC, Burkhoff D, et al. Normalized diastolic properties after left ventricular assist result from reverse remodeling of chamber geometry. Circulation 2001;104 Suppl I:I229–32.

11. Dipla K, Mattiello JA, Jeevanandam V, et al. Myocyte recovery after mechanical circulatory support in humans with end-stage heart failure. Circulation 1998;97:2316–22.

12. Zafeiridis A, Jeevanandam V, Houser SR, et al. Regression of cellular hypertrophy after left ventricular assist device support. Circulation 1998;98:656–62.

13. Heerdt PM, Holmes JW, Cai B, et al. Chronic unloading by left ventricular assist device reverses contractile dysfunction and alters gene expression in end-stage heart failure. Circulation 2000;102:2713–9.

14. Mital S, Loke KE, Addonizio LJ, et al. Left ventricular assist device implantation augments nitric oxide dependent control of mitochondrial respiration in failing human hearts. J Am Coll Cardiol 2000;36:1897–902.

15. Ogletree-Hughes ML, Stull LB, Sweet WE, et al. Mechanical unloading restores beta-adrenergic responsiveness and reverses receptor downregulation in the failing human heart. Circulation 2001;104:881–6.

16. Carpentier A, Chachques JC. Clinical dynamic cardiomyoplasty method and outcome. Semin Thorac Cardiovasc Surg 1991;3:136–9.

17. Moreira LF, Bocchi EA, Stolf NA, et al. Dynamic cardiomyoplasty in the treatment of dilated cardiomyopathy: current results and perspectives. J Cardiac Surg 1996;11:207–13.

18. Kass DA, Baughman KL, Pak PH, et al. Reverse remodeling from cardiomyoplasty in human heart failure: external constraint versus active assist. Circulation 1995;91:2314–8.

19. Patel HJ, Polidori DJ, Pilla JJ, et al. Stabilization of chronic remodeling by asynchronous cardiomyoplasty in dilated cardiomyopathy: effects of a conditioned muscle wrap. Circulation 1997;96:3665–71.

20. Power JM, Raman J, Dornom A, et al. Passive ventricular constraint amends the course of heart failure: a study in an ovine model of dilated cardiomyopathy. Cardiovasc Res 1999;44:549–55.

21. Chaudhry PA, Mishima T, Sharov VG, et al. Passive epicardial containment prevents ventricular remodeling in heart failure. Ann Thorac Surg 2000;70:1275–80.

22. Sabbah HN, Sharov VG, Chaudhry PA, et al. Chronic therapy with the Acorn cardiac support device in dogs with chronic heart failure: three- and six-month hemodynamic, histologic and ultrastructural findings (abstr). J Heart Lung Transplant 2001;20:189.

23. Sabbah HN, Levine TB, Gheorghiade M, et al. Hemodynamic response of a canine model of chronic heart failure to intravenous dobutamine, nitroprusside, enalaprilat, and digoxin. Cardiovasc Drugs Ther 1993;7:349–56.

24. Sabbah HN, Sharov VG, Lesch M, et al. Progression of heart failure: a role for interstitial fibrosis. Mol Cell Biochem 1995;147:29–34.

25. Sabbah HN, Shimoyama H, Kono T, et al. Effects of long-term monotherapy with enalapril, metoprolol, and digoxin on the progression of left ventricular dysfunction and dilation in dogs with reduced ejection fraction. Circulation 1994;89:2852–9.

26. Liu CP, Tunin C, Kass DA. Transient time course of cocaine-induced cardiac depression versus sustained peripheral vasoconstriction. J Am Coll Cardiol 1993;21:260–8.

27. Konertz WF, Shapland JE, Hotz H, et al. Passive containment and reverse remodeling by a novel textile cardiac support device. Circulation 2001;104 Suppl I:I270–5.

28. Gengo PJ, Sabbah HN, Steffen RP, et al. Myocardial beta-adrenoceptor and voltage sensitive calcium channel changes in a canine model of chronic heart failure. J Mol Cell Cardiol 1992;24:1361–9.

29. Senzaki H, Isoda T, Paolocci N, et al. Improved mechanoenergetics and cardiac rest and reserve function of in vivo failing heart by calcium sensitizer EMD-57033. Circulation 2000;101:1040–8.

30. Glower DD, Spratt JA, Snow ND, et al. Linearity of the Frank-Starling relationship in the intact heart: the concept of preload recruitable stroke work. Circulation 1985;71:994–1009.

31. Bella JN, Wachtell K, Palmieri V, et al. Relation of left ventricular geometry and function to systemic hemodynamics in hypertension: the Losartan Intervention For Endpoint reduction in hypertension (LIFE) study. J Hypertens 2001;19:127–34.

32. Burkhoff D, Holmes JW, Madigan J, et al. Left ventricular assist device–induced reverse ventricular remodeling. Prog Cardiovasc Dis 2000;43:19–26.

33. Madigan JD, Barbone A, Choudhri AF, et al. Time course of reverse remodeling of the left ventricle during support with a left ventricular assist device. J Thorac Cardiovasc Surg 2001;121:902–8.

34. Morawietz H, Szibor M, Goettsch W, et al. Deloading of the left ventricle by ventricular assist device normalizes increased expression of endothelin ET_A receptors but not endothelin-converting enzyme-1 in patients with end-stage heart failure. Circulation 2000;102 Suppl III:III188–93.

35. Bartling B, Milting H, Schumann H, et al. Myocardial gene expression of regulators of myocyte apoptosis and myocyte calcium homeostasis during hemodynamic unloading by ventricular assist devices in patients with end-stage heart failure. Circulation 1999;100 Suppl II:II216–23.

36. Barbone A, Holmes JW, Heerdt PM, et al. Comparison of right and left ventricular responses to left ventricular assist device support in patients with severe heart failure: a primary role of mechanical unloading underlying reverse remodeling. Circulation 2001;104:670–5.

37. Batista R, Santos J, Takeshita N, et al. Partial left ventriculectomy to improve left ventricular function in end-stage heart disease. J Cardiol Surg 1996;11:96–7.

38. Starling RC, McCarthy PM, Buda T, et al. Results of partial left ventriculectomy for dilated cardiomyopathy: hemodynamic, clinical and echocardiographic observations. J Am Coll Cardiol 2000;36:2098–103.

39. McCarthy PM, Takagaki M, Ochiai Y, et al. Device-based change in left ventricular shape: a new concept for the treatment of dilated cardiomyopathy. J Thorac Cardiovasc Surg 2001;122:482–90.

40. Patel HJ, Pilla JJ, Polidori DJ, et al. Long-term dynamic cardiomyoplasty improves chronic and acute myocardial energetics in a model of left ventricular dysfunction. Circulation 1998;98 Suppl II:II346–51.

41. Schreuder JJ, van der Veen FH, van der Velde ET, et al. Left ventricular pressure–volume relationships before and after cardiomyoplasty in patients with heart failure. Circulation 1997;96:2978–86.

42. Dauterman K, Pak PH, Nussbacher A, et al. Contribution of external forces to left ventricle diastolic pressure: implications for the clinical use of the Frank-Starling law. Ann Intern Med 1995;122:737–42.

43. Raman JS, Hata M, Storer M, Power JM, Buxton BF, Alferness C, Hare D. The mid-term results of ventricular containment (Acorn wrap) for end-stage ischemic cardiomyopathy. Ann Thorac Cardiovasc Surg 2001;7:278–81.

313

Reverse remodeling and enhancedadrenergic reserve from passive externalsupport in experimental dilated heart failure

W. Federico Saavedra, Richard S. Tunin, Nazareno Paolocci, Takayuki Mishima, George Suzuki, Charles W. Emala, Pervaiz A. Chaudhry, Petros Anagnostopoulos, Ramesh C. Gupta, Hani N. Sabbah and David A. Kass

This information is current as of October 30, 2006

Updated Information & Services	including high-resolution figures, can be found at: http://content.onlinejacc.org/cgi/content/full/39/12/2069
References	This article cites 43 articles, 22 of which you can access for free at: http://content.onlinejacc.org/cgi/content/full/39/12/2069#BIBL
Citations	This article has been cited by 16 HighWire-hosted articles: http://content.onlinejacc.org/cgi/content/full/39/12/2069#otherarticles
Rights & Permissions	Information about reproducing this article in parts (figures, tables) or in its entirety can be found online at: http://content.onlinejacc.org/misc/permissions.dtl
Reprints	Information about ordering reprints can be found online: http://content.onlinejacc.org/misc/reprints.dtl

314

Circulation Research

Reversal of Chronic Molecular and Cellular Abnormalities Due to Heart Failure by Passive Mechanical Ventricular Containment

Hani N. Sabbah, Victor G. Sharov, Ramesh C. Gupta, Sudhish Mishra, Sharad Rastogi, Albertas I. Undrovinas, Pervaiz A. Chaudhry, Anastassia Todor, Takayuki Mishima, Elaine J. Tanhehco and George Suzuki

The online version of this article, along with updated information and services, is located on the World Wide Web at:

http://circres.ahajournals.org/cgi/content/full/93/11/1095

315

Reversal of Chronic Molecular and Cellular Abnormalities Due to Heart Failure by Passive Mechanical Ventricular Containment

Hani N. Sabbah, Victor G. Sharov, Ramesh C. Gupta, Sudhish Mishra, Sharad Rastogi,
Albertas I. Undrovinas, Pervaiz A. Chaudhry, Anastassia Todor, Takayuki Mishima,
Elaine J. Tanhehco, George Suzuki

Abstract—Passive mechanical containment of failing left ventricle (LV) with the Acorn Cardiac Support Device (CSD) was shown to prevent progressive LV dilation in dogs with heart failure (HF) and increase ejection fraction. To examine possible mechanisms for improved LV function with the CSD, we examined the effect of CSD therapy on the expression of cardiac stretch response proteins, myocyte hypertrophy, sarcoplasmic reticulum Ca^{2+}-ATPase activity and uptake, and mRNA gene expression for myosin heavy chain (MHC) isoforms. HF was produced in 12 dogs by intracoronary microembolization. Six dogs were implanted with the CSD and 6 served as concurrent controls. LV tissue from 6 normal dogs was used for comparison. Compared with normal dogs, untreated HF dogs showed reduced cardiomyocyte contraction and relaxation, upregulation of stretch response proteins (p21ras, c-fos, and p38 α/β mitogen-activated protein kinase), increased myocyte hypertrophy, reduced SERCA2a activity with unchanged affinity for calcium, reduced proportion of mRNA gene expression for α-MHC, and increased proportion of β-MHC. Therapy with the CSD was associated with improved cardiomyocyte contraction and relaxation, downregulation of stretch response proteins, attenuation of cardiomyocyte hypertrophy, increased affinity of the pump for calcium, and restoration of α- and β-MHC isoforms ratio. The results suggest that preventing LV dilation and stretch with the CSD promotes downregulation of stretch response proteins, attenuates myocyte hypertrophy and improves SR calcium cycling. These data offer possible mechanisms for improvement of LV function after CSD therapy. (*Circ Res*. 2003;93:1095-1101.)

Key Words: heart failure ∎ myocyte hypertrophy ∎ sarcoplasmic reticulum ∎ myosin heavy chain

Heart failure (HF) is a progressive disorder mediated through multiple signaling pathways. Once initiated, HF is characterized by increased neurohumoral activation and ventricular dilation. Although such compensatory changes are initially beneficial, over the long-term they cause adverse structural and functional changes collectively referred to as ventricular remodeling. Ventricular dilation also causes increased mechanical stress and myocardial stretch. Upregulation of stretch response proteins, such as p21ras,[1] c-fos,[2,3] and p38 α/β mitogen-activated protein kinase (MAPK),[4] have been shown to induce cardiomyocyte hypertrophy.

The Acorn Cardiac Support Device (CSD) has been shown to halt progressive left ventricular (LV) dilation and improve ejection fraction.[5–7] However, the mechanism(s) underlying the improved cardiac function has not been elucidated. In the present study, we tested the hypothesis that improvement in LV systolic function in dogs with HF after long-term therapy with the CSD results, in part, from downregulation of stretch response proteins, attenuation of cardiomyocyte hypertrophy,[1–4] and improvement of sarcoplasmic reticulum (SR) calcium cycling. To further understand the mechanisms for

the improvement in LV systolic function, we also explored the influence of this form of therapy on the expression of cardiac α- and β-myosin heavy chain (MHC) isoforms.[8,9]

Materials and Methods

Animal Model

The canine model of chronic HF used in this study was previously described in detail.[10] Chronic LV dysfunction is produced by multiple sequential intracoronary embolization with polystyrene Latex microspheres (70 to 102 μm in diameter), which results in loss of viable myocardium. The model manifests many of the sequelae of HF observed in humans with HF, including marked depression of LV systolic and diastolic function, reduced cardiac output, increased LV filling pressures, and enhanced activity of the sympathetic nervous system.[10] Moreover, this model demonstrates progression of HF long after the cessation of coronary microembolizations. In the present study, 12 healthy mongrel dogs (Marshall Farms, North Rose, NY), weighing between 21 and 31 kg, underwent serial coronary microembolizations to produce HF. Embolizations were performed 1 to 3 weeks apart and were discontinued when LV ejection fraction was between 30% and 40%. Microembolizations were performed during cardiac catheterization under general anesthesia and sterile conditions. The anesthesia regimen consisted of a combination of intra-

316

venous injection of oxymorphone (0.22 mg/kg), diazepam (0.17 mg/kg), and sodium pentobarbital (150 to 250 mg) to effect.

Study Protocol

Dogs underwent a left and right heart catheterization at baseline, before any coronary microembolizations. At 2 weeks after the last coronary microembolization, dogs underwent another left and right heart catheterization (pretreatment) while anesthetized. The 2-week period was allowed to ensure that all infarctions produced by the last microembolization were completely healed. The CSD was surgically implanted in 6 dogs as previously described.[5] The remaining 6 dogs served as concurrent controls. All CSD-treated dogs and controls were followed up for 3 months during which time no cardioactive drugs were used. At the end of the follow-up period, a final left and right heart catheterization was performed. After the final catheterization, and while under general anesthesia, the chest was opened and the heart removed and the tissue prepared for histological and biochemical examination. LV tissue from 6 normal dogs was prepared in an identical manner and used for comparison. The study was approved by the Henry Ford Hospital Care of Experimental Animals Committee and conformed to the "Position of the American Heart Association on Research Animal Use."

Angiographic Measurements

Single-plane left ventriculograms were obtained during left heart catheterization with the dog placed on its right side. Ventriculograms were recorded on 35-mm cine film at 30 frames per second during the injection of 20 mL of contrast material (Reno-M-60, Squibb). Correction for image magnification was made with a radiopaque calibrated grid placed at the level of the LV. LV end-systolic and end-diastolic volumes (ESV and EDV, respectively) were calculated from LV silhouettes using the area-length method,[11] LV EF as previously described.[10]

Determination of Stretch Response Proteins

Expression of stretch response proteins, specifically p21ras, c-fos, and p38 α/β MAPK, was determined by Western blotting using homogenate of cardiomyocytes isolated from the LV free wall.[12,13] In parallel, expression of calsequestrin (CSQ), a protein that is not altered in HF, was also determined and used as internal control. All stretch response proteins were normalized to CSQ. The Western blot membranes were incubated with primary (p21 rabbit polyclonal IgG; p38 α/β MAPK rabbit polyclonal IgG; c-fos rabbit polyclonal IgG; all from Santa Cruz, Inc) and then with secondary (goat-anti-rabbit HRP conjugated; Chemicon) antibody for 2 hours each. The antibody-bound antigen was identified by chemiluminescence (Renaissance Western Blot Chemiluminescence Reagent, Perkin Elmer Life Sciences Inc), followed by autoradiography. The density of bands was quantified using a densitometer.

Contraction and Relaxation of Isolated Cardiomyocytes

Cardiomyocytes were isolated from the LV free wall as previously described.[14] Cardiomyocyte contraction and relaxation were recorded using an edge detection algorithm.[15] Contraction was evoked by electrical field stimulation at a frequency of 1.0 Hz. Percent cardiomyocyte shortening, peak velocity of shortening, and peak velocity of relengthening were measured in 5 to 10 cardiomyocytes from each dog selected at random. For each cardiomyocyte, 20 consecutive cycles were averaged to obtain a representative value, which was then used to calculate the average measures for each dog.

Determination of Cardiomyocyte Hypertrophy

Cardiomyocyte hypertrophy was determined by assessing average cardiomyocyte cross-sectional area from frozen LV tissue sections using computer-assisted planimetry.[5,16] The length and width of isolated cardiomyocytes were also determined. Isolated cardiomyocytes were visualized using a Labophot-2 Nikon microscope with objective 20. The field was transferred to a computer using a digital video camera and projected on a digital screen. The maximum length

and width of approximately 1200 rod shaped cardiomyocytes from each dog were measured using computer-assisted planimetry.

Determination of SR Ca²⁺ Uptake and Cardiac SR Ca²⁺-ATPase (SERCA2a) Activity

Oxalate-dependent Ca^{2+} uptake was determined in LV homogenate as previously described.[17] Briefly, an aliquot of 50 μL of 0.25 mg/mL LV homogenate was incubated at 37°C for 1 minute in 0.4 mL of Ca^{2+} uptake buffer consisting of 50 mmol/L imidazole-HCl (pH 7.0), 100 mmol/L KCl, 6 mmol/L $MgCl_2$, 10 mmol/L NaN_3 (included to inhibit mitochondrial Ca^{2+} uptake), 10 mmol/L potassium oxalate, 20 μmol/L ruthenium red (included to inhibit SR Ca^{2+} release), 0.5 mmol/L EGTA, and 0.01 to 10 μmol/L free Ca^{2+} ($^{45}CaCl_2$, 10 000 dpm/nmol). The reaction was initiated by adding an aliquot of 50 μL of 50 mmol/L ATP, the assay was terminated 2 minutes later, radioactivity retained on filter paper was counted, and oxalate-dependent Ca^{2+} uptake was calculated as previously described.[17] SR Ca^{2+} uptake, expressed as nmol $^{45}Ca^{2+}$ sequestered/min per mg of noncollagen protein, was determined as previously described.[17] For thapsigargin-sensitive SERCA2a activity measurements, membrane vesicles were prepared from LV tissue as previously described.[18] SERCA2a activity was determined in the absence and presence of thapsigargin at varying calcium concentration (0.1 to 10.0 μmol/L) as previously described[18] and the activity expressed as μmol Pi released/min per mg of noncollagen protein.

Determination of Expression of SERCA2a, Phospholamban (PLB), and PLB Phosphorylation

To determine SR protein levels of SERCA2a and PLB, sodium-dodecyl sulfate (SDS) extract of LV homogenate was prepared as previously described.[17,18] To freeze the phosphorylation state of the proteins, LV tissue was homogenized in the presence of the inhibitors of protein kinases (1 mmol/L EDTA, 1 mmol/L EGTA) and protein phosphatases (2 mmol/L sodium pyrophosphate and 10 mmol/L sodium fluoride). Five micrograms or the indicated amount of the SDS-extract was separated on 4% to 20% linear polyacrylamide (BioRad), transferred electrophoretically on nitrocellulose membrane, and the resulting membrane was incubated with primary antibody as previously described.[17,18] The accuracy of the electrotransfer was confirmed by staining the membrane with 0.1% amido black. Polyclonal antibodies for phosphorylated PLB at threonine-17 (Thr17) and serine-16 (Ser16) or monoclonal antibody for PLB was diluted to 500-fold or 2500-fold, respectively. Primary-antibody binding protein was visualized by incubating the blot with a second antibody, a peroxidase-conjugated anti-mouse in case of monoclonal or anti-rabbit in case of polyclonal antibodies, and the enhanced chemiluminescence assay was used as described by the supplier (Dupont-NEN). In parallel, CSQ was also determined in the LV homogenate. The intensity of the bands was quantified using a Bio-Rad model GS-670 imaging densitometer. The density of the phosphorylated PLB at Thr17 or Ser16 was normalized to the amount of PLB present in LV tissue. Protein levels of PLB and SERCA2a were normalized to CSQ. Before quantifying protein expression levels, the protein dependency of the immunodetectable bands for all proteins was established. In this study, a linear correlation was observed between densitometric units and protein content (<30 μg) for each immunodetectable protein.

Gene Expression of Cardiac α- and β-MHC

Total RNA from LV myocardium was isolated as described previously.[19] Tissue samples were homogenized in RNA Stat-60 solution (150 mg tissue/1.5 mL RNA Stat 60) followed by extraction with chloroform, precipitation with isopropanol, and finally washing the precipitated RNA with 75% (v/v) ethanol. The RNA obtained was dissolved in RNase free water. The concentration of RNA was determined by spectrophotometry. Total RNA was diluted to 0.1 mg/mL concentration and denatured at 95°C for 5 minutes followed by rapid cooling in ice bath. Approximately 10 μg of total RNA was primed with 0.5 μg of oligo (dT)15 primer. Total RNA was reversed transcribed by using a cDNA synthesis kit (Promega Inc). After

TABLE 1.   Angiographic Measurements Obtained at Baseline (Base) Before Any Coronary Microembolizations, Before Initiating Therapy or Follow-Up (Before), and 3 Months After Initiating Therapy or Follow-Up (After)

	Untreated HF Controls			CSD-Treated		
	Base	Before	After	Base	Before	After
LV EDV, mL	55±4	67±5†	83±8*	59±3	68±4†	61±4*
LV ESV, mL	25±3	43±3†	60±7*	28±2	45±7†	36±7*
LV EF, %	55±1	36±1†	28±2*	53±2	34±1†	42±1*

LV indicates left ventricular; EDV, end-diastolic volume; ESV, end-systolic volume; and EF, ejection fraction.

†$P<0.05$ Base vs Before; *$P<0.05$ Before vs After.

incubating the samples at 42°C for 1 hour, the reaction was terminated at 95°C for 5 minutes. The mRNA levels of α- and β-MHC were analyzed by amplification of cDNA by reverse transcriptase-polymerase chain reaction[12] followed by restriction enzyme digestion and then identified by agarose gel electrophoresis and ethidium bromide staining. Fluorescent bands corresponding to α- and β-MHC were quantified in densitometric units, each normalized to total MHC (α-MHC+β-MHC) and each reported as percent of total MHC.

Data Analysis

Within group comparisons between baseline, pretreatment, and posttreatment angiographic measures were made using repeated measures analysis of variance (ANOVA) with α set at 0.05. If significance was attained, pairwise comparisons between groups was determined using the Student-Newman-Kuels test with a value of $P<0.05$ considered significant. Comparisons of biochemical measures between normal, HF controls and CSD-treated HF dogs were based on one-way analysis of variance (ANOVA) with α set at 0.05. If significance was attained, pairwise comparisons between groups were determined using the Student-Newman-Kuels test with a value of $P<0.05$ considered significant. All data are reported as the mean±SEM.

Results

There were no significant differences at baseline and at pretreatment in EDV, ESV, or EF between dogs that were subsequently treated with the CSD and dogs assigned as concurrent controls (Table 1). After treatment, EF significantly decreased in untreated controls but increased significantly in CSD-treated dogs. This was accompanied by a significant increase in both ESV and EDV in untreated controls and by a significant reduction in both ESV and EDV in CSD-treated dogs (Table 1).

Cardiomyocyte Contraction and Relaxation

Results of cardiomyocyte contraction and relaxation are shown in Table 2. Percent cardiomyocyte shortening, peak velocity of shortening, and peak velocity of relengthening

TABLE 2.   Contraction and Relaxation of Isolated Cardiomyocytes

	Normal	Untreated HF Controls	CSD-Treated
S, %	4.9±0.3	1.5±0.2*	2.8±0.3*†
Peak dS/dt, μm/sec	111±10	26±1*	48±9*†
Peak dR/dt, μm/sec	124±4	13±2*	40±6*†

S indicates percent of cardiomyocyte shortening; dS/dt, velocity of shortening; and dR/dt, velocity of relengthening.

*$P<0.05$ Normal vs HF; †$P<0.05$ CSD-Treated vs Untreated HF Controls.

decreased significantly in untreated HF dogs compared with normal dogs. In contrast, in dogs treated with the CSD all three measures were significantly higher than in untreated HF dogs.

Stretch Response Proteins

Western blots depicting changes in p21Ras, c-fos, and p38 α/β MAPK are shown in Figure 1. The summary data for all 6 dogs in each of the three groups are shown in Table 3. All three stretch response proteins, normalized to CSQ, increased significantly in untreated HF dogs compared with normal dogs. In HF dogs treated with the CSD, all three stretch response protein levels were similar to those seen in normal dogs (Figure 1, Table 3).

Cardiomyocyte Hypertrophy

Cardiomyocyte cross-sectional area increased significantly in dogs with HF compared with normal dogs. This increase was significantly attenuated by CSD treatment (Figure 2). Cardiomyocyte length and width were significantly greater in untreated HF dogs compared with normal dogs; whereas treatment with the CSD was associated with a significantly lesser change in length and width of the cardiomyocytes compared with untreated controls (Figure 2).

SERCA2a Activity and Ca²⁺ Uptake

Maximal velocity (V_{max}) and the affinity of SERCA2a for calcium ($K_{0.5}$) are shown in Table 3. V_{max}, but not $K_{0.5}$, decreased significantly in control HF dogs compared with normal dogs. Therapy with the CSD did not change V_{max}
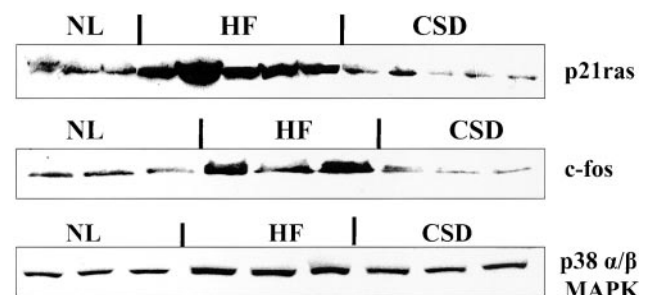

Figure 1. Representative Western blot for the stretch response proteins p21ras, c-fos, and p38 α/β MAPK. Implantation of the CSD significantly reduced the expression of all 3 proteins (see Table 3). NL indicates normal; HF, heart failure; and CSD, cardiac support device–treated dogs.

318

TABLE 3. Changes in Stretch Response Protein Levels, Sarcoplasmic Reticulum Ca^{2+} Uptake, and SERCA2a Activity, and Expression of Other Sarcoplasmic Reticulum Proteins Depicted in Densitometric Units

	Normal	Untreated HF Controls	CSD-Treated
p21ras/CSQ	0.24±0.02	0.92±0.20*	0.35±0.10**
c-fos/CSQ	0.41±0.04	0.96±0.20*	0.33±0.05**
p38 α/β MAPK/CSQ	1.18±0.07	2.99±0.37*	1.25±0.10**
CSQ	4.91±0.35	5.11±0.33	5.22±0.22
Ca^{2+} uptake			
V_{max}	22.5±2.0	11.6±1.0*	12.3±1.0*
Ka	0.52±0.03	0.53±0.03	0.28±0.01**
SERCA2a Activity			
V_{max}	0.36±0.02	0.23±0.02*	0.25±0.02*
$K_{0.5}$	0.45±0.03	0.48±0.03	0.32±0.02**
SERCA2a/CSQ	2.26±0.10	1.74±0.11*	1.76±0.10*
PLB/CSQ	3.63±0.19	1.57±0.21*	2.23±0.31*
PLB-Ser16/PLB	0.28±0.01	0.18±0.03*	0.40±0.02**
PLB-Thr17/PLB	0.54±0.07	0.30±0.03*	0.88±0.02**

CSQ indicates calsequestrin; MAPK, mitogen-activated protein kinase; HF, heart failure; Ca^{2+}, calcium; SERCA2a, Ca^{2+}-ATPase; PLB, phospholamban; PLB-Ser16, phosphorylated phospholamban at serine-16; and PLB-Thr17, phosphorylated phospholamban at threonine-17.

*$P<0.05$ Normal vs HF; **$P<0.05$ CSD-Treated vs Untreated HF Controls.

compared with control but was associated with a significant decrease in $K_{0.5}$ compared with HF controls, indicating a higher SERCA2a affinity for calcium after CSD therapy (Table 3). V_{max} for SR Ca^{2+} uptake but not affinity (Ka) decreased in control HF dogs compared with normal dogs. V_{max} for Ca^{2+} uptake did not change after CSD therapy, whereas Ka decreased indicating an increase in the affinity after CSD therapy (Table 3).

Expression of SERCA2a, PLB, and PLB Phosphorylation

Western blots showing expression of SERCA2a, PLB, PLB at Ser16 and Thr17, and CSQ are shown in Figure 3. All
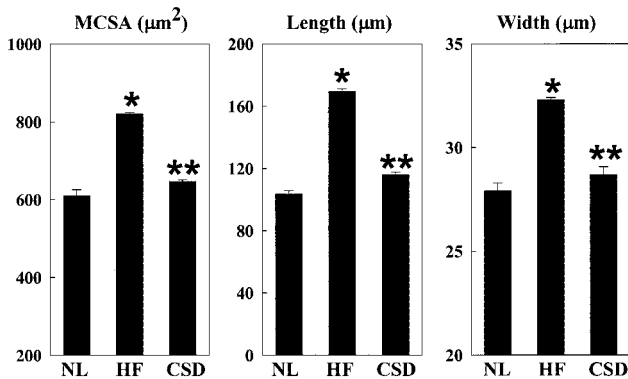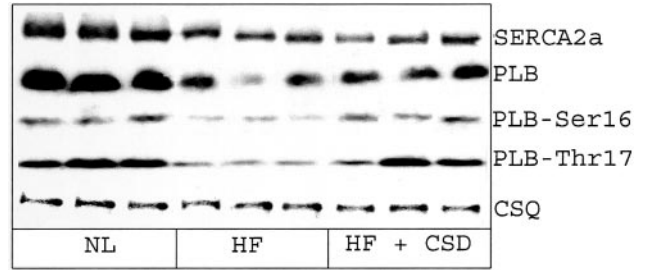

Figure 3. Western blot showing immunodetectable sarcoplasmic reticulum proteins in left ventricular myocardium of 3 normal dogs (NL), 3 dogs with heart failure that are not treated (HF), and 3 dogs with heart failure treated with the cardiac support device (HF+CSD). SERCA2a indicates Ca^{2+}-ATPase; PLB, phospholamban; PLB-Ser16, phosphorylated phospholamban at serine-16; PLB-Thr17, phosphorylated phospholamban at threonine-17; and CSQ, calsequestrin.

proteins, with the exception of CSQ, decreased significantly in control HF dogs compared with normal dogs. Densitometric analyses in Table 3 show that expression of SERCA2a and PLB was not changed in CSD-treated dogs compared with HF controls, whereas expression of phosphorylated PLB at Ser16 and Thr17 increased with CSD therapy compared with controls.

Expression of α- and β-MHC

Changes in the proportion of cardiac α- and β-MHC between normal dogs, untreated HF dogs, and CSD-treated HF dogs are shown in Table 4. In untreated HF dogs, gene expression of LV α-MHC decreased significantly compared with expression in LV of normal dogs. Three months of chronic treatment with the CSD LV expression of α-MHC was similar to that seen in normal dogs (Table 4). In untreated HF dogs, expression of LV β-MHC increased significantly compared with normal dogs, whereas treatment with the CSD was associated with LV expression of β-MHC that was similar to that seen in normal dogs (Table 4, Figure 4).

Discussion

Heart failure is characterized by progressive LV dysfunction and dilation. Regardless of the type of initiating injury, compensatory mechanisms are evoked to maintain adequate organ perfusion that includes neurohumoral activation, ventricular dilation, and cardiomyocyte hypertrophy. These responses are beneficial initially, but in the long-term cause maladaptive changes in myocardial structural and function recognized as ventricular remodeling. Thus, sustained neurohumoral activation and increased LV mechanical stretch and

Figure 2. Bar graphs depicting changes in cardiomyocyte size. Treatment group abbreviations same as in Figure 1. Implantation of the CSD significantly reduced cardiomyocyte hypertrophy. MCSA indicates myocyte cross-sectional area. *$P<0.05$ compared with NL; **$P<0.05$ compared with HF.

TABLE 4. mRNA Expression of α- and β-Myosin Heavy Chain Depicted as Percent of Total Myosin Heavy Chain

	Normal	Untreated HF Controls	CSD-Treated
α-MHC	23.5±1.0	14.1±1.0*	24.6±0.6**
β-MHC	76.5±1.0	85.9±1.0*	75.4±0.6**

MHC indicates myosin heavy chain; HF, heart failure.

*$P<0.05$ Normal vs Untreated HF Controls; **$P<0.05$ CSD-Treated vs Untreated HF Controls.
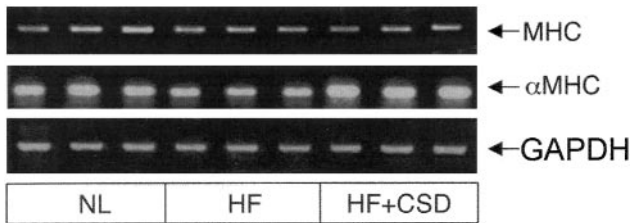
Figure 4. Ethidium bromide–agarose gel showing mRNA encoding total myosin heavy chain (MHC); α-myosin heavy chain (αMHC) and glyceraldehyde 1,3 diphosphate dehydrogenase (GAPDH) in LV myocardium of 3 normal dogs (NL), 3 dogs with heart failure that are not treated (HF), and 3 dogs with heart failure treated with the cardiac support device (HF+CSD).

wall stress associated with ventricular dilation represent key mediators that precipitate progression of HF.

In recent years, attenuation of maladaptive ventricular remodeling has become an important goal for the treatment of HF. Numerous pharmacological interventions have been developed to block various neurohumoral factors and, in doing so, attenuate remodeling. Drug therapy with angiotensin-converting enzyme inhibitors and β-adrenergic receptor blockers represent the current standard of care in patients with HF and have been shown to attenuate LV remodeling and, in the case of β-blockers, reverse the maladaptive process, albeit partially.[9,20] However, the existence of multiple molecular signaling pathways that can trigger HF progression suggest that even the use of multiple pharmacological agents may not completely block all pathways responsible for the progression of LV remodeling. In particular, drugs may not be as effective at blocking the effects of mechanical signals such as wall stress and myocardial stretch. The latter can have direct consequences on biochemical and molecular effector systems that can mediate LV remodeling.[1–4,25]

It has long been accepted that certain surgical approaches can be combined with optimal medical therapy to provide better survival and improved quality of life in patients with advanced HF. Functional mitral regurgitation, a common feature of the failing heart, can be eliminated or attenuated by repair or replacement of the mitral valve, a procedure that can improve forward stroke output.[21] Experience with LV assist devices (LVADs) indicates that unloading the heart can promote reduction in LV chamber size, improvement in LV performance, and normalization of gene expression.[22,23] Cardiomyoplasty is another surgical technique, in which the primary mode of action was originally thought to involve an active assist during contraction. The procedure involved wrapping a skeletal muscle around the heart and electrically stimulating the muscle to squeeze the heart and augment cardiac function. Even though the procedure involved extensive surgery and was plagued with technical difficulties, patients showed symptomatic improvement.[24,25] However, several experimental[26,27] and clinical[28] studies have suggested that the improvement was derived primarily from the passive girdling of the heart and not from active contraction of the skeletal muscle. Several studies in various animal models of HF have shown that progressive LV dilation can be prevented or attenuated by wrapping synthetic materials around the

cardiac ventricles to elicit containment.[5–7,29] These passive mechanical devices and surgical approaches attempted to treat HF by directly preventing progressive LV enlargement and, in doing so, limit the adverse effects of increased wall stress and myocardial stretch.

The CSD is one such device designed to prevent progressive LV dilation and attenuate myocardial stretch and chamber sphericity.[5,25] Mechanical stretch has been shown to directly and/or indirectly stimulate cardiomyocyte hypertrophy through upregulation of so-called stretch response proteins.[1–4] The resulting maladaptive hypertrophy is invariably associated with abnormal SR calcium cycling, shifts in myosin isoforms, and other changes associated with ventricular remodeling.[1–4,8,10,22,23] Thus, reducing mechanical stress and preventing excessive myocardial stretch may downregulate stretch response proteins and block an important signaling pathway for HF progression.

Findings from our laboratory and others have demonstrated that long-term monotherapy with the CSD in animals with experimentally induced HF can prevent progressive LV dilation and improve LV ejection fraction.[5–8,25] Although one would expect that a passive mechanical device such as the CSD can prevent progressive LV dilation, the mechanism by which the CSD leads to improved LV systolic function is not as clear. The present study addressed this issue by exploring the potential biochemical and molecular alterations that occurred as a consequence of CSD therapy.

In the present study, improvement of global LV function with CSD therapy was associated with lesser extent of intrinsic contractile dysfunction of cardiomyocytes compared with no treatment at all. Therapy with the CSD was also associated with lower tissue levels of stretch response proteins specifically p21ras, c-fos, and p38 α/β MAPK compared with no treatment at all. Expression of these proteins has been shown to increase in HF.[1–4] These proteins are known to be direct stimuli for cardiomyocyte hypertrophy.[1–4] Maladaptive cardiomyocyte hypertrophy plays a key role in the progression of HF.[30,31] In this study, long-term CSD therapy resulted in attenuation of cardiomyocyte hypertrophy as evidenced by decreased cardiomyocyte cross-sectional area, length, and width compared with control.

Findings of this study also showed that CSD therapy was associated with increased affinity of SERCA2a for calcium. This increase in affinity may have been due to increased phosphorylation of PLB. Increased affinity of SERCA2a for calcium can lead to improved calcium cycling within the SR particularly at low cytosolic calcium concentrations. Given that abnormalities in Ca^{2+} handling may, in part, underlie the decrease in contractile function in HF, we propose that increased affinity of the pump for calcium as seen with CSD therapy may have contributed to the observed improvement of LV function.

Marked differences in the phosphorylation of PLB were observed in the present study and warrant discussion. Phosphorylation of PLB was decreased in HF controls compared with normal dogs. It would be expected that phosphorylation of PLB would be greater in HF dogs due to the increase in plasma norepinephrine associated with the HF state. However, this increase in circulating plasma norepinephrine is

accompanied by downregulation of β_1 adrenoceptors in the heart and uncoupling between the receptors and their G proteins. In addition, phosphorylation of PLB was increased in the CSD group compared with the HF group despite the improvement of LV function, which is normally associated with decreased plasma norepinephrine. One possible explanation is that in addition to augmented plasma norepinephrine, an increase in phosphatase activity has also been documented in HF.[32–36] A decrease in PLB phosphorylation has been previously noted in our canine model of HF.[32,34] It is possible, albeit unproven, that the balance of phosphorylation/phosphatase activation may have favored dephosphorylation in the HF dogs, while reverting to phosphorylation in the CSD-treated animals.

Cardiomyocytes express both α- and β-MHC isoforms. In the rat heart, these two isoforms differ on the basis of ATPase activity, with α-MHC being more active than β-MHC.[37,38] Compared with cardiac β-MHC, α-MHC is associated with faster velocity of shortening.[37,38] Studies in LV tissue obtained form explanted failed human hearts showed loss of α-MHC expression with increased expression of β-MHC, a condition that can argue in favor of diminished contractile function. Other studies have shown that this maladaptation in the proportion of cardiac α-MHC and β-MHC isoforms can be reversed in animal models of HF after drug or surgical therapy.[39–41] In the present study, the proportion of cardiac α-MHC was significantly reduced in HF dogs that were untreated, and the proportion β-MHC was increased. Long-term treatment with the CSD was associated with expression of both MHC isoforms that was close to normal levels, a condition that may have also contributed to the improvement of LV function seen with CSD therapy.

In conclusion, results of this study suggest that the observed improvement in LV function after long-term therapy with the CSD may be due, in part, to the effects of the CSD on limiting LV wall stress and myocardial stretch. These changes were associated with attenuation of muscle cell hypertrophy and improvement of SR calcium cycling. The improvement of LV function with CSD therapy may have also been due, in part, on its effects on the expression of cardiac MHC isoforms.

Acknowledgments

References

1. Sadoshima J, Izumo S. Mechanical stretch rapidly activates multiple signal transduction pathways in cardiac myocytes: potential involvement of an autocrine/paracrine mechanism. *EMBO J*. 1993;12:1681–1692.
2. Sadoshima J, Izumo S. Signal transduction pathways of angiotensin II induced c-fos gene expression in cardiac myocytes in vitro: roles of phospholipid-derived second messengers. *Circ Res*. 1993;73:424–438.
3. Sadoshima J, Jahn L, Takahashi T, Kulik TJ, Izumo S. Molecular characterization of the stretch-induced adaptation of cultured cardiac cells. An in vitro model of load-induced cardiac hypertrophy. *J Biol Chem*. 1992; 267:10551–10560.
4. Sadoshima J, Qiu Z, Morgan JP, Izumo S. Angiotensin II and other hypertrophic stimuli mediated by G protein-coupled receptors activate tyrosine kinase, mitogen-activated protein kinase, and 90-kD S6 kinase in cardiac myocytes: the critical role of Ca^{2+}-dependent signaling. *Circ Res*. 1995;76:1–15.
5. Chaudhry PA, Mishima T, Sharov VG, Hawkins J, Alferness C, Paone G, Sabbah HN. Passive epicardial containment prevents ventricular remodeling in heart failure. *Ann Thorac Surg*. 2000;70:1275–1280.
6. Saaverda EF, Tunin RS, Paolocci N, Mishima T, Suzuki G, Emala CW, Chaudry PA, Anagnostopoulos P, Gupta RC, Sabbah HN, Kass DA. Reverse remodeling and enhanced adrenergic reserve from passive external support in experimental dilated heart failure. *J Am Coll Cardiol*. 2002;39:2069–2076.
7. Power JM, Raman J, Dornom A, Farish SJ, Burrell LM, Tonkin AM, Buxton B, Alferness CA. Passive ventricular constraint amends the course of heart failure: a study in an ovine model of dilated cardiomyopathy. *Cardiovasc Res*. 1999;44:549–555.
8. Nakao K, Minobe W, Roden R, Bristow MR, Leinwand LA. Myosin heavy chain gene expression in human heart failure. *J Clin Invest*. 1997; 100:2362–2370.
9. Lowes BD, Gilbert EM, Abraham WT, Minobe WA, Larrabee P, Ferguson D, Wolfel EE, Lindenfeld J, Tsvetkova T, Roberston AD, Quaife RA, Bristow MR. Myocardial gene expression in dilated cardiomyopathy treated with beta-blocking agents. *N Engl J Med*. 2002;346: 1357–1365.
10. Sabbah HN, Stein PD, Kono T, Gheorghiade M, Levine TB, Jafri S, Hawkins ET, Goldstein S. A canine model of chronic heart failure produced by multiple sequential intracoronary microembolizations. *Am J Physiol*. 1991;260:H1379–H1384.
11. Dodge HT, Sandler H, Baxley WA, Hawley RR. Usefulness and limitations of radiographic methods for determining left ventricular volume. *Am J Cardiol*. 1966;18:10–24.
12. Symington J, Green M, Brackman K. Immunoautoradiographic detection of proteins after electrophoretic transfer from gels to diazo-paper: analysis of adenovirus encoded proteins. *Proc Natl Acad Sci U S A*. 1981;78: 177–181.
13. Todor A, Sharov VG, Tanhehco EJ, Silverman N, Bernabei A, Sabbah HN. Hypoxia-induced cleavage of caspase-3 and DFF45/ICAD in human failed cardiomyocytes. *Am J Physiol*. 2002;283:H990–H995.
14. Maltsev VA, Sabbah HN, Higgins RSD, Silverman N, Lesch M, Undrovinas AI. Novel, ultraslow inactivating sodium current in human ventricular cardiomyocytes. *Circulation*. 1998;98:2545–2552.
15. Maltsev VA, Sabbah HN, Tanimura M, Lesch M, Goldstein S, Undrovinas AI. Relationship between action potential, contraction-relaxation pattern, and intracellular Ca^{2+} transient in cardiomyocytes of dogs with chronic heart failure. *Cell Mol Life Sci*. 1998;54:597–605.
16. Tanimura M, Sharoc VG, Shimoyama H, Mishima T, Levine TB, Goldstein S, Sabbah HN. Effects of AT$_1$-receptor blockade on progression of left ventricular dysfunction in dogs with heart failure. *Am J Physiol*. 1999;276:H1385–H1392.
17. Gupta RC, Mishra S, Mishima T, Goldstein S, Sabbah HN. Reduced sarcoplasmic reticulum Ca^{2+}-uptake and expression of phospholamban in left ventricular myocardium of dogs with heart failure. *J Moll Cell Cardiol*. 1999;31:1381–1389.
18. Gupta RC, Shimoyoma H, Tanimura M, Nair R, Lesch M, Sabbah HN. Reduced SR Ca^{2+}-ATPase activity and expression in ventricular myocardium of dogs with heart failure. *Am J Physiol*. 1997;273:H12–H18.
19. Feldman AM, Ray PE, Silan CM, Mercer JA, Minobe W, Bristow MR. Selective gene expression in failing human heart: quantification of steady-state levels of messenger RNA in endomyocardial biopsies using the polymerase chain reaction. *Circulation*. 1991;83:1866–1872.
20. Sabbah HN, Shimoyama H, Kono T, Gupta RC, Sharov VG, Scicli G, Levine B, Goldstein S. Effects of long-term monotherapy with enalapril, metoprolol, and digoxin on the progression of left ventricular dysfunction and dilation in dogs with reduced ejection fraction. *Circulation*. 1994;89: 2852–2859.
21. Bolling SF. Mitral reconstruction in cardiomyopathy. *J Heart Valve Dis*. 2002;11(suppl 1):S26–S31.
22. Madigan JD, Barbone A, Choudhri AF, Morales DL, Cai B, Oz MC, Burkhoff D. Time course of reverse remodeling of the left ventricle during support with a left ventricular assist device. *J Thorac Cardiovasc Surg*. 2001;121:902–908.
23. Burkhoff D, Holmes JW, Madigan J, Barbone A, Oz MC. Left ventricular assist device-induced reverse ventricular remodeling. *Prog Cardiovac Dis*. 2000;43:19–26.
24. Capouya ER, Gerber RS, Drinkwater DC, Pearl JM, Sack JB, Aharon AS, Barthel SW, Kaczer EM, Chang PA, Laks H. Girdling effect of non-

stimulated cardiomyoplasty on left ventricular function. *Ann Thorac Surg*. 1993;56:867–871.

25. Kass DA, Baughman KL, Pak PH, Cho PW, Levin HR, Gardner TJ, Halperin HR, Tsitlik JE, Acker MA. Reverse remodeling from cardiomyoplasty in human heart failure: external constraint versus active assist. *Circulation*. 1995;91:2314–2318.

26. Vaynblat M, Chiavarelli M, Shah HR, Ramdev G, Aron M, Zisbrod Z, Cunningham JN. Cardiac binding in experimental heart failure. *Ann Thorac Surg*. 1997;64:81–85.

27. Patel HJ, Polidori DJ, Pilla JJ, Plappert T, Kass D, St John Sutton M, Lankford EB, Acker MA. Stabilization of chronic remodeling by asynchronous cardiomyoplasty in dilated cardiomyopathy: effects of a conditioned muscle wrap. *Circulation*. 1997;96:3665–3671.

28. Hagege AA, Desnos M, Fernandez F, Besse B, Mirochnik N, Castaldo M, Chachques JC, Carpentier A, Guerot C. Clinical study of the effects of latissimus dorsi muscle flap stimulation after cardiomyoplasty. *Circulation*. 1995;92(suppl):II-210–II-215.

29. McCarthy PM, Takagaki M, Ochiai Y, Young JB, Tabata T, Shiota T, Qin JX, Thomas JD, Mortier TJ, Schroeder RF, Schweich J, Fukamachi K. Device-based change in left ventricular shape: a new concept for the treatment of dilated cardiomyopathy. *J Thorac Cardiovasc Surg*. 2001;122:482–490.

30. Molkentin JD, Dorn II GW 2nd. Cytoplasmic signaling pathways that regulate cardiac hypertrophy. *Annu Rev Physiol*. 2001;63:391–426.

31. Francis GS. Changing the remodeling process in heart failure: basic mechanisms and laboratory results. *Curr Opin Cardiol*. 1998;13:156–161.

32. Gupta RC, Mishra S, Rastogi S, Imai M, Habib O, Sabbah HN. Cardiac SR-coupled type 1 protein phosphatase activity and expression are increased and inhibitor protein 1 protein expression is decreased in the failing heart. *Am J Physiol Heart Circ Physiol*. In press.

33. Huang B, Wang HB, Qin D, Boutjdir M, El-Sherif N. Diminished basal phosphorylation level of phospholamban in the postinfarction remodeled rat ventricle: role of β adrenergic pathway, G_i protein, phosphodiesterase, and phosphatases. *Circ Res*. 1999;85:848–855.

34. Mishra S, Gupta RC, Towari N, Sharov VG, Sabbah HN. Molecular mechanisms of reduced sarcoplasmic reticulum Ca^{2+} uptake in human failing left ventricular myocardium. *J Heart Lung Trans*. 2002;21:366–373.

35. Sande JB, Sjaastad I, Hoen IB, Bokenes J, Tonnessen T, Holt E, Lunde PK, Christensen G. Reduced level of serine (16) phosphorylated phospholamban in the failing rat myocardium: a major contributor to reduced SERCA2 activity. *Cardiovasc Res*. 2002;53:382–391.

36. Mishra S, Sabbah HN, Jain JC, Gupta RC. Reduced Ca^{2+}-calmodulin-dependent protein kinase activity and expression in LV myocardium of dogs with heart failure. *Am J Physiol Heart Circ Physiol*. 2003;284:H876–H883.

37. Pope B, Hoh JF, Weeds A. The ATPase activities of rat cardiac myosin isoenzymes. *FEBS Lett*. 1980;118:205–208.

38. Miyata S, Minobe W, Bristow MR, Leinwand LA. Myosin heavy chain isoform expression in the failing and nonfailing human heart. *Circ Res*. 2000;86:386–390.

39. Bauersachs J, Galuppo P, Fraccarollo D, Christ M, Ertl G. Improvement of left ventricular remodeling and function by hydroxymethylglutaryl coenzyme a reductase inhibition with cerivastatin in rats with heart failure after myocardial infarction. *Circulation*. 2001;104:982–985.

40. Liu X, Sentex E, Golfman L, Takeda S, Osada M, Dhalla NS. Modification of cardiac subcellular remodeling due to pressure overload by captopril and losartan. *Clin Exp Hypertens*. 1999;21:145–156.

41. Pauletto P, Vescovo G, Scannapieco G, Angelini A, Pessina AC, Dalla Libera L, Carraro U, Dal Palu C. Changes in rat ventricular isomyosins with regression of cardiac hypertrophy. *Hypertension*. 1986;8:1143–1148.